Mechanistic understanding of glycolysis in Japanese encephalitis virus infected neuronal cells with special reference to hypoxia-inducible factor-1α and pyruvate Kinase M2

Thesis submitted in partial fulfilment of the requirements for the award of the degree of

DOCTOR OF PHILOSOPHY

By

Vijay Singh Bohara

Under the Supervision of

Prof. Sachin Kumar

Viral Immunology Laboratory

Department of Biosciences and Bioengineering

INDIAN INSTITUTE OF TECHNOLOGY GUWAHATI

Guwahati-781039, Assam, India

November, 2025

Dedicated to my parents and my teachers

Indian Institute of Technology Guwahati

Department of Biosciences and Bioengineering

DECLARATION

I hereby declare that the research work embodied in this thesis, entitled **"Mechanistic understanding of glycolysis in Japanese encephalitis virus infected neuronal cells with special reference to hypoxia-inducible factor-1α and pyruvate Kinase M2"** is the result of scientific investigation carried out by me in the Department of Biosciences and Bioengineering, Indian Institute of Technology Guwahati for the award of the degree of Doctor of Philosophy under the supervision of Prof. Sachin Kumar.

As per the general norms of the reporting of scientific findings, due acknowledgements have been made wherever the findings of other investigators have been cited in this thesis.

Date: 30th November, 2025

Vijay Singh Bohara
(Roll No. 196106107)
Department of Biosciences and Bioengineering,
Indian Institute of Technology Guwahati,
Assam, India

Indian Institute of Technology Guwahati

Department of Biosciences and Bioengineering

CERTIFICATE

This is to certify that the thesis entitled **"Mechanistic understanding of glycolysis in Japanese encephalitis virus infected neuronal cells with special reference to hypoxia-inducible factor-1α and pyruvate Kinase M2"** submitted by Vijay Singh Bohara for the award of the degree of Doctor of Philosophy is an authentic record of the original work carried out by him under my supervision and guidance at the Department of Biosciences and Bioengineering, Indian Institute of Technology Guwahati, India. This work has not been submitted elsewhere for the award of any other degree or diploma to the best of my knowledge.

Date: 30th November, 2025

Prof. Sachin Kumar
(Thesis supervisor)
Department of Biosciences and Bioengineering,
Indian Institute of Technology Guwahati,
Assam, India

Acknowledgements

I would like to express my heartfelt gratitude to everyone who has been part of this long journey, guiding me and believing in me through every challenge that I faced. Though their contributions are beyond what words can describe, I will do my best to acknowledge each one of them for the support they have given me in achieving this milestone in my life.

First, I want to extend my deepest regard and indebtedness to my thesis supervisor, **Prof. Sachin Kumar**, for providing the financial support for my research and for unwavering trust, motivation, and insightful guidance throughout this journey. Beyond scientific research, he taught me to stay calm and composed, seeking the best alternative options available. His passion for research and never-give-up mindset have pushed me beyond my limits. It was always my privilege to work under his guidance.

I am sincerely thankful to my Doctoral Committee members, **Dr. Rajkumar P. Thummer (Chairman)**, **Prof. Manish Kumar**, and **Dr. Kusum K. Singh**, for their constructive criticism, valuable suggestions, and advice, which enabled me to improve my work. I am also indebted to my teachers from Sri Guru Tegh Bahadur Khalsa College, University of Delhi and Tezpur University for shaping my early academic foundation.

My heartfelt thanks to all the respected faculty members and staff of the **Department of Biosciences and Bioengineering, Indian Institute of Technology Guwahati**, for creating an environment that not only nurtures scientific learning but also the overall personality of a student. I also acknowledge the **Ministry of Education, Government of India**, for providing me with a research fellowship to pursue my research and the Department of Biosciences and Bioengineering, Indian

Institute of Technology Guwahati, for providing state-of-the-art facilities to conduct my experiments.

I am grateful to my seniors of Viral Immunology Laboratory, **Dr. Anjali Gupta, Dr. Kamal Shokeen, Dr. Rakesh Kumar,** and **Dr. Sudhir Morla** for their generous support, valuable advice to troubleshoot my experiments and constant encouragement. I would also like to thank the Postdoctoral fellows, **Dr. Purvita Chowdhury** and **Dr. Diptesh**, for their continuous guidance. I was fortunate to work with these amazing people. I am also thankful to the current members of the laboratory, **Shivani, Priyanka, Nilave, Sushil, Shinjini, Kiran, Aditya, Deepa, Satyendu, Shurti** and **Sayani**. I am also grateful to **Shubham Gaurav, Anushka, Abhay, Maitreyee, Subhadwip, Imdhiyas,** and **Achal** for their assistance. I especially thank seniors beyond my laboratory, Siddhartha bhaiya, Sonya dee, Robin bhaiya, Gaurav bhaiya, and Satakshi dee, who have been my last resort for help.

I am blessed to have some great people in my life, my friends **Surabhi, Sanya, Dwipjyoti, Bhoomika, Rashmi, Malaya,** and **Shomina**. Thanks for standing by me at every step of my journey. Above all, I offer my deepest respect and love to my parents and elder brother for their blessings. They have always been my greatest strength and role model.

Finally, I bow my head in front of **Lord Shiva** for granting me strength, guiding me through challenges, and showering his divine blessings upon me.

Signing off with a quote from the Bhagavad Gita.

"You are what you believe in, you become that which you believe you can become"

Vijay

Table of contents

List of figures

List of tables

List of Abbreviations

JEV	Japanese encephalitis virus
JE	Japanese encephalitis
HIF-1α	Hypoxia-inducible factor-1alpha
PHD	Prolyl hydoxylases
PKM2	Pyruvate kinase M2
ROS	Reactive oxygen species
STAT3	Signal transducer and activator of transcription 3
TNF-α	Tumor necrosis factor-alpha
IL-1β	Interleukin-1beta
UTR	Untranslated regions
GAGs	Glycosaminoglycans
ATP	Adenosine triphosphate
ADP	Adenosine diphosphate
AMP	Adenosine monophosphate
TCA	Tricarboxylic acid cycle
WNV	West Nile virus
YFV	Yellow fever virus
SARS-CoV-2	Severe acute respiratory syndrome coronavirus 2
HCV	Hepatitis C virus
RSV	Respiratory syncytial virus
HK	Hexokinase
PDH	Pyruvate dehydrogenase
PFK	Phosphofructokinase
PK	Pyruvate kinase
LDH	Lactate dehydrogenase
GAPDH	Glyceraldehyde 3-phosphate dehydrogenase
NDV	Newcastle disease virus
PDK4	Pyruvate dehydrogenase kinase 4
CVB3	Coxsachievirus B3
PRRSV	Porcine reproductive and respiratory syndrome virus
HPV	Human papillomavirus
SVA	Senecavirus A
ARV	Avian reovirus
HIV	Human immunodeficiency virus
GLUT	Glucose transporter
SIRT3	Sirtuin 3
AMPK	AMP-activated protein kinase
FOXO	Forkhead box O
mTOR	Mammalian target of rapamycin
P13K	Phosphoinositide 3-kinase
IDH3β	Isocitrate dehydrogenase 3 subunit beta
GDH	Glutamate dehydrogenase
eIF4E	Eukaryotic translation initiation Factor 4E
2-DG	2-Deoxy-D-glucose
SOP	Sodium pyruvate
DCA	Dichloroacetate

ECAR	Extracellular acidification rate
ERK1/2	Extracellular signal-regulated kinase 1/2
FBP	Fructose-1,6-bisphosphate
GPI	Glucose-6-phosphate isomerase
ALD	Aldolase
TPI	Triose phosphate isomerase
PGK1	Phosphoglycerate kinase 1
hnRNP	Heterogeneous nuclear ribonucleoprotein
EGFR	Epidermal growth factor receptor
PPARγ	Peroxisome proliferator-activated receptor γ
PPRE	PPARγ response elements
NF-κβ	Nuclear factor kappa-light chain-enhancer of activated B cells
PKCε	Protein kinase C
SAICAR	Succinyl-5-aminoimidazole-4-carboxamide-1-ribose-5'-phosphate
NADP	Nicotinamide adenine dinucleotide phosphate
CENPF	Centromere protein F
HSP90	Heat shock protein 90
PPP	Pentose phosphate pathway
HDAC3	Histone deacetylase 3
PTB	Polypyrimidine-tract-binding protein
C-MYC	Cellular myelocytomatosis
PAK2	p21-activated kinase 2
TG1F2	TGF-β-induced factor homeobox 2
CDH1	Cadherin-1
MEK5	Mitogen-activated protein kinase 5
ROCK2	Rho-associated coiled-coil containing protein kinase 2
SNAP23	Synaptosomal-associated protein 23
BCL-2	B-cell lymphoma 2
JMJD5	Jumonji Domain-containing 5
HMGB1	High mobility group box 1
BUB3	Budding uninhibited by benzimidazoles
SOCS3	Suppressor of cytokine signaling 3
1L-17	Interleukin-17
TNFR1	Tumor necrosis factor receptor 1
DMEM	Dulbecco’s Modified Eagle Medium
FBS	Fetal Bovine Serum
LPS	Lipopolysaccharide
BHK-21	Baby hamster kidney-21
MTT	3-(4,5-dimethylthiazol-2-yl)-2,5-diphenyl tetrazolium bromide
DMSO	Dimethyl sulfoxide
RIPA	Radioimmunoprecipitation assay
TBST	Tris-buffered Saline with Tween 20
HPLC	High-performance liquid chromatography
PBS	Phosphate Buffered Saline
BSA	Bovine serum albumin
DAPI	4',6'-diamidino-2-phenylindole
GFP	Green fluorescence protein
MOI	Multiplicity of infection
DCFH-DA	2',7'-dichlorodihydrofluorescein diacetate
RIG-I	Retinoic acid-inducible gene I

MDA5	Melanoma differentiation-associated protein 5
MAVS	Mitochondrial antiviral signaling protein
IFN-β	Interferon-beta
PEP	Phosphoenol pyruvate
PDK	Pyruvate dehydrogenase kinase
RMSD	Root Mean Square Deviation
RMSF	Root Mean Square Fluctuation
SASA	Solvent Accessible Surface Area
CDK1	Cyclin-dependent kinase 1
JNK1	c-Jun N-terminal kinase 1
JAK2	Janus kinase 2

Abstract

Viruses impose substantial metabolic stress on the host cells, which drives the increased biosynthesis of nucleotides, lipids, and proteins required for supporting rapid virus multiplication in the infected cells. In the current study, we have shown that Japanese encephalitis virus (JEV) profoundly reprograms neuronal metabolism by stimulating glycolysis. This was reflected by increased glycolytic flux in JEV-infected Neuro-2a cells. Further, the replication was augmented by enhanced extracellular glucose levels and insulin treatment. Conversely, treatment with glycolytic inhibitors markedly restricted viral replication, which highlights the enhanced utilization of glucose upon JEV infection. This glycolytic reprogramming was found to be orchestrated by key glycolytic enzymes in the infected cells. Moreover, the enhanced expression of Hypoxia-inducible factor-1 (HIF-1α), a known transcription factor for glycolytic genes, was also observed in the infected cells. Additionally, the stabilization of HIF-1α expression by cobalt chloride ($CoCl_2$) treatment enhanced JEV replication, while its knockdown reduced the replication. This reflects that HIF-1α is a positive regulator of JEV replication in neurons. The study also uncovers a mechanistic perspective, as enhanced reactive oxygen species (ROS) accumulation was observed in the infected cells. We speculate that enhanced ROS stabilizes HIF-1α in the infected cells, which in turn increases the transcription of glycolytic genes such as glycolytic enzymes to support glycolysis. In the current study, we also describe a novel host cell factor, pyruvate kinase isoform M2, regulating JEV replication in neuronal cells, by inducing the activation of Signal Transducer and Activator of Transcription (STAT3), which then modulates the expression of proinflammatory cytokines such as Tumor necrosis factor alpha (TNF-α) and Interleukin-1beta (IL-1β). The study also delineates the cellular co-localization and interaction of PKM2 with the NS1 protein of JEV. However, the functional implication of this interaction remains to

be uncovered. Altogether, the study highlights the mechanism of glycolytic reprogramming by JEV in neuronal cells. Targeting these glycolytic enzymes and host factors can help in designing virus-specific therapies.

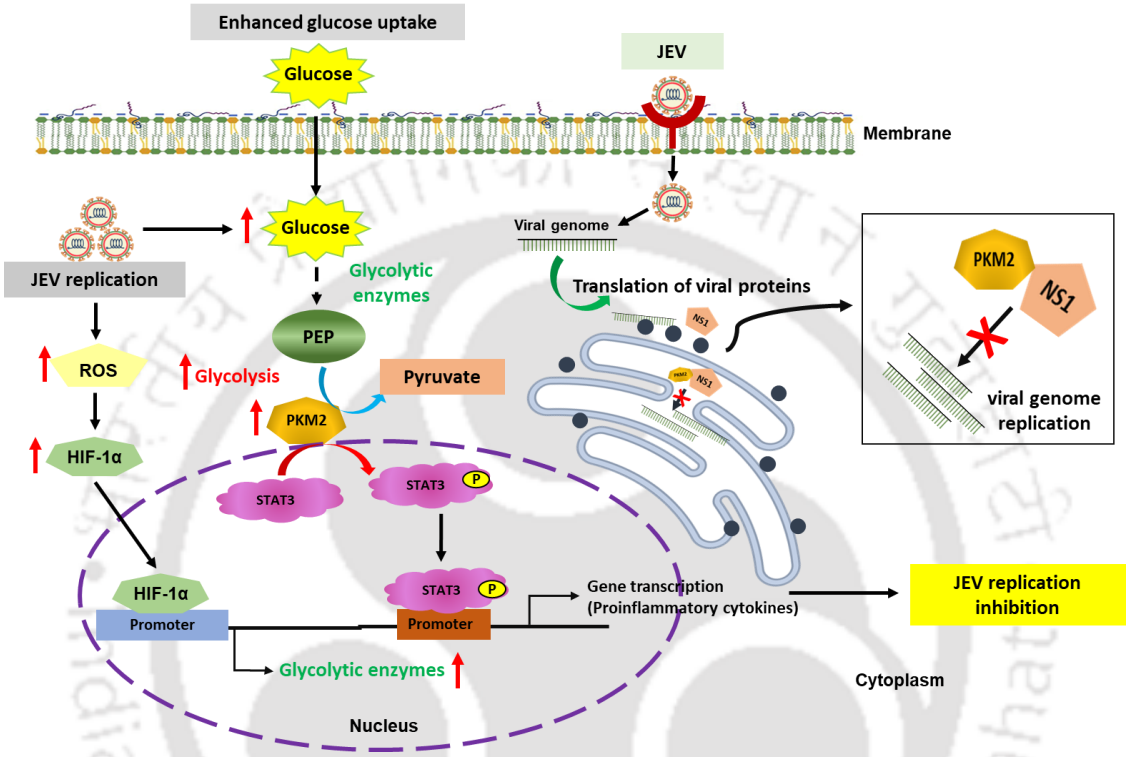

Graphical thesis abstract

Chapter 1
Introduction

Brief overview of the Chapter

The chapter begins with an overview of the epidemiology of Japanese encephalitis and its causative agent, providing a concise description of the transmission cycle of the Japanese encephalitis virus. It then outlines the structure of the virus, its genome organization, and the functions of structural and non-structural proteins. Subsequently, the chapter focuses on the replication cycle of the virus along with the viral proteins involved in the replication. At last, the concept of replication-induced glycolytic reprogramming has also been introduced.

1.1 Introduction

Japanese encephalitis (JE) is a neurotropic disease caused by the mosquito-borne Japanese encephalitis virus (JEV) (Pinapati et al., 2023). According to the WHO, JE is regarded as the predominant cause of viral encephalitis in Asia, with an estimated yearly incidence of 50,000 to 100,000 cases, with the majority occurring in children and young adults (Li et al., 2025). The early symptoms of JEV infection include headache, altered consciousness, and vomiting (Mohsin et al., 2022). JE is estimated to have a fatality rate of about 30%, with up to 50% of survivors experiencing long-term neurological consequences (Kulkarni et al., 2018; Mohsin et al., 2022). The most common mode of transmission of JEV is through the bite of an infected female *Culex* mosquito (Srivastava et al., 2023). Certain species of *Anopheles* mosquitoes, including *Anopheles subpictus*, *Anopheles peditaeniatus*, and *Anopheles hyrcanus*, are also implicated in the transmission of JEV (Srivastava et al., 2023). Pigs and wading birds are considered amplifying hosts and significant contributors to the

transmission of JEV to mosquitoes. Humans are dead-end hosts as they do not develop infect breeding mosquitoes (Figure 1.1) (Turtle and Solomon, 2018).

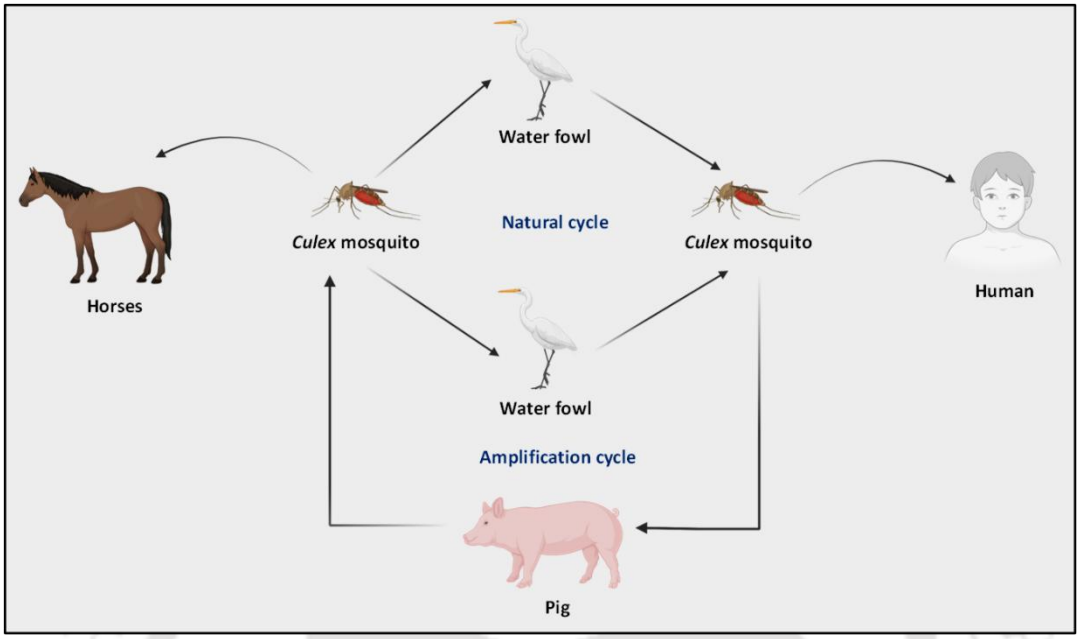

Figure 1.1 Schematic representation of the transmission cycle of JEV.

1.2 Structure and genome organization

JEV belongs to the genus *Orthoflavivirus* and is 40-50 nm in diameter (Unni et al., 2011). It has a spheroid shape, with a core composed of nucleocapsid containing the genome and core (C) protein (Lindenbach and Rice, 2003). The structure of JEV was elucidated using X-ray crystallographic techniques (Wang et al., 2017b). It was discovered that, like other *Orthoflavivirus,* its outer surface is smooth and comprises envelope and membrane proteins. Envelope proteins form homodimers arranged in a head-to-tail fashion, resulting in an icosahedron (Luca et al., 2012; Wang et al., 2017b). It is surrounded by a lipid bilayer, which it acquires from its host. The genome is positive-stranded, single-stranded and 10.7 kb in length, containing a single ORF flanked by untranslated regions (UTR) at both 5' and 3' ends (Unni et al., 2011). The genome possesses a 5' cap but lacks a poly A tail (Dong et al., 2014; Ray et al., 2006). It encodes a single polyprotein of 3400 amino acids, which is cleaved

by viral or host proteases to form 10 proteins (Kim et al., 2015). Out of 10 proteins, structural proteins are capsid (C), pre-membrane (prM/M), and envelope (E), while non-structural proteins are NS1, NS2A/2B, NS3, NS4A/4B and NS5 (Figure 1.2) (Yun and Lee, 2018).

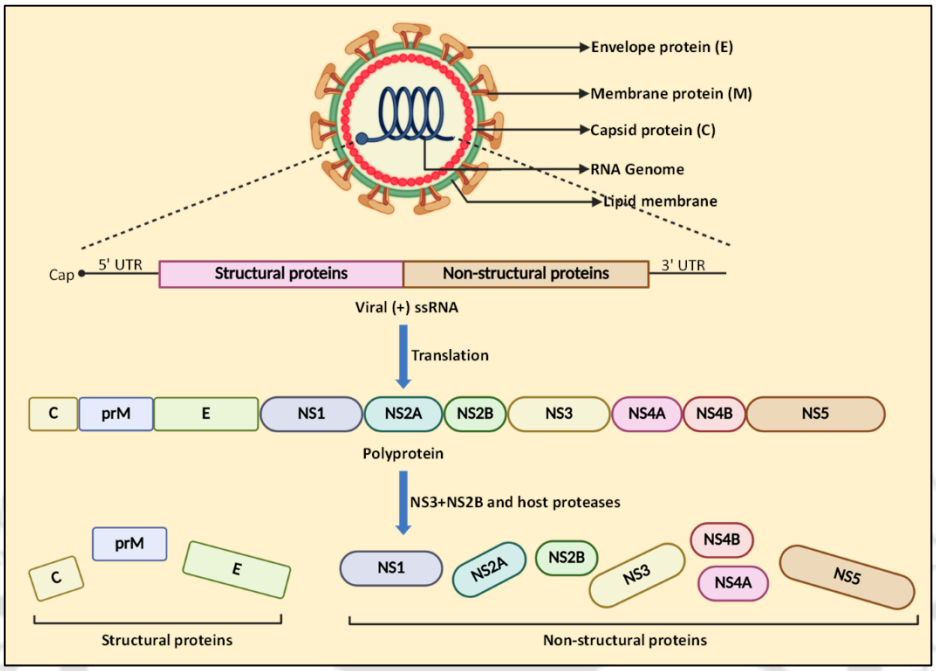

Figure 1.2 Diagrammatic illustration of the structure and genome organization of JEV.

1.2.1 Structural proteins

The mature capsid is a ~11-12 kDa protein involved in genome packaging and forms the nucleocapsid (Dey et al., 2021). It has a helix-rich structure, leading to the formation of stable homodimers (Poonsiri et al., 2019). It interacts with both the envelope protein and the virus genome, forming an enclosure around the genome (Poonsiri et al., 2019). Envelope is a ~55 kDa protein with 12 conserved cysteine residues (Lai et al., 2008). It possesses a hydrophobic fusion loop, which, upon attachment to the host cell membrane, results in the fusion of the host and the viral membrane, forming endocytic vesicles (Lai et al., 2008). Inside endosomes, the acidic pH induces the dissociation of the dimers into monomers, which later acquire an irreversible trimeric conformation, thereby facilitating

the release of the nucleocapsid into the host cytoplasm (Allison et al., 1995; Bressanelli et al., 2004; Modis et al., 2004). The prM is a ~18 kDa protein (Markoff, 1989; Markoff et al., 1994; Rice et al., 1985). It is associated with the fusion loop of the E protein and prevents the nascent virions from undergoing premature fusion with the host cell membrane (Li et al., 2008; Lorenz et al., 2002; Yu et al., 2008). During the maturation of virions, it is cleaved by furin proteases into the pr and M in the lumen of the Golgi apparatus (Elshuber et al., 2003; Stadler et al., 1997). The acidic pH of the Golgi lumen keeps the prM peptide associated with the E protein until it is dissociated from the E protein upon exposure to a neutral extracellular environment (Li et al., 2008).

1.2.2 Non-structural proteins

NS1 is a 46-55 kDa multifunctional glycosylated protein (Wang et al., 2021). It is translocated to the ER lumen, where it undergoes glycosylation, leading to its dimerization (Xie et al., 2025). The dimeric NS1 interacts with the ER membrane and initiates the formation of the replication complex along with other non-structural proteins (Xie et al., 2025). Multimeric NS1 is secreted from the infected cell and is involved in the modulation of the immune responses (Flamand et al., 1999; Muller and Young, 2013). NS2A is a ~22 kDa membrane-associated protein (Wu et al., 2015). It transports the viral RNA and both structural and non-structural viral proteins to the site of virion assembly (Xie et al., 2019). NS2B is a ~14 kDa hydrophobic protein (Li et al., 2016). The NS2B binds with NS3, resulting in a functional serine protease that cleaves viral polyprotein into functional proteins (Li et al., 2016). The central region is hydrophilic, with its N-terminal (49-67 residues) forming a β-strand and facilitating the proper folding of the NS3, while the C-terminal, a β-hairpin region, forms a substrate binding domain (Luo et al., 2015; Zhang et al., 2016). The membrane-associated domain provides a scaffold for the replication complex and helps to anchor NS3 at the site of replication (Li et al., 2015b). NS3 is the second largest protein with a molecular weight of ~70 kDa (Yusof et al., 2000). Along with NS2B, it forms an active protease complex (Bessaud et al., 2006). Its C-terminal has helicase and

NTPase activity; helicase unwinds RNA while NTPase activity caps newly formed RNA (Luo et al., 2008; Wang et al., 2018). Along with NS2A, it supports the assembly and packaging of newly synthesized RNA (Liu et al., 2003). NS4A is a ~17 kDa protein, with a crucial role in the formation of the replication complex along with NS2A, NS2B and NS4B (Zou et al., 2015). NS4A forms membrane curvature, resulting in the formation of a scaffold for the replication complex (Teo and Chu, 2014). NS4B is a ~27 kDa protein (Zou et al., 2014). It augments the processivity of NS3 by enhancing its activity and is also involved in the dislodging of RNA from its helicase domain (Umareddy et al., 2006). It also acts as a bridge, linking NS1 to the replication complex (Youn et al., 2012). NS5 is the largest protein with a molecular weight of ~103 kDa (Tay et al., 2016). It has RNA-dependent RNA polymerase (RdRp) activity on its N-terminal motif, while methyltransferase activity is at the C-terminal end (Yap et al., 2007; Zhao et al., 2015). It also acts as an interferon antagonist (Lin et al., 2006).

1.3 Replication cycle of JEV

JEV binds to the host cell through specific interactions of glycoprotein E with host cell surface factors (Zhu et al., 2023). E protein has 3 domains: E-DI, E-DII and E-DIII (Wang et al., 2017b). Glycosylation of E-DI and the presence of Arg-Gly-Asp (RGD) motif in E-DIII suggest the probable interaction of N-glycans and RGD motif with lectins and integrins on the target cell surface (Fan et al., 2017; Shimojima et al., 2014). The presence of conserved basic residues in E-DI also acts as a binding site for glycosaminoglycans (GAGs) (Liu et al., 2015). After attachment, the virus enters the host cell through clathrin-dependent or clathrin-independent endocytosis (Pierson and Kielian, 2013). The endosomal acidification induces structural rearrangements in the E-M heterotetramers, leading to the dissociation of heterotetramers and formation of E homotrimer (Yun and Lee, 2018). This exposes the hydrophobic fusion loop of E-proteins, and pinches it partly into the outer leaflet of the host membrane. These structural changes in the E protein leads to the fusion of the virus and host membrane and release

of the nucleocapsid in the cytoplasm (Hu et al., 2021). After release, the viral genome is translated into two overlapping polyproteins in the endoplasmic reticulum (ER). Polyproteins are processed co- or post-translationally into mature functional, structural, and non-structural proteins by both viral and host proteases (Kumar et al., 2022). Replication of the viral genome occurs in a "replication complex" formed by non-structural proteins (Kumar et al., 2022). The positive-strand genomic RNA is transcribed into a negative-strand RNA, which then acts as a template to synthesize progeny positive-stranded genomes. Newly synthesised viral genome and C protein form a complex which is budded into the lumen of the ER as immature virions. Inside the lumen, prM and E are also incorporated (Konishi and Mason, 1993). Thereafter, immature virions are carried to the trans-Golgi network through the cellular secretory pathway (Leyssen et al., 2000). Due to the acidic environment in the trans-Golgi, immature virions undergo structural rearrangements, resulting in the exposure of the cleavage site of prM to the furin proteases (Yun and Lee, 2018). The cleavage of the prM protein into M protein results in the maturation of virions. Complete and partial mature virions are then budded into the extracellular environment via exocytosis (Figure 1.3) (Yun and Lee, 2018).

1.4 Replication-induced reprogramming of glycolysis by RNA viruses

Viruses lack metabolism and rely entirely on the host cells for their replication. They hijack the host cellular machinery to synthesize nucleotides for genome replication and lipids for viral membrane formation, facilitating their rapid multiplication in the host cell (Mayer et al., 2019b). As a result, virus replication imposes a significant energy burden on the host cell (Thaker et al., 2019a). Glycolysis is a much faster process to generate ATP than oxidative phosphorylation, despite producing fewer ATP per molecule of glucose (Epstein et al., 2014; Locasale and Cantley, 2011; Vander Heiden et al., 2009). Therefore, most viruses fulfil this excessive energy demand by instigating glycolysis in the host cell (Kavanagh Williamson et al., 2018; Kraut et al., 1986; Lee et al., 2020; Ritter et al., 2010). This enhanced glycolysis in the infected cells is supported by increased glucose uptake and overexpression

of key glycolytic genes (Bhatt et al., 2022b; Gong et al., 2022; Lee et al., 2020; Qian et al., 2022; Singh et al., 2020). Several host signaling pathways, such as PI3K/AKT and mTORC1/eIF4E/HIF-1α, are involved in the regulation of glycolysis by viruses. Inhibition of these pathways has been shown to significantly impede virus replication (Chi et al., 2018; Passalacqua et al., 2019).

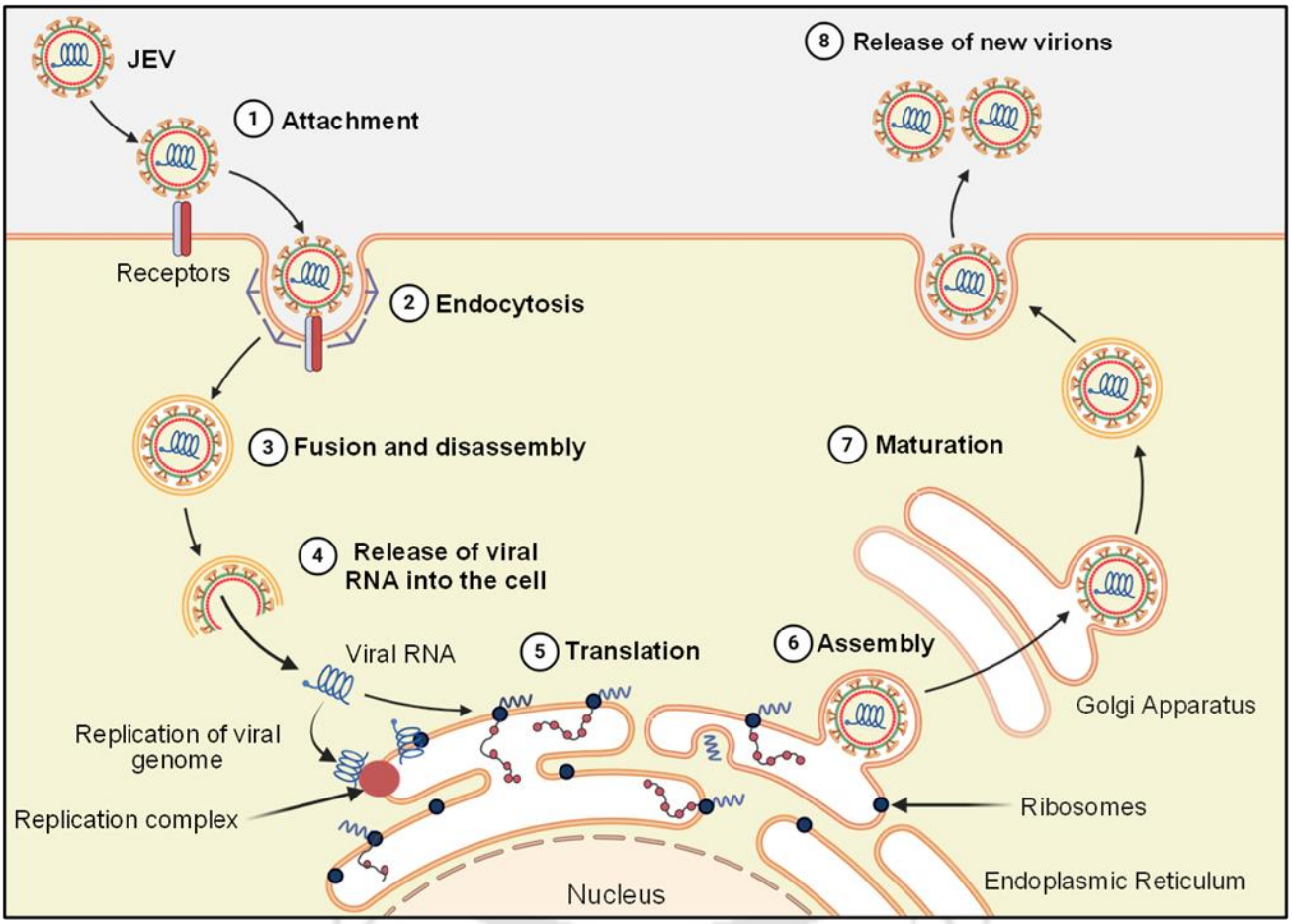

Figure 1.3 Diagrammatic representation of the life cycle of JEV.

Chapter 2
Review of Literature

Brief overview of the chapter

The chapter begins with an overview of the RNA virus-induced glycolysis reprogramming in the host cells, which is a phenomenon known as the Warburg effect. This metabolic shift supports viral replication by providing essential macromolecular precursors and energy. Further, the key components of glycolysis, including glucose transporters and glycolytic enzymes involved in the regulation of glycolysis by RNA viruses, have also been discussed. The chapter also elaborates the molecular mechanisms involved in the regulation of glycolysis by RNA viruses. Subsequently, a multifunctional glycolytic enzyme, pyruvate kinase M2 (PKM2), has been discussed in detail with a focus on regulation of its activity, role in glycolysis, and its non-metabolic functions. Diving more into detail, the chapter describes the regulation of immune responses by PKM2 and its role in viral pathogenesis. The chapter ends with the research gap in the understanding of the regulation of glycolysis in JEV-infected neuronal cells and the role of PKM2 in its replication.

2.1 The Warburg effect by RNA viruses

Cancer and RNA virus-infected cells exhibit the Warburg effect, resulting in enhanced glycolysis to produce reducing equivalents and precursors for macromolecules essential for replication (Bilz et al., 2018; Fontaine et al., 2015b; Heyward and Eisenhofer, 1985). The Warburg effect refers to the conversion of pyruvate, the end-product of glycolysis, into lactate in the presence of oxygen. It results in the accumulation of lactic acid, a decrease in glycolytic intermediates that contribute to the TCA cycle, and an enhanced uptake of glucose (Goyal and Rajala, 2023a). Several studies suggest that

RNA viruses modulate the central carbon metabolism of host cells by enhancing glycolysis. For example, viruses belonging to the genus *orthoflavivirus*, such as dengue virus, Zika virus, and West Nile virus (WNV), have been reported to induce glycolysis in the infected cells (Fontaine et al., 2015b; Goyal and Rajala, 2023a; Mingo-Casas et al., 2023). Other RNA viruses, such as the influenza virus, severe acute respiratory syndrome coronavirus 2 (SARS-CoV-2), hepatitis C virus (HCV), and respiratory syncytial virus (RSV), have also been shown to induce glycolysis in the infected cells (Guarnieri et al., 2023; Levy et al., 2016; Mazzoni et al., 1986; Ren et al., 2021a; Ripoli et al., 2010). The molecular mechanisms regulating glycolysis differ among these viruses, with each virus affecting distinct signaling pathways, modulating specific glycolytic enzymes, and inducing glucose uptake in to optimize their replication and meet metabolic needs in a specific host cell type.

2.2 Regulation of glycolytic enzymes by RNA viruses

RNA viruses have been shown to regulate the expression of essential regulatory enzymes of glycolysis, such as hexokinase (HK), phosphofructokinase (PFK), pyruvate kinase (PK), and lactate dehydrogenase (LDH). Hexokinase (HK) catalysis the rate-limiting first step of glycolysis, which is the phosphorylation of glucose to glucose-6-phosphate (Roberts and Miyamoto, 2015). Several RNA viruses, such as Newcastle disease virus (NDV), dengue virus, Zika virus and SARS-CoV-2, have been reported to upregulate HK2 expression to promote glycolysis in the infected cells (Bhatt et al., 2022b; Gong et al., 2022; Lee et al., 2020; Singh et al., 2020).

PFK, a glycolytic enzyme which is responsible for the breakdown of fructose-6-phosphate to fructose-1,6-bisphosphate, was regulated by coxsackievirus B3 (CVB3) (Qian et al., 2022). Similarly, PK**,** another critical enzyme in the glycolytic pathway, is targeted by RNA viruses such as CVB3, H1N1 influenza virus and SARS-CoV-2 (McElvaney et al., 2020a; Qian et al., 2022; Ren et al., 2021a).

Lactate dehydrogenase A (LDHA) is an enzyme that catalysis the last step of the pathway, which is the conversion of pyruvate (the end-product of glycolysis) into lactate**.** This conversion is

particularly significant in anaerobic conditions (or low oxygen), as it regenerates NAD+, mandatory for the maintenance of glycolysis (Pathria et al., 2018). Multiple studies have highlighted the role of LDHA in RNA virus infection. For example, metabolomics and transcriptomic analysis of H1N1 influenza A-infected A549 cells have revealed enhanced glycolysis, along with significant upregulation of HK2 and LDHA (Zhang et al., 2024b). Studies on porcine reproductive and respiratory syndrome virus (PRRSV) have reported that inhibition of LDHA using sodium oxamate reduces replication in Marc-145 cells (Zhang et al., 2023). Elevated LDH levels have also been observed in the mice infected with WNV and JEV (Argade and Banerjee, 1990). Therefore, glycolytic enzymes serve as critical regulators in the reprogramming of glycolytic flux by RNA viruses.

2.3 Molecular mechanisms regulating glycolysis during RNA virus infection

HIF is a protein consisting of two distinct subunits, HIF-1α and HIF-1β (Wang et al., 1995). HIF-1β is constitutively expressed, while HIF-1α, under normal conditions, undergoes rapid hydroxylation by prolyl hydroxylases (PHD) and is subsequently degraded through ubiquitin-mediated proteasomal pathways (Berra et al., 2003; Bruick and McKnight, 2001; Dayan et al., 2006; Hon et al., 2002; Matsuzawa and Yamamoto, 1975). However, under low oxygen conditions, hydroxylation is inhibited, and HIF-1α is translocated to the nucleus, regulating the expression of several genes, including glycolytic enzymes and GLUTs (Luo et al., 2011; Mathupala et al., 2001; Maxwell et al., 2001; Wheaton and Chandel, 2011). HIF-1α has been reported to be targeted by RNA viruses to promote their replication in the host cells. RNA viruses have been shown to activate the mitochondrial ROS-HIF-1α-mediated glycolytic pathway in the infected cells (Chen et al., 2023a; Zhang et al., 2024b). Virus infection often leads to mitochondrial damage, resulting in the increased production of ROS. Elevated ROS levels inhibit the hydroxylation of HIF-1α, resulting in its stabilization and accumulation in the infected cells. This, in turn, upregulates glycolytic flux to compensate for the energy deficit caused by mitochondrial dysfunction (Figure 2.1). This metabolic

shift towards glycolysis not only restores cellular energy balance but also supports virus replication and the release of progeny virions (Ren et al., 2021a; Zhang et al., 2024b). For example, HCV interacts with cellular mitochondria, resulting in the generation of ROS and an increase in HIF-1α expression. This activates glycolysis and enhances viral replication (Jung et al., 2016b). Similarly, it has been shown that NDV infection induces a transition from mitochondrial fusion to fission, instigating energy stress characterized by an imbalance in ATP, ADP, and AMP levels. This impairs mitochondria, which are then degraded by selective autophagy. NDV-induced mitophagy also results in the elimination of SIRT3. Consequently, the degradation of SIRT3 in damaged mitochondria elevates cellular mitochondrial ROS levels, stabilising HIF-1α and inducing the expression of its downstream targeted genes in NDV-infected cells, thereby shifting mitochondrial bioenergetic metabolism towards aerobic glycolysis (Gong et al., 2022).

AMPK regulates glucose, lipid, and protein metabolism in response to metabolic stress (Long and Zierath, 2006). Under low glucose conditions, AMPK promotes glucose uptake and glycolysis by enhancing the surface expression of GLUT1 and GLUT4 (Bratthauer, 1994; Wu et al., 2013). It plays a pivotal role in regulating the activity of FOXO (Forkhead box O) transcription factors, which maintain cellular redox balance and promote cell survival. FOXO proteins are activated by AMPK and regulate the expression of genes involved in antioxidant production and glucose metabolism (Greer et al., 2007). AMPK can also negatively regulate the Warburg effect and suppress tumor growth (Faubert et al., 2013). However, in the context of RNA virus infection, AMPK has been shown to negatively regulate glycolysis and inhibit virus replication (Singh et al., 2020).

AKT is a crucial protein associated with cellular energy sensing across a variety of cell types (Hung et al., 2017; Roberts et al., 2013). AKT enhances glycolysis by promoting the movement of GLUT1 to the cell surface, which increases glucose uptake, and by inducing the expression of glycolytic enzymes such as HK and PFK (Coloff et al., 2011). Under sufficient glucose conditions, AKT is activated and subsequently stimulates mTOR signaling to promote glucose metabolism and

protein synthesis (Paul et al., 1987). Several RNA viruses have been reported to regulate the AKT signaling pathway (Fan et al., 2024; Hajari et al., 2025; Lahon et al., 2021; Li et al., 2021a; Tang et al., 2023). Notably, increased phosphorylation of AKT has been observed following norovirus infection, indicating its critical role in virus replication. In particular, norovirus infection in RAW cells showed an increase in AKT phosphorylation, which in turn promoted glycolysis to support its replication. Interestingly, Inhibition of glycolysis by 2-DG suppressed AKT activation and reduced its infection significantly (Passalacqua et al., 2019). Multiple studies have shown that Zika virus infection in several human cell lines, including those derived from liver, neuroblastoma, neural progenitor, and embryonic kidney, depends on the activation of the AKT/mTORC signaling pathway. (Chan et al., 2018; Gratton et al., 2019; Holbrook, 2017; Kong et al., 2020). In all cellular models, the suppression of the mTOR or phosphatidylinositol 3-kinase PI3K/AKT pathways has negatively impacted its replication. Similarly, other RNA viruses, such as dengue virus and YFV, also depend on this pathway not only for their replication but also for the modulation of immune responses (Altenberg and Greulich, 2004; Carter et al., 2022; Chan et al., 2018; De Wied and De Kloet, 1987; Liang et al., 2016; Sahoo et al., 2020). Interestingly, avian reovirus (ARV) was also shown to elevate α-ketoglutarate levels by upregulating isocitrate dehydrogenase 3 subunit beta (IDH3β) and glutamate dehydrogenase (GDH), leading to the activation of mTORC1. Activated mTORC1 further increases eIF4E, boosting the translation of HIF-1α, which in turn promotes the expression of glycolytic enzymes, leading to enhanced glycolytic flux (Chi et al., 2018). All these studies suggest that RNA viruses can upregulate the glycolytic pathway by regulating PI3K/AKT signalling (Figure 2.1).

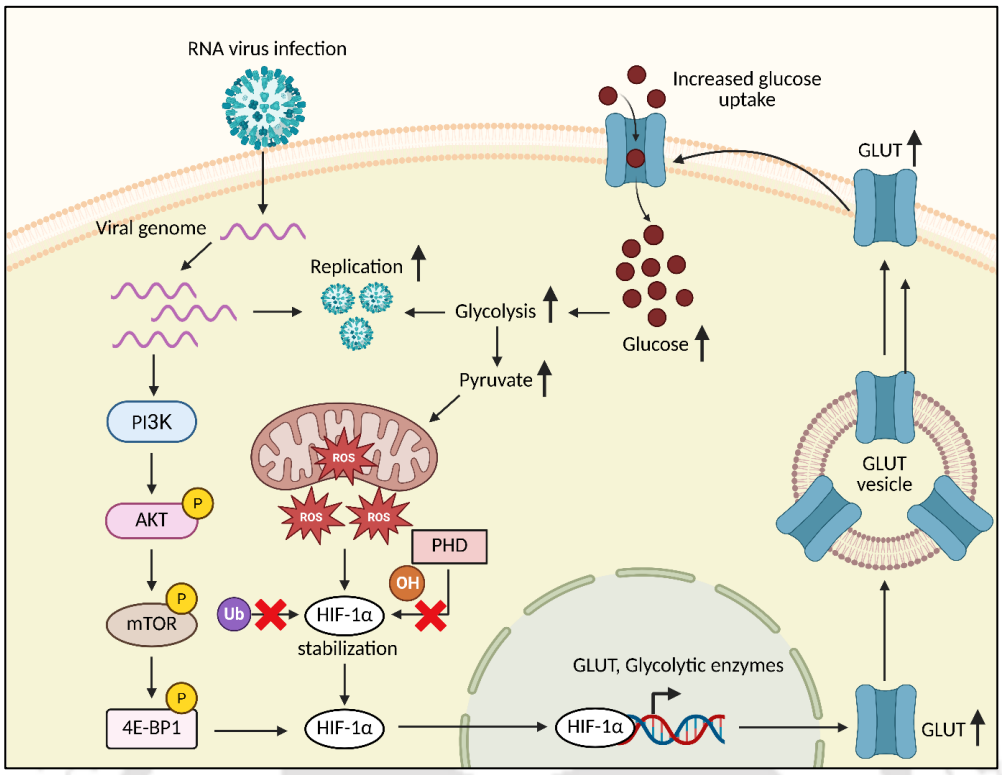

Figure 2.1 Schematic representation of glycolysis-mediated regulation of RNA virus infection. Virus infection activates the PI3K/AKT/mTOR pathway and induces mitochondrial ROS. Subsequently, ROS inhibits PHD, an enzyme responsible for the hydroxylation of HIF-1α, which prevents ubiquitin-mediated proteasomal degradation of HIF-1α, leading to the HIF-1α accumulation and its translocation to the nucleus. Inside the nucleus, it activates the expression of genes encoding glycolytic enzymes and GLUTs. Glycolytic enzymes facilitate enhanced glycolysis while GLUTs are translocated to the cell surface to provide more glucose for fuelling glycolysis, thereby supporting virus replication.

2.4 Therapeutic approaches against RNA viruses targeting glucose uptake and its metabolism

Different compounds have been tested for inhibiting the replication of RNA viruses by targeting glycolytic enzymes. 2-DG is the most widely used compound for inhibiting glycolysis. 2-DG targets HK, an important rate-limiting enzyme of the glycolytic pathway. Inhibition of glycolysis by using 2-DG has shown a significant reduction in the replication of several RNA viruses such as influenza A virus (H1N1), CVB3, dengue virus, WNV, etc. (Fontaine et al., 2015b; Mingo-Casas et al., 2023; Qian et al., 2022; Ren et al., 2021a). HK can also be inhibited by 3-bromopyruvate and Favipiravir, and

thus, can be a potent glycolytic inhibitor for inhibiting viral infection (Kohio and Adamson, 2013; Kulkarni and Padmanabhan, 2022). Another compound, oxamate, an inhibitor of LDH, is also a potential inhibitor of glycolysis and has been shown to impair the replication of influenza A, Senecavirus A (SVA) and dengue virus (Fontaine et al., 2015b; Li et al., 2023a; Ren et al., 2021a). Another potent compound that can inhibit glycolysis is Dichloroacetate (DCA), which targets the PDK4 enzyme. The inhibitory effect of DCA has been shown for different viruses such as H1N1, SVA and WNV (Li et al., 2023a; Mingo-Casas et al., 2023; Ren et al., 2021a). Apart from glycolytic enzyme inhibitors, GLUT inhibitors have also been used to inhibit glucose uptake as a strategy to suppress virus replication. Some examples of GLUT inhibitors are Indinavir, Fasentin, Dexamethasone and Niclosamide. Fasentin, which inhibits GLU1/4, have been shown to reduce the virus-induced glucose uptake in RSV-infected Hep-2 cells. Moreover, a significant reduction in ECAR, a key indicator of glycolytic flux, was also observed (Chen et al., 2023a). Dexamethasone reduces the expression of GLUT1 by inhibiting HIF-α (Clayton et al., 2023). It has been reported that treatment of human immunodeficiency virus (HIV) infected HC69 glial cells with dexamethasone reduces the abundance of viral transcripts in the infected cells (Shytaj et al., 2021). Niclosamide, an anti-helminthic drug, was shown to inhibit glucose uptake in NDV-infected DF-1 (Chicken embryo fibroblast) cells. Moreover, the expression of GLUT1 and HK was also found to be reduced in infected cells. However, whether these genes are direct targets of niclosamide is not known (Vashi et al., 2023). Thus, GLUT inhibitors can be a promising antiviral strategy by limiting glucose uptake and perturbing the virus-induced metabolic reprogramming.

Targeting the pathways that are involved in glucose metabolism can also be explored for developing interventions to inhibit viral infections. A study investigated the role of AMPK in Zika virus infection and reported a decreased active phosphorylated state of AMPK in infected cells. Treatment of Zika virus-infected HRvEC and HUVEC cells with AMPK agonist AICAR abolished infection and significantly reduced the titres in the infected cells. Similar results were observed when

Zika virus-infected HRvEC cells were treated with GSK621 (AMPKα-specific activator) (Singh et al., 2020). Rhinovirus has been shown to upregulate glucose uptake in infected cells in a PI3K-dependent manner. When rhinovirus-infected primary human fibroblasts and HeLa cells were treated with PI3K inhibitors, PP242 and LY294002, glucose uptake reverted to normal conditions (Gualdoni et al., 2018). RSV has been shown to upregulate glycolysis in infected cells by regulating HIF-1α expression. HIF-1α is the core transcription factor that regulates glycolysis and controls the expression of glucose transporters and glycolytic enzymes. RSV-infected HEp-2 cells showed activation of IR/PI3K/AKT signalling, which led to increased HIF-1α expression. Pharmacological inhibition of HIF-1α with PX-478 significantly reduced RSV infection *in vitro* and *in vivo*. Glucose uptake and glycolysis were also reduced by using BMS-754807, an insulin receptor (IR) inhibitor and LY294002, a PI3K inhibitor (Chen et al., 2023a).

Table 1: List of RNA viruses regulating different glycolytic enzymes along with signaling pathways involved.

S.No	Virus	signaling pathway	Glycolytic proteins	Viral protein	References
1.	Newcastle disease virus	HIF-1α	NA	NA	(Gong et al., 2022; Lan et al., 2010)
2.	Respiratory syncytial virus	PI3K/Akt, HIF-1α	HK1, HK2	M	(Chen et al., 2023a; Hu et al., 2023; Morris et al., 2020)
3.	Dengue virus	PI3K/Akt/mTOR	HK2, GAPDH	NS1	(Allonso et al., 2015; Fontaine et al., 2015b; Lahon et al., 2021; Lee et al., 2020)
4.	Human immunodeficiency virus	PI3K, HIF-1α	HK1	Vpr	(Deshmane et al., 2009; Kavanagh Williamson et al., 2018; Loisel-Meyer et al., 2012; Palmer et al., 2014; Rivas et al., 1997; Sorbara et al., 1996)
5.	Influenza A virus	mTOR/PI3K	HK2, PKM2, GAPDH, PFK PDK3, LDH GP1, FBP, ALD, TPI, PK	M1	(Mishra et al., 2020; Ren et al., 2021a; Ritter et al., 2010; Smallwood et al., 2017)

6.	Mayaro virus	NA	PFK	NA	(El-Bacha et al., 2004)
7.	SARS-CoV-2	HIF-1α	NA	NA	(Codo et al., 2020b; Rochowski et al., 2024)
8.	Murine norovirus	Akt	NA	NA	(Passalacqua et al., 2019)
9.	Coxsackievirus B3	PI3K/Akt, ERK1/2	HK2, PFKM, PKM2	NA	(Luo et al., 2002; Qian et al., 2022)
10.	West Nile virus	NA	HK2, HK3, PDK4	NS1	(Mingo-Casas et al., 2023; Wessel et al., 2021)
11.	Rhinovirus	PI3K	NA	NA	(Gualdoni et al., 2018)
12.	Senecavirus A	NA	HK2, PFKM, PKM, PGK1	NA	(Li et al., 2023a)
13.	Zika virus	PI3K/Akt/mTOR, AMPK, HIF-1α	HK1, HK2, GAPDH, LDH, TPI	NS4A, NS4B	(de Farias et al., 2025b; Liang et al., 2016; Singh et al., 2020)
14.	Porcine reproductive and respiratory syndrome virus	HIF-1α	HK2	nsp1β	(Pang et al., 2022; Zhang et al., 2023)
15.	Avian reovirus	HIF-1α	HK, PFK, TPI, PK	σA	(Chi et al., 2018; Hsu et al., 2023)
16.	Rous sarcoma virus	NA	HK, PFK, PK, LDH, G-6-P dehydrogenase	pp60src	(Presek et al., 1980; Salter et al., 1982; Singh et al., 1974a; Singh et al., 1974b)

Table 2: List of glycolytic inhibitors used against different RNA viruses.

S.No	Virus	Inhibitor	Target	References
1.	Influenza A virus	BEZ235 3- Bromopyruvate 2-DG Oxamate	PI3K/mTOR HK HK and GPI LDH	(Kleinehr et al., 2023; Kohio and Adamson, 2013; Ren et al., 2021a; Smallwood et al., 2017)
2.	Newcastle disease virus	Sodium oxamate Niclosamide	LDH Glycolysis	(Vashi et al., 2023)
3.	Coxsackievirus B3	2-DG Sodium citrate Shikonin	HK PFKM PKM2	(Qian et al., 2022; Thompson et al., 1987)
4.	West Nile virus	AL-429 Sodium oxamate 2-DG Dichloroacetate	Glycolysis LDH HK PDK4	(Mingo-Casas et al., 2023)

5.	Human immunodeficiency virus	Dexamethasone	Glycolysis	(Shytaj et al., 2021)
6.	Rhinovirus	2-DG PP242 LY294002	HK PI3K PI3K	(Gualdoni et al., 2018)
7.	Senecavirus A	2-DG Oxamate Dichloroacetate	HK LDH PDK4	(Li et al., 2023a)
8.	Dengue virus	2-DG Oxamate 6-Amino-Nicotinamide	HK LDH NADH biosynthesis	(Fontaine et al., 2015b; Ogire et al., 2024)
9.	Norovirus	2-DG	HK	(Passalacqua et al., 2019)
10.	Respiratory syncytial virus	PX-478 BMS-754807 LY294002 Fasentin	HIF-1α IR PI3K GLUT	(Chen et al., 2023a)
11.	SARS-CoV-2	2-DG	HK	(Bhatt et al., 2022b)
12.	Semliki forest virus	2-DG	HK	(Findlay and Ulaeto, 2015)
13.	Sindbi virus	Lonidamine Oxamate	HK LDH	(Findlay and Ulaeto, 2015)
14.	Zika virus	2-DG	HK	(Singh et al., 2020)

2.5 PKM2: A multi-functional glycolytic enzyme

PK is a crucial enzyme of the glycolytic pathway which catalysis the conversion of phosphoenolpyruvate to pyruvate while coupling ATP synthesis (Israelsen and Vander Heiden, 2015). It has four different isoforms: L, R, M1, and M2 (Gupta and Bamezai, 2010). L-isoform is mainly present in the liver, kidney, pancreas and intestine; R-isoform is present in RBCs; M1 is present in muscle, kidney and brain tissue, and M2 is present in the brain, lung, liver, kidney, heart, embryonic tissues and cancer cells (Lu, 2012). These isoforms are encoded by two genes: PKLR (which encodes the L and R isoforms) and PKM (which encodes the M1 and M2 isoforms) (Noguchi et al., 1986; Noguchi et al., 1987). PKM1 and PKM2 are produced by the alternate splicing of the same gene, PKM, at exon 9 and exon 10, respectively (Figure 2.2) (Noguchi et al., 1986; Takenaka et al., 1991). PKM2

can form a dimer or a tetramer, while PKM1 can only create a monomer. The dimeric and tetrameric forms of PKM2 perform distinct functions: the tetrameric form plays a catalytic role in glycolysis, while the dimeric form exhibits low catalytic activity and is involved in the biosynthesis of precursor biomolecules (Dong et al., 2016a). Dimeric PKM2 can localize to different cellular compartments, such as the ER and nucleus. In the nucleus, it activates the transcription of several genes, or it can associate with other transcription factors to regulate gene expression and inside the ER, it regulates the ER stress (Zhang et al., 2019). Dimeric PKM2 can bind to the outer mitochondrial membrane to regulate its function (Christofk et al., 2008a; Liang et al., 2017). Therefore, depending on its isomeric state, PKM2 can perform a range of different functions inside the cell.

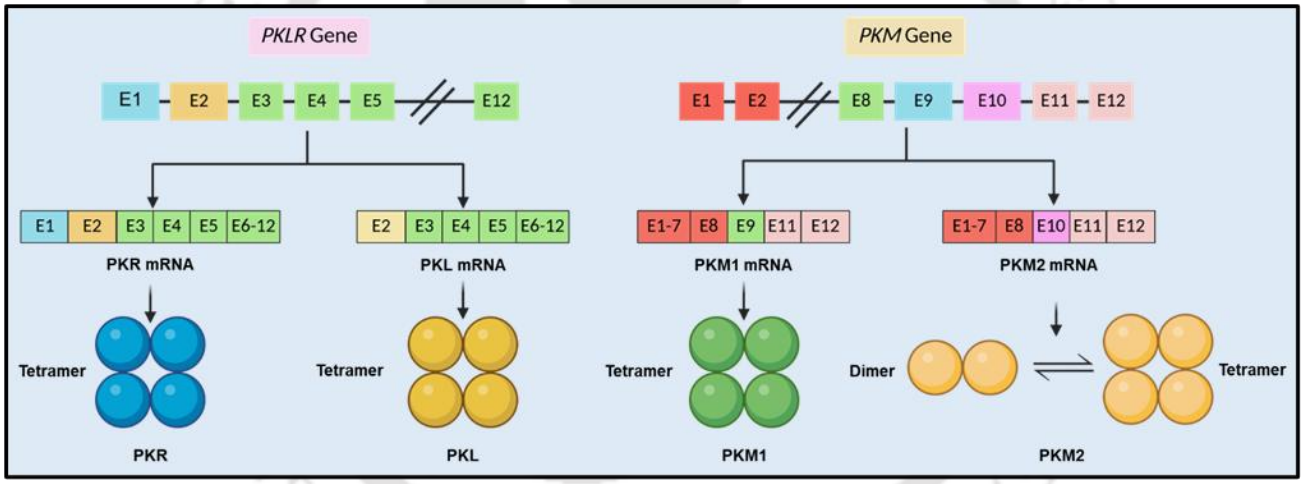

Figure 2.2 Schematic illustration of different isoforms of Pyruvate kinase encoded by the *PKLR* and *PKM* genes through alternative splicing

2.5.1 Regulatory mechanism of PKM2 expression

Several factors regulate PKM2 expression. As previously discussed, alternative splicing, performed by riboproteins (hnRNPL, hnRNP1, and hnRNP2), controls the transcription switch from PKM1 to PKM2 (Clower et al., 2010). Several non-coding RNAs, such as miR-138, miR-148a, miR-

152, miR-199a, miR-22, and let-7a, have been proposed to downregulate the expression of PKM2 by directly interacting with the UTRs of its mRNA transcript (Guo et al., 2017; Xu et al., 2015; Zhang et al., 2015). It has been shown in most cancer cells P13K/mTOR signaling pathway promotes PKM2 expression through HIF-1α-mediated expression of c-Myc (Iqbal et al., 2013; Sun et al., 2011). c-Myc upregulates PKM2 expression by inducing the expression of hnRNPs involved in alternative splicing (Deming, 1991; Iqbal et al., 2013; Mazurek, 2007; Sun et al., 2011). Peroxisome proliferator-activated receptor γ (PPARγ) and epidermal growth factor receptor (EGFR) also induce the expression of PKM2, as its promoter contains binding sites for PPARγ known as PPARγ response elements (PPRE) (Panasyuk et al., 2012). EGFR-mediated activation of NF-κβ via mono-ubiquitinylation of PKCε also activates PKM2 expression (Yang et al., 2012b).

2.5.2 Regulation of PKM2 activity

The existence of PKM2 in tetrameric and dimeric forms depends on allosteric regulation. Tetramers can exist in either the catalytically inactive T-state or active R-state, while dimeric PKM2 possess protein kinase activity (Chen et al., 2020b; Wang et al., 2015). Fructose-1,6-bisphosphate (FBP), a glycolytic intermediate, binds to the allosteric region of PKM2 and stabilizes its active tetrameric form (Jurica et al., 1998). Serine can also act as an allosteric activator of PKM2, stabilizing its tetrameric form (Chaneton et al., 2012). The binding of succinyl-5-aminoimidazole-4-carboxamide-1-ribose-5′-phosphate (SAICAR) induces the protein kinase activity of PKM2 (Keller et al., 2014). PKM2 activity is also regulated through several post-translational modifications. Phosphorylation of PKM2 at Tyr105 induces the conversion of tetrameric PKM2 into dimeric form by disrupting its interaction with FBP, thereby reducing pyruvate kinase activity (Hitosugi et al., 2009). Studies have reported that acetylation of PKM2 at Lys305 and Lys433 inhibits pyruvate kinase activity by disrupting its interaction with phosphoenolpyruvate. Phosphorylation of PKM2 by JNK1 at Thr365 enhances PKM2 activity (Iansante et al., 2015). Succinylation of PKM2 at K498 enhances its activity (Xiangyun

et al., 2017). Phenylalanine inhibits the pyruvate kinase activity of PKM2 by stabilizing its inactive tetrameric state (Morgan et al., 2013). Structural analogs of pyruvate, such as oxalate and malonate, have been shown to stabilize active R-state tetramers of PKM2 (Armilla, 1967). Thyroid hormone was also shown to inhibit the pyruvate kinase activity of PKM2 by stabilizing its inactive monomers (Morgan et al., 2013). In several cancers, ERK2, upon activation by EGFR, induces the translocation of PKM2 and promotes its protein kinase activity (Yang et al., 2012c; Yang et al., 2012d).

2.5.3 PKM2 and its association with glucose metabolism

The active tetrameric form of PKM2 acts as a glycolytic enzyme, while the dimeric form of PKM2 induces the accumulation of glycolytic intermediates through PPP and glycerol synthesis, which boosts the production of nucleotides and NADP (Anastasiou et al., 2011; Chen et al., 2014; Zahra et al., 2020). In the cancer cells, the balance between tetrameric and dimeric PKM2 is critical in determining the fate of glucose, whether it will be utilized for ATP production via oxidative decarboxylation or diverted towards biosynthesis of amino acids, lipids and nucleotides (Wu and Le, 2013). This ratio is controlled by oncogenes, tumor suppressor genes, and intermediate metabolites (Li et al., 2014; Zhang et al., 2019). At the time of rapid proliferation, cancer cells exhibit augmented levels of dimeric PKM2, promoting accumulation of glycolytic intermediates such as 3-phosphoglycerate, dihydroxyacetone phosphate and FBP (Li et al., 2014). These glycolytic intermediates are utilized to fuel the biosynthesis of amino acids, lipids and nucleotides (Li et al., 2014). When FBP reaches beyond a particular threshold level, cancer cells temporarily halt proliferation, and the low activity dimer then undergoes conformational change to form an active tetramer (Gupta et al., 2010). This allosteric conversion is triggered by activators like phenylalanine, serine, glycine, cysteine, alanine, thyroid hormone, growth hormone, intracellular ROS levels and FBP (Akhtar et al., 2009; Vander Heiden et al., 2009). This increases the active tetrameric form of PKM2 to enhance glucose metabolism, providing energy until these allosteric activators decline below

threshold levels (Akhtar et al., 2009; Vander Heiden et al., 2009). Additionally, when cancer cells are exposed to stress upon drug treatment, they overexpress HIF-1α, which increases PKM2 expression and promotes its tetramerization. This catalytically active PKM2 supports the TCA cycle and electron transport chain, helping to scavenge the ROS generated under stressed conditions (Yang et al., 2011). Studies have linked chromosomal segregation during mitosis to glucose metabolism in prostate cancer (Morgan et al., 2013). It was shown that CENPF, a microtubule-binding protein, regulates cancer metabolism through its effect on PKM2 phosphorylation. Upon silencing of CENPF, phosphorylation of PKM2 increased at Tyr105, inactivating its pyruvate kinase function, crucial for glycolysis (Shahid et al., 2018). In HCC cells, it was shown that HSP90/GSK-3β mediates phosphorylation of PKM2 at Thr328, induces its stabilisation, promoting glycolysis and inhibiting apoptosis (Xu et al., 2017).

2.5.4 Non-metabolic roles of PKM2

Apart from pyruvate kinase activity, PKM2 can act as a protein kinase and as a transcriptional co-activator. PKM2 translocates to the nucleus and phosphorylates histone proteins, and activates transcription of several genes. PKM2 is involved in instigating tumorigenesis through the activation of EGFR. Activated EGFR signaling promotes the nuclear localization of PKM2 by ERK2. Once PKM2 enters the nucleus, it interacts and phosphorylates β-catenin at Y333 (Yang et al., 2011). The PKM2-β-catenin complex is recruited to the promoter site of *CCND1* gene to phosphorylate H3 histone, leading to its separation from HDAC3. This results in the stimulation of cyclin D1 expression, promoting tumor cell proliferation and growth (Yang et al., 2011). Nuclear PKM2 can also act as a co-activator of β-catenin, which further promotes the expression of c-myc. C-myc induces upregulation of GLUT1, LDHA and PTB-dependent expression of PKM2; all these enzymes promote the Warburg effect in cancer cells (Yang et al., 2011). Upon EGFR activation, PKM2 can also directly phosphorylate H3 histone at T11, inducing the dissociation of HDAC3 from *CCDN1* and *MYC* promoter regions and acetylation of H3 histone at K9 (Yang et al., 2012c). This initiates the expression of cyclin D1, a key

regulator of cell-cycle progression, and c-MYC, a transcription factor that regulates the expression of glycolytic enzymes, thereby promoting the Warburg effect and tumorigenesis (Yang et al., 2012c). Nuclear PKM2 phosphorylates PAK2, preventing its ubiquitination and proteasomal degradation. This stabilizes PAK2, enhancing cell mobility and metastasis (Cheng et al., 2018). Dimeric nuclear PKM2 interacts with TGIF2 and promotes its ubiquitin-mediated proteasomal degradation (Hamabe et al., 2014). This results in exposing the *CDH1* promoter to HDAC3, which deacetylates H3 histone and suppresses the transcription of *CDH1*, thereby promoting metastasis and tumour progression (Hamabe et al., 2014). PKM2 can also directly bind to STAT3 at Tyr705, which subsequently activates transcription of MEK5 and HIF-1α (Cheng et al., 2018). PKM2 associates and phosphorylates Bub3 at Tyr207 during mitosis (Jiang et al., 2014a). Bub3 is a spindle checkpoint protein, and its phosphorylation by PKM2 is crucial for precise chromosomal segregation (Jiang et al., 2014a). Phosphorylation of PKM2 at Thr45 by Aurora B induces its binding to MLC2, resulting in its phosphorylation at Tyr118. Phosphorylated MLC2 associates with ROCK2, resulting in the phosphorylation of MLC2 at Ser15 by ROCK2, which is essential for inducing cytokinesis and cell division (Jiang et al., 2014b). This highlights the role of protein kinase activity of PKM2 in regulating cell-cycle progression in cancer cells. PKM2 also activates mTORC1 signaling by phosphorylating its inhibitor, AKT1S1 at Ser202/203, leading to inhibition of growth and autophagy in cancer cells (Chen et al., 2020b). Nuclear PKM2 associates with H2AX histone, inducing genome instability in cancer cells (Xia et al., 2017). PKM2 can regulate the tumor microenvironment by phosphorylating the SNAP-23 protein at Ser95, thereby inducing the release of exosomes. Additionally, in response to oxidative stress. PKM2 can translocate the outer membrane of mitochondria and phosphorylate BCL2 at Thr69, leading to its stabilization. This inhibits apoptosis induced during oxidative stress (Liang et al., 2017). Under hypoxic conditions, PKM2 interacts with JMJD5, which prevents its tetramerization, thereby promoting nuclear translocation and interaction with HIF-1α. This facilitates the binding of HIF-1α to the HRE and regulates the transcription of metabolic genes, such as PKM2, LDHA, ENO1,

and GLUT1 (Wang et al., 2014). Moreover, dimeric PKM2 also acts as a co-activator of HIF-1α, which, along with PHD3, induces the transcription of HIF-1α-regulated genes (Luo et al., 2011; Luo and Semenza, 2011).

2.5.5 PKM2-mediated regulation of immune responses

Research has demonstrated that PKM2 contributes to the regulation of immune cell metabolism by modulating the Warburg effect (Liu et al., 2021b). As previously described, dimeric PKM2 drives aerobic glycolysis while the active tetrameric form provides pyruvate for the TCA cycle (Zhang et al., 2019). LPS-activated macrophages have been shown to exhibit higher PKM2 expression, predominantly in its inactive monomeric or dimeric forms (Palsson-McDermott et al., 2015a; Shirai et al., 2016). The LPS-induced PKM2 translocates to the nucleus and associates with HIF-1α to form a complex. This complex directly binds to the promoter of the *IL-1β* gene and activates its transcription (Palsson-McDermott et al., 2015a). When activated macrophages were treated with DASA-58 and TEPP-46 to drive the conversion of dimeric PKM2 into its active tetrameric form, this abrogated the LPS-induced expression of IL-1β and other HIF-1α-regulated genes (Palsson-McDermott et al., 2015a). Moreover, PKM2 also regulates the expression of HMGB1, a potent pro-inflammatory cytokine in activated macrophages, through its interaction with HIF-1α. Moreover, the knockdown of PKM2 using specific shRNA or its inhibition by shikonin resulted in the reduced expression of HMGB1 and glycolytic-related genes (Bichler et al., 1989). In addition, in colorectal carcinoma cells treated with LPS, PKM2 was associated with the enhanced expression of proinflammatory cytokines (Shirai et al., 2016). It was shown that treatment with LPS induced the nuclear localization of PKM2, where it interacts with the promoter of STAT3, directly inducing its transcription. Moreover, nuclear localization of dimeric PKM2 in LPS-activated CAD macrophages phosphorylates and activates STAT3, which in turn boosts the expression of IL-1β and IL-6 (Shirai et al., 2016). When dimeric PKM2 was induced to convert into tetrameric conformation by treatment with ML265, it reduced its

nuclear translocation and phosphorylation of STAT3, which also led to a decrease in the expression of proinflammatory cytokines (Shirai et al., 2016). Inhibition of dimeric PKM2 by shikonin protected the mice from LPS-induced endotoxemia (Yang et al., 2014b). In agreement with these observations, PKM2 expression was upregulated in different inflammatory diseases, such as Crohn's disease (Tang et al., 2015). In line with this, mice suffering from TNBS-induced colitis also showed marked upregulation of PKM2 (Bertrand et al., 2015). Notably, proteomics analysis of synovial tissue from the arthritis patient also revealed that PKM2 was one of the 33 genes that were found to be upregulated (Li et al., 2013). PKM2 is also involved in the differentiation of Th17 cells through its interaction with STAT3, enhancing its activation and differentiation (Damasceno et al., 2020). Th17 cells produce IL-17, a proinflammatory cytokine and are involved in the development of several autoimmune diseases such as rheumatoid arthritis, diabetes mellitus, psoriasis, and multiple sclerosis. Moreover, studies have also revealed that PKM2 can drive macrophages to the M1 phenotype by regulating the expression of proinflammatory mediators (Shirai et al., 2016). Dendritic cells play an important role in inducing tumour-specific immune responses by presenting tumour-specific antigens on their surface (Armstrong et al., 1998; Huang et al., 1994). However, dendritic cells are mostly ineffective in the tumor microenvironment (Bennaceur et al., 2008). It was demonstrated that SOCS3, induced by cytokines and tumour-induced factors in DCs, interact directly with PKM2, leading to reduced ATP synthesis, which ultimately reduces the antigen-presenting ability of DCs (Zhang et al., 2010). Inflammatory diseases and cancer lead to the accumulation of lactate (Haas et al., 2015; Weyand et al., 2017). The lactate induces the expression of lactate transporter SLC5A12 in $CD4^+$ T cells, which, through PKM2/STAT3 signaling, promotes the expression of IL-17 and enhances fatty acid synthesis (Pucino et al., 2019). The glycolysis-inactive PKM2 was also shown to be involved in the manifestation of allergic airway disease by eliciting IL-1β signaling through STAT3 phosphorylation (van de Wetering et al., 2020). This suggests that PKM2 is a crucial target for treating inflammatory diseases due to its role in regulating the expression of proinflammatory cytokines.

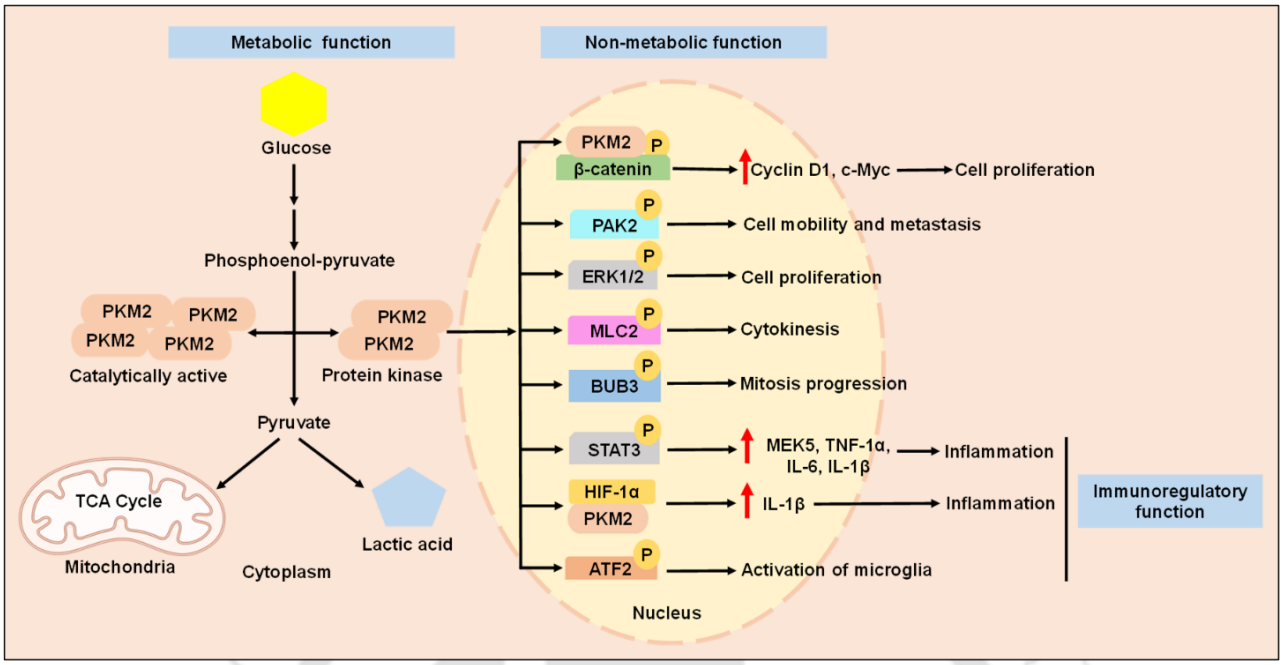

Figure 2.3 Schematic representation of metabolic, non-metabolic and immunoregulatory functions of PKM2.

2.5.6 PKM2 and viruses

Several viruses have been shown to enhance PKM2 expression to regulate their infection in the host cells (Qian et al., 2022). PKM2 was found to be involved in the replication and pathogenesis of HCV by interacting with NS5B, which is the viral RNA-dependent RNA polymerase, and its downregulation in HCV9B cells was shown to inhibit its replication (Wu et al., 2008). Studies in HBV have shown that activation of PKM2 upon treatment with TEPP-46 inhibits the expression of viral proteins (Wu et al., 2021). Contrary to this, HPV16 E7 oncoprotein induces the proliferation of cervical cancer cells by activating non-metabolic functions of PKM2 (Lee et al., 2021). PKM2 was also shown to interact with NS4A and NS5A, promoting their expression in the infected cells. Moreover, PKM2 was shown to promote CSFV replication by inducing mitophagy through the activation of the AMPK/mTOR pathway (Liu et al., 2024). Very recently, it was demonstrated that cyclophilin-A

restricts respiratory syncytial virus infection by inhibiting glycolysis through downregulation of PKM2 (Zhang et al., 2025a). In the case of dengue virus-infected huh cells, PKM2 was downregulated, while in U937 cells, dengue virus infection resulted in the upregulation of PKM2 (Martínez-Betancur and Martínez-Gutierrez, 2016; Pando-Robles et al., 2014). A549 cells infected with the H1N1 influenza virus have also shown higher expression of glycolytic enzymes, including PKM2 (Ren et al., 2021a). Studies in COVID-19 patients have shown that the increased expression of cytokines such as IL-6, IL-5, IL-1β and sTNFR1, along with the increased expression of cytosolic PKM2, phosphorylated PKM2 and HIF-1α (McElvaney et al., 2020a).

2.6 Knowledge gap and scope of current research

Glycolysis is the first stage in glucose metabolism, which is the breaking down of glucose into pyruvate while generating ATP and NADH. The glucose-6-phosphate produced in glycolysis can be utilized in the PPP to synthesize nucleotides. Similarly, pyruvate, which is the end-product of glycolysis, is converted to acetyl-CoA and is used in the synthesis of cholesterol and other lipids. As a central metabolic pathway, glycolysis is closely linked with other metabolic processes. Its regulation can directly or indirectly impact the overall metabolomics of a cell. Consequently, many viruses reprogram glycolysis to support their multiplication in the host cell. Multiple pathways, enzymes, and transcription factors are involved in this regulation. Inhibitors of key glycolytic enzymes have also been shown to be very effective in restricting the viral infection. However, no studies have clearly outlined the mechanisms regulating glycolysis during JEV infection in neuronal cells. Understanding the enzymes and factors regulating glycolysis during JEV infection could help in the development of virus-specific antiviral therapies. One of the glycolytic enzymes, Pyruvate kinase M2, not only plays a central role in glycolysis but also carries out several non-glycolytic functions, such as regulating immune response, particularly the expression of inflammatory cytokines. Most of the previous studies have concentrated on its glycolytic function in controlling viral infections. To date, there are no studies

which have specifically explored the non-metabolic role of PKM2 in JEV-infected neuronal cells. This work aims to elucidate the role of glycolysis in JEV infection, its regulatory mechanism, the role of the glycolytic enzyme PKM2 in JEV neuropathogenesis and its potential interaction with JEV NS1 protein.

2.7 Objectives

Based on the knowledge gap, we proposed the following objectives

1. To understand the regulation of glycolysis in Japanese encephalitis virus-infected neuronal cells
2. To understand the role of pyruvate kinase M2 in Japanese encephalitis virus replication
3. Investigating the interaction and cellular co-localization of pyruvate kinase M2 and the non-structural protein 1 of Japanese encephalitis virus

Chapter 3

Japanese encephalitis virus promotes its replication in neuronal cells by enhancing glycolysis via hypoxia-inducible factor-1α

Brief overview of the chapter

Glycolysis is one of the crucial metabolic pathways regulated by most RNA viruses. In this chapter, we investigated the regulation of glycolysis by JEV, with a specific focus on the regulation of glycolytic enzymes. We demonstrated that JEV replication induces a time-dependent increase in glycolysis, as evidenced by reduced glucose and elevated lactic acid levels in the supernatant of infected cells. Furthermore, treatment with glycolytic inhibitors, such as 2-DG and sodium oxamate, reduced virus replication. Moreover, supplementation with sodium pyruvate, an alternative energy source, and treatment with insulin promoted JEV replication, highlighting their positive role in enhancing JEV replication during metabolic stress. In addition, several glycolytic enzymes were found to be upregulated in JEV-infected cells. Later, we identified HIF-1α, a known transcription factor for controlling the expression of glycolytic genes, as a critical regulator of glycolysis during JEV infection, as its expression was upregulated following infection. Besides this, $CoCl_2$-induced stabilization of HIF-1α enhanced JEV replication, while its knockdown abrogated this effect in treated cells. At last, we concluded that JEV modulates host glucose metabolism via HIF-1α to facilitate its replication and highlighted glycolytic inhibitors as potential antivirals for JEV infection.

3.1 Introduction

Viruses rely on the host cellular metabolic machinery for their replication and propagation. Specifically, they stimulate anabolism to produce the macromolecules required for virion replication and assembly (Thaker et al., 2019a). Both DNA and RNA viruses reprogram many facets of host carbon metabolism, including enhanced glycolysis and the PPP to facilitate nucleotide synthesis, amino acid production, and lipid biosynthesis (Dunn et al., 2021; Krishnan et al., 2021a; Moreno et al., 2022; Thaker et al., 2019b; Vastag et al., 2011). Glucose is the primary energy source involved in cellular metabolism. Glycolysis and the tricarboxylic acid cycle are the two basic mechanisms involved in glucose metabolism (Bose et al., 2021). Many viruses have been shown to regulate glucose metabolism in the host cells by targeting glycolytic enzymes and GLUTs (Codo et al., 2020b; Gong et al., 2022; Kavanagh Williamson et al., 2018; Ritter et al., 2010; Zhang et al., 2023). Viruses often modulate pathways such as PI3K/Akt and mTORC1/eIF4E/HIF-1α to regulate the expression of glycolytic enzymes (Chi et al., 2018; Lahon et al., 2021; Li et al., 2021a; Liao et al., 2024). Viruses of the genus *Orthoflavivirus,* such as dengue virus, Zika virus and WNV, have been reported to depend on glycolysis for their replication (Fontaine et al., 2015b; Mingo-Casas et al., 2023; Singh et al., 2020). Dengue virus infection in human foreskin fibroblast cells was reported to induce glycolysis mediated by the overexpression of GLUT1 and HK2 (Fontaine et al., 2015b). Similarly, Zika virus replication in HUVEC cells promoted glycolysis, facilitated by enhanced expression of glycolytic genes such as GLUT1 and HK (Singh et al., 2020). LDH was also found to be upregulated in WNV and JEV-infected mice (Argade and Banerjee, 1990; Zhou et al., 2024). Additionally, another glycolytic enzyme, aldolase, was also shown to be upregulated upon JEV infection (Tien et al., 2014). Several past studies have shown that glycolysis inhibitors are very effective in reducing virus replication, indicating critical role of glycolysis in viral pathogenesis (Fontaine et al., 2015b; Mingo-Casas et al., 2023; Qian et al., 2022). HIF-1α is a critical regulator of glucose metabolism in several tumor types (Rankin and Giaccia, 2008). HIF-1 is a heterodimeric protein, comprising HIF-1α and HIF-1β (Erbel et al., 2003). Under normal conditions, HIF-1α is hydroxylated by prolyl hydroxylases, leading to pVHL (von-

Hippel-Lindau protein) dependent ubiquitination and proteasomal degradation of HIF-1α, while HIF-1β is constitutively expressed (Lee et al., 2004; Zhang et al., 2025b). Under hypoxic conditions, the hydroxylation of HIF-1α is inhibited, leading to its accumulation and translocation to the nucleus, where it regulates the transcription of glycolytic genes, especially glycolytic enzymes (Strowitzki et al., 2019). Enhanced expression of glycolytic enzymes promotes glycolysis, leading to increased glucose uptake. Several RNA viruses have been shown to induce glycolysis in the infected cells by stabilizing HIF-1α (Chen et al., 2023b; Jung et al., 2016a; Pang et al., 2022; Zhang et al., 2024c). A previous study has reported that JEV replication modulates glycolysis, the PPP and lipid metabolism in neuronal cells (Li et al., 2021b). However, the precise mechanism by which JEV modulates glycolysis remains elusive. Elucidating the specific glycolytic enzymes regulated during JEV replication, along with their mechanism of regulation, may offer critical avenues for JEV-specific antiviral therapy. The current study highlights HIF-1α as a critical metabolic checkpoint for regulating glucose metabolism in JEV-infected cells.

3.2 Materials and Methods

3.2.1 Cells and virus

The mouse neuroblastoma cells (Neuro-2a) and the baby hamster kidney cells (BHK-21) were obtained from the National Centre for Cell Sciences (NCCS), Pune, India. The cells were cultured in DMEM supplemented with 10% FBS and 1% antibiotic-antimycotic (GIBCO) cocktail at 37 °C in a humidified incubator with 5% CO2. The JEV strain SA14-14-2 (GenBank accession number JN604986) used in this study was procured from the Department of Health and Family Welfare, Government of Assam, India.

3.2.2 Chemical reagents and antibodies

2-DG, Tokyo Chemical Industry (TCI), Sodium oxamate, SIGMA (02751-5G), Sodium pyruvate, SIGMA (S8636-100ML), Recombinant human insulin, HIMEDIA (TCL035), Cobalt chloride (II) hexahydrate, SRL. The following primary and secondary antibodies were used: JEV NS1 (GeneTex, GTX633820), hexokinase 2 (Cell Signaling Technology, #2867), Glyceraldehyde-3-phosphate dehydrogenase (Cell Signaling Technology, #5174), Pyruvate kinase M1/M2 (Cell Signaling Technology, #3190), Pyruvate dehydrogenase (Cell Signaling Technology, #3205), Hypoxia inducing factor-1α (ABclonal, A7684), β-actin (Invitrogen, MA1-140).

3.2.3 Virus stock preparation

For the preparation of virus stock, BHK-21 cells were cultured in T75 culture flasks and allowed to reach 80 % confluency. The cells were infected with JEV at 0.01 MOI, and the virus was allowed to adsorb on the cell surface for 2 hours. After the adsorption, the infection media were substituted with fresh DMEM supplemented with 2% FBS. The infected cells were placed at 37 ˚C in a 5% CO_2 incubator for 72 hours for sufficient virus replication and release of progeny virions. Afterwards, the cells were lysed through successive freeze-thaw cycles for the release of entrapped virions. Cell debris was removed by centrifugation at 1,500 g for 5 minutes, and the clear supernatant containing JEV was collected and stored at -80 °C until further use.

3.2.4 Plaque assay

JEV titration was performed using plaque assay in BHK-21 cells. Cells were seeded 12 hours before infection in a 12-well plate. Virus dilution was prepared in plain DMEM, and the seeded cells were infected. After 2 hours of virus adsorption, the infection media were discarded, and the cells were washed with PBS, followed by overlaying with methylcellulose DMEM supplemented with 2% FBS. Plates were incubated for at least 72 hours at 37 ˚C in 5% CO_2 incubator. Overlay media was dispensed, and cells were fixed with chilled methanol for 10 minutes. After fixation, cells were stained with 1%

crystal violet and washed under tap water. The number of plaques was manually counted, and the titer was represented as plaque-forming units per milliliter of supernatant (PFU/mL).

3.2.5 Cell cytotoxicity assay

The cytotoxicity of the chemical compounds dissolved in milli-Q water was estimated using the MTT assay. Neuro-2a cells were seeded on a 96-well plate with a seeding density of 10^4 cells/well and allowed to attach overnight. The cells were then treated with different concentrations of the respective chemical compounds and incubated at 37 ˚C CO_2 incubator for different time points depending on the compound. Post-incubation cells were treated with 3-(4,5-dimethylthiazol-2-yl)-2,5-diphenyl tetrazolium bromide (MTT) and incubated in a 37 ˚C incubator for 3 hours. The MTT reagent was discarded, and DMSO was added to dissolve the formazan crystals. The plate was incubated in the dark for 10 minutes, following which absorbance was measured at 570 nm using Multiscan Go (Thermo Scientific, USA) microplate reader.

3.2.6 Western blotting

Estimation of targeted proteins in a whole cell lysate was performed using western blotting. Cells were lysed in RIPA buffer, and proteins were separated on a 12% SDS-PAGE gel. Separated proteins from the gel were transferred to a 0.4 µm nitrocellulose membrane. Thereafter, the membrane was blocked with 5% skim milk in TBST for 1 hour to prevent non-specific binding of antibodies. Following blocking, primary antibody dilution was prepared in 2% BSA (Bovine Serum Albumin) and incubated at 4 ˚C overnight. After incubation, the membrane was washed with TBST at least three times for 5 minutes each, followed by incubation with HRP-conjugated secondary antibody for 1 hour at room temperature. Protein bands were detected using ECL reagent (BioRad, USA) under chemiluminescence. Quantitative analysis was performed using ImageJ software.

3.2.7 Glucose and lactic acid estimation

Neuro-2a cells were cultured in a 6-well plate overnight. Cells were infected with 0.1 MOI JEV, and supernatant was collected at 24-, 48- and 72-hours post-infection for glucose and lactic acid estimation. The cell supernatant was first passed through a 0.22-µm filter and subsequently analyzed using HPLC (Shimadzu system) equipped with a refractive index detector. The concentrations of lactic acid and glucose were measured using a mobile phase of 5 millimolar sulfuric acid, eluted at a rate of 0.6 mL/min on an aminex 87H HPLC column (Bio-Rad) maintained at 50 °C.

3.2.8 Treatment with glycolytic inhibitors

To inhibit glycolysis, 2-DG and sodium oxamate were used. 2-DG is a structural analog of glucose that inhibits HK, an enzyme catalysing the first step of glycolysis, conversion of glucose to glucose-6-phosphate (Barban and Schulze, 1961). Sodium oxamate is a LDH inhibitor, an enzyme that catalyses the conversion of pyruvate to lactate (Kolesnik et al., 2023). Neuro-2a cells were cultured in a 6-well plate and infected with JEV at 0.1 MOI. Virus was allowed to adsorb for two hours, following which cells were maintained in DMEM with 2% FBS supplemented with 2-DG and sodium oxamate for 48 hours. Virus supernatant was collected for titration, and protein lysate was prepared for further analysis.

3.2.9 Nuclear and cytoplasmic fractionation

The Neuro-2a cells were cultured in a 6-well plate and infected with 0.1 MOI JEV. At 48 hours post-JEV infection, cells were collected and washed with PBS twice. The cells were lysed in lysis buffer containing PBS, 1 mM Dithiothreitol, protease inhibitor cocktail (TaKaRa), and 1% NP 40 for 10 minutes at room temperature. The lysate was centrifuged at 1000g at 4 ˚C for 10 minutes. The supernatant containing the cytoplasmic fraction was collected in separate tubes. The nuclear pellet was washed with PBS twice and lysed in 40 µl of 1% SDS. The collected fractions were then subjected to

SDS-PAGE followed by western blotting. GAPDH and H3 histone served as internal controls for fractionation.

3.2.10 Overexpression of HIF-1α

For the overexpression studies, $CoCl_2$, a well-known chemical inducer of hypoxia, was used to stabilize HIF-1α and promote its accumulation in the cells. Neuro-2a cells were pre-treated with $CoCl_2$ for 12 hours, and then the cells were infected with JEV at 0.1 MOI. 48 hours post-infection, protein lysate and supernatant were collected. Proteins were analyzed by western blotting, and the extracellular virus in the supernatant was quantified using the plaque assay.

3.2.11 knockdown studies

The knockdown of endogenous HIF-1α was achieved with a shRNA plasmid procured from Addgene (Catalog No. #21104), submitted by Connie Cepko's laboratory (Chen and Cepko, 2009). The HIF-1α RNAi target sequence: GGGTTGAAACTCAAGCAACTG. Scrambled shRNA plasmid gifted by Robert Friedlander was used as a negative control (Addgene #89912) (Yano et al., 2014). Neuro-2a cells were cultured overnight and transfected with 2 µg of plasmid with Lipofectamine 2000 (Invitrogen, USA) as per the manufacturer's protocol. Post-transfection cells were maintained in 2% DMEM supplemented with $CoCl_2$ (100 µM) for 12 hours. After which, cells were infected with 0.1 MOI JEV and maintained for 48 hours.

3.2.12 ROS quantification

Neuro-2a cells were seeded in a 35 mm dish and incubated at 37 ˚C in 5% CO_2 incubator for 12 hours. Thereafter, cells were infected with JEV at 0.1 MOI, and uninfected cells were kept as a negative control. At 24 and 48-hours post-infection, cells were collected in 500 µL PBS, treated with 10 µM of DCFH-DA dye and incubated in the dark at 37 ˚C for 30 min. The cells were then analyzed

using CytoFLEX flow cytometer (Beckman Coulter, USA). The cells treated with 100 µM of H_2O_2 were used as a positive control for the estimation of ROS. The FITC filter channel was used to record the emission intensity of DCFH-DA dye.

3.2.13 Statistical Analysis

All the results were shown as mean ± standard deviation. All the experiments were reproduced at least three times. Statistical tests were performed using GraphPad Prism software. The significance level among different groups was represented as *, **, ***, where * is for $P < 0.05$, ** for $P < 0.01$, and *** for $P < 0.001$. $P < 0.05$ was considered significant.

3.3 Results

3.3.1 JEV infection induces glycolysis in neurons.

To understand the role of glucose in virus replication, Neuro-2a cells were infected with JEV at 0.1 MOI. Increased acidification of supernatant was observed in infected cells compared to uninfected cells (Figure 3.1A). Supernatant from the infected cells was collected at different time intervals post-infection to quantify glucose and lactic acid in the supernatant. The glucose concentration in the supernatant of infected cells was found to be significantly lower compared to uninfected cells at 48- and 72-hours post-infection (Figure 3.1B). However, lactic acid concentration in the supernatant of infected cells increased significantly compared to uninfected cells at 48- and 72-hours post-infection (Figure 3.1C). To further investigate this correlation, the dependence of JEV infection on exogenous glucose was investigated by infecting the cells under low (5 mM), medium (10 mM) and high (25 mM) glucose conditions. We observed a gradual increase in NS1 expression with an increase in exogenous glucose. (Figure 3.1D and 3.1E). The extracellular viral particles in the supernatant were also titratedusing plaque assay (Figure 3.1F), which showed an increase in extracellular virus titer with increasing exogenous glucose (Figure 3.1G).

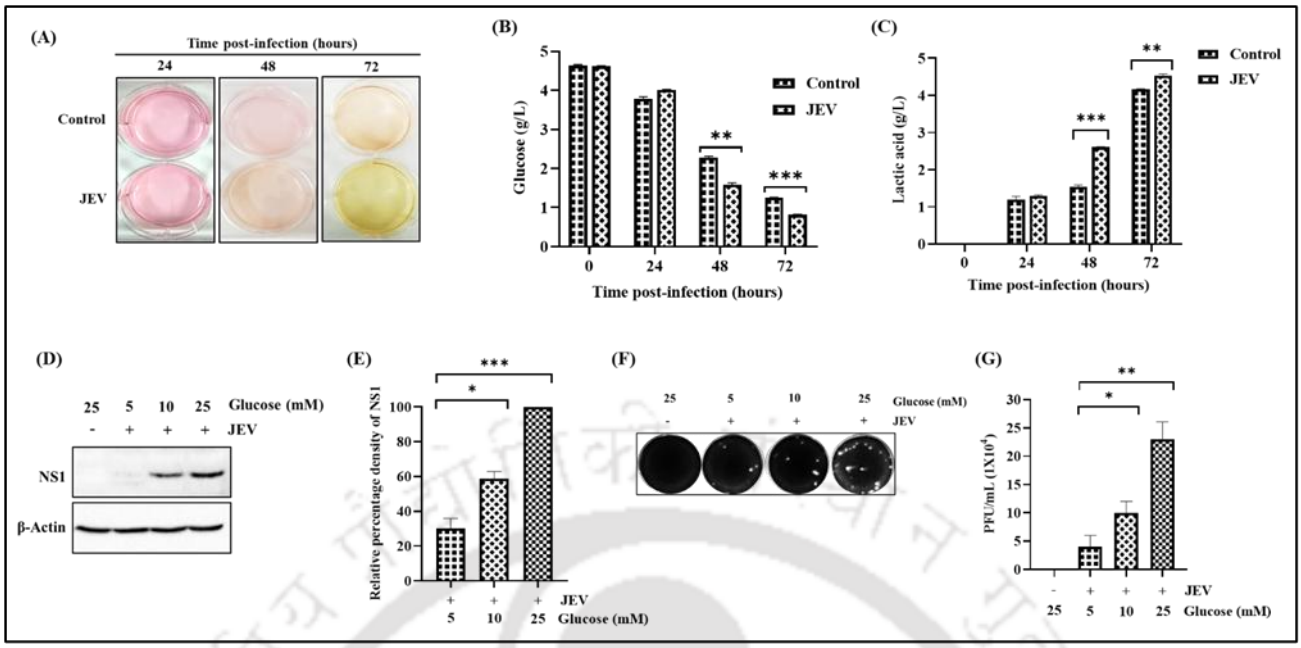

Figure 3.1 JEV infection induces glycolysis in neurons. Picture showing enhanced acidification of supernatant at 48 hours post-infection (A). Graph depicting glucose concentration in the supernatant at different time intervals post-infection compared to uninfected cells (B). Graph representing lactic acid concentration in the supernatant at different time intervals post-infection compared to uninfected cells (C). Immunoblot showing NS1 expression with increasing concentration of glucose in supernatant (D). Graph showing the relative percentage density of NS1 in infected cells under increasing glucose (E). Plaque image showing increased extracellular virus titer in the supernatant of infected cells treated with increasing glucose concentration (F). Graph showing enhanced virus titer with an increase in glucose concentration (G). Represented values are mean ± SD. Statistical analyses were performed using student's t-test for (B) and (C), while one-way ANOVA was used for (E) and (G).

3.3.2 Cytotoxicity assay and glycolysis inhibition upon treatment with glycolytic inhibitors

Cellular cytotoxicity of the glycolytic inhibitors was determined 48 hours post-treatment by MTT assay. Treatment with 5 mM of 2-DG resulted in about 82% cell viability (Figure 3.2A), whereas about 89% of the cells were viable upon treatment with 5 mM oxamate (Figure 3.2D). Next, we estimated the glucose and lactic acid concentration in the supernatant of the cells treated with 5 mM of glycolytic inhibitors. The glucose uptake by cells treated with 2-DG and oxamate was found to be

significantly lower than untreated cells (Figure 3.2B and 3.2E), and the lactic acid released in the supernatant was also significantly lower in the treated cells compared to the untreated cells (Figure 3.2C and 3.2F). These results indicated reduced glycolysis upon treatment with glycolytic inhibitors.

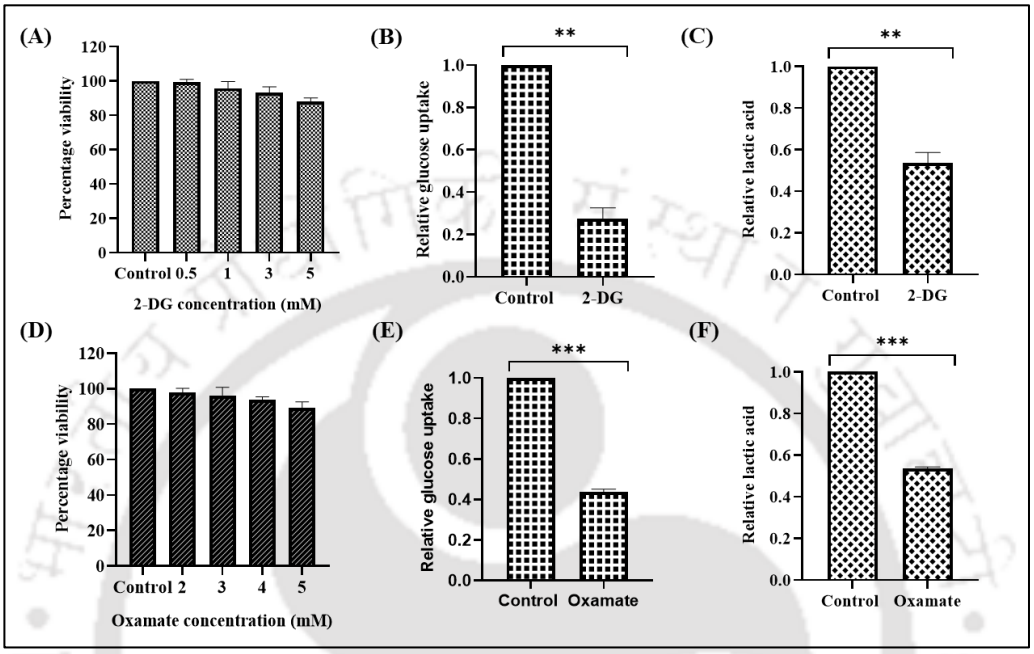

Figure 3.2 Cytotoxicity assay and glycolysis inhibition upon treatment with glycolytic inhibitors. Graph showing percentage cell viability upon treatment with different concentrations of 2-DG (A). Graph showing relative glucose uptake, 48 hours post-treatment with 2-DG (B). Graph showing lactic acid concentration in the supernatant, 48 hours post-treatment with 2-DG (C). Graph representing percentage cell viability upon treatment with different concentrations of oxamate (D). Graph showing relative glucose uptake, 48 hours post-treatment with oxamate (E). Graph showing lactic acid concentration in the supernatant, 48 hours post-treatment with oxamate (F). Represented values are mean ± SD. Statistical analyses were performed using student's t-test.

3.3.3 Treatment with glycolytic inhibitors impairs JEV replication.

To understand the reason behind increased glucose uptake and the role of glycolysis in the JEV-infected cells. We pharmacologically inhibited glycolysis by using 2-DG and sodium oxamate. Treatment with glycolytic inhibitors resulted in a significant reduction of JEV replication in a dose-dependent manner. Treatment with 5 mM 2-DG resulted in a 68% reduction in NS1 expression (Figure

3.3A and 3.3B) while treatment with 5 mM sodium oxamate resulted in about 56% reduction in NS1 expression (Figure 3.3C and 3.3D). Plaque assay was performed to examine viral particles in the supernatant of the infected cells (Figure 3.3E). Treatment with 2-DG resulted in about 85% reduction in virus titer, while treatment with sodium oxamate resulted in around 59% reduction in virus titer compared to untreated infected cells (Figure 3.3F).

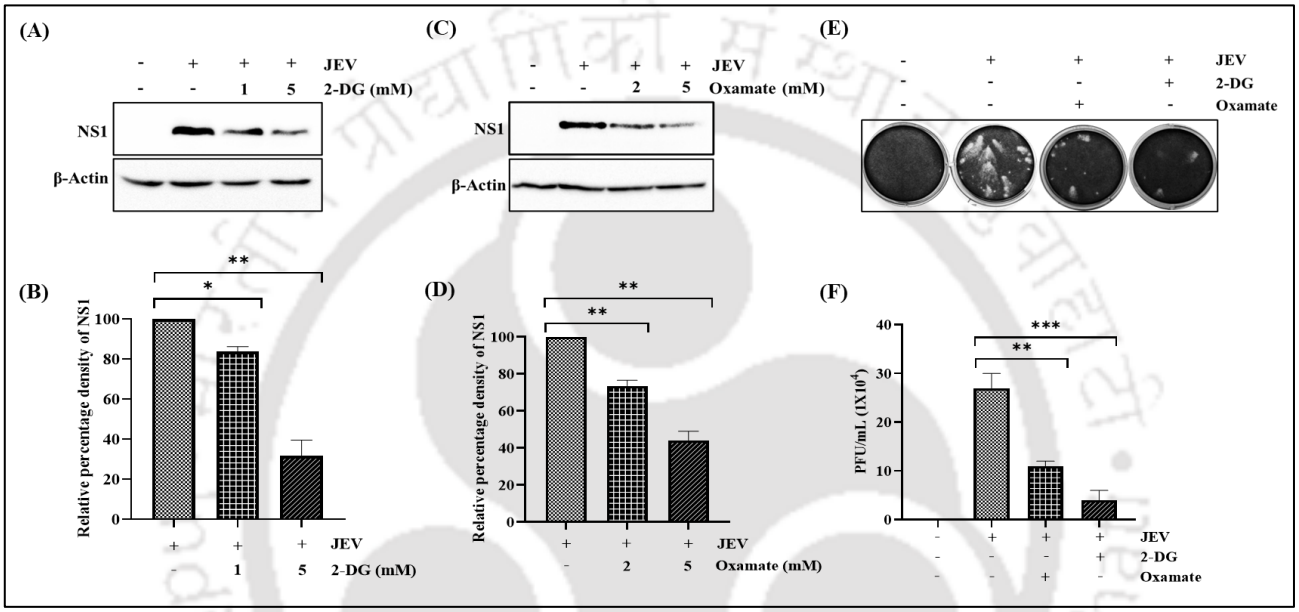

Figure 3.3 Treatment with glycolytic inhibitors inhibited JEV replication. Immunoblot representing NS1 protein expression upon treatment with 2-DG (A). Graph showing relative percentage density of NS1 protein upon treatment with 2-DG compared to untreated infected cells (B). Western blot depicting NS1 protein expression upon treatment with sodium oxamate (C). Graph showing relative percentage density of NS1 protein upon treatment with sodium oxamate compared to untreated infected cells (D). Picture showing a decrease in virus titer in the form of plaques upon treatment with glycolytic inhibitors (2-DG and sodium oxamate) compared to untreated infected cells (E). Graph showing extracellular viral titer in 2-DG and sodium oxamate-treated infected cells compared to untreated infected cells (F). Represented values are mean ± SD. Statistical analyses were performed using one-way ANOVA.

3.3.4 Treatment with sodium pyruvate enhances JEV replication.

Sodium pyruvate (SOP) is one of the intermediates in the glycolytic pathway. It acts as an alternate carbon source in addition to glucose. Since JEV infection leads to enhanced glycolysis to support the growing energy demand required to facilitate its replication. Therefore, we hypothesised that this high energy demand could be met by utilizing sodium pyruvate as an alternate energy source. Firstly, the percentage cell viability of cells treated with different concentrations of SOP for 48 hours was determined using the MTT assay. Treatment up to 5 mM of SOP did not affect the cell viability (Figure 3.4A). Next, to test the effect of SOP on JEV replication, JEV-infected cells were treated with 5 mM SOP in addition to the basal level already present in high glucose culture media, followed by immunoblotting to quantify NS1. Treatment with 5 mM SOP resulted in a significant increase in NS1 expression compared to untreated infected cells (Figure 3.4B and 3.4C). Extracellular virus titer was also examined (Figure 3.4D), which showed up to 68% increase in JEV titer upon treatment with SOP compared to untreated infected cells (Figure 3.4E).

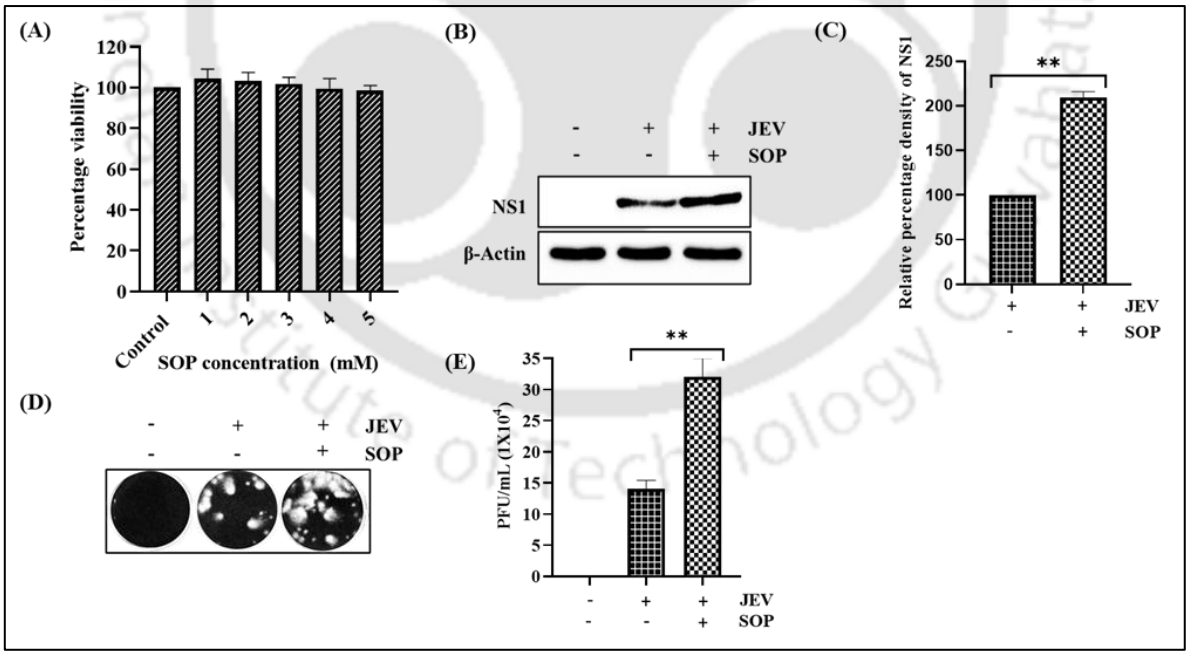

Figure 3.4 Treatment with sodium pyruvate enhances JEV replication. Graph representing percentage cell viability upon treatment with different concentrations of SOP (A). Immunoblot picture showing NS1 expression upon treatment with SOP (B). Graph representing relative percentage densitometric quantification of NS1 upon treatment with SOP compared to untreated infected cells (C). Plaque image

showing enhanced extracellular viral titer upon SOP treatment (D). Graph depicting virus titer in the supernatant collected from infected cells upon SOP treatment compared to untreated infected cells (E). Sodium pyruvate is represented as SOP. Represented values are mean ± SD. Statistical analyses were performed using student's t-test.

3.3.5 Treatment with insulin positively modulates JEV replication.

Neuro-2a cells were treated with 100 nM insulin for 6 hours, and glucose uptake was estimated 48 hours post-treatment. Treatment with insulin resulted in a 2.7-fold increase in glucose uptake relative to untreated cells (Figure 3.5A). To check the effect of insulin on JEV replication, infected cells were treated with 10 nM and 100 nM of insulin for the same duration, followed by western blot analysis. In the 100 nM insulin-treated cells, there was a significant increase in NS1 expression compared to untreated infected cells (Figure 3.5B and 3.5C). Extracellular virus titer was also quantified (Figure 3.5D), and about a 71% increase in virus titer was observed upon treatment with 100 nM insulin compared to untreated infected cells. However, there was no significant difference in JEV titer upon treatment with 10 nM of insulin (Figure 3.5E).

3.3.6 Modulation of glycolytic enzymes and HIF-1α upon JEV replication.

To further understand the role of glycolysis in JEV replication, the expression of key glycolytic enzymes at different time intervals post-infection was analyzed. We observed that there was a significant increase in the expression of HK2, PKM and PDH at 24- and 48-hour post-infection. However, there was no change in the expression of GAPDH (Figure 3.6A and 3.6B). To understand the mechanism of regulation of glycolysis in JEV-infected neuronal cells, the expression of HIF-1α was analyzed at 24-, 48- and 72-hours post-infection. The expression of HIF-1α was enhanced significantly in JEV-infected cells at 24- and 48-hour post-infection. There was no change in the expression of HIF-1α at 72 hours post-infection (Figure 3.6C and 3.6D). We also observed an increase in the nuclear localization of HIF-1α in JEV-infected cells compared to uninfected control (Figure 3.6E

and 3.6F).

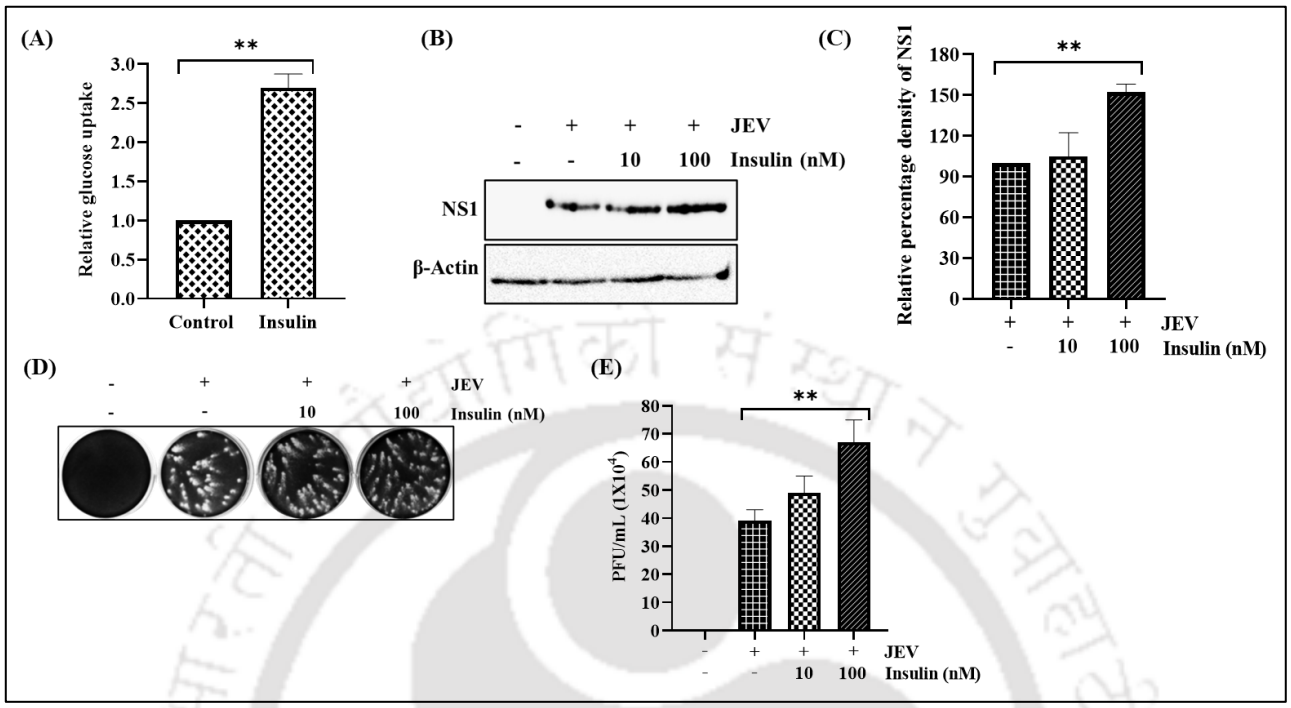

Figure 3.5 Treatment with insulin positively modulates JEV replication. Graph showing relative glucose uptake upon treatment with 100 nM for 6 hours (A). Immunoblot picture showing NS1 expression upon treatment with insulin (B). Graph representing the relative percentage density of NS1 upon treatment with insulin compared to untreated infected cells (C). Plaque image showing extracellular viral titer upon insulin treatment (D). Graph depicting virus titer in the supernatant collected from infected cells upon insulin treatment compared to untreated infected cells (E). Represented values are mean ± SD. Statistical analyses were performed using one-way ANOVA. $P < 0.05$ (*), $P < 0.01$ (**), and $P < 0.001$ (***) were considered significant.

3.3.7 $CoCl_2$-induced stabilization of HIF-1α promotes JEV replication.

To assess the cytotoxicity of $CoCl_2$, cells were pre-treated with varying concentrations of $CoCl_2$ for 12 hours, followed by replacement with fresh media. After 48 hours, the MTT assay was performed. Approximately 75-80 % of the cell viability was observed at 150 µM of $CoCl_2$ (Figure 3.7A). Therefore, we used 100 µM of $CoCl_2$ to achieve maximum viable cells. Next, to understand the role of HIF-1α, its stabilization was induced in the Neuro-2a cells by pre-treating the cells with $CoCl_2$ for

12hours. Treatment with 100 µM and 200 µM of $CoCl_2$ significantly increased the expression of HIF-1α compared to untreated control (Figure 3.7B). Neuro-2a cells were pre-treated with 100 µM of $CoCl_2$ for 12 hours, followed by JEV infection for 48 hours. This resulted in a significant increase in NS1 expression compared to untreated infected cells (Figure 3.7C and 3.7D).

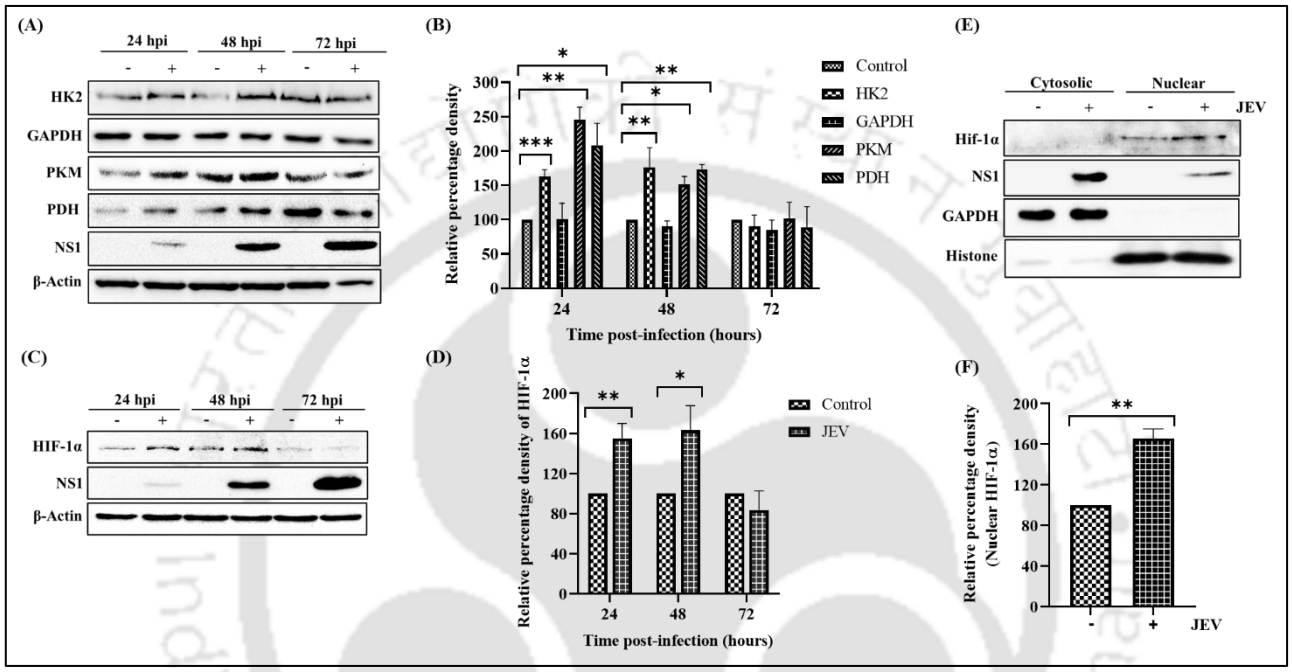

Figure 3.6 Modulation of glycolytic enzymes and HIF-1α upon JEV replication. Blot showing expression of different glycolytic enzymes at different time intervals post-infection (A). Relative percentage densitometric quantification of different glycolytic enzymes at different time points post-infection (B). Immunoblot showing time-dependent expression of HIF-1α (C). Graph depicting relative percentage density of HIF-1α expression at different time intervals post-infection (D). Immunoblot representing nuclear HIF-1α expression in uninfected and JEV-infected cells (E). Graph showing relative percentage density of nuclear HIF-1α in infected cells compared to uninfected cells (F). Represented values are mean ± SD. Statistical analyses were performed using two-way ANOVA for (B) and (D), while the student's t-test was used for (F).

3.3.8 HIF-1α knockdown abrogated the effect of $CoCl_2$ on JEV replication.

To determine whether the effect of $CoCl_2$ on JEV replication was specifically mediated by HIF-

1α, cells treated with $CoCl_2$ were transfected with HIF-1α-specific shRNA. Treatment with HIF-1α-specific shRNA significantly reduced HIF-1α expression in $CoCl_2$ treated cells (Figure 3.8A and 3.8B). When cells transfected with HIF-1α-specific shRNA were treated with $CoCl_2$, there was no difference in the NS1 expression compared to untreated infected cells. However, compared to scrambled shRNA-transfected and CoCl2-treated cells, NS1 expression was significantly reduced in cells transfected with HIF-1α shRNA along with $CoCl_2$ treatment (Figure 3.8A and 3.8C). Extracellular virus titer also did not show any significant difference. Nevertheless, there was a significant reduction in JEV titer upon HIF-1α downregulation compared to the cells treated with $CoCl_2$ and transfected with scrambled shRNA (Figure 3.8D and 3.8E). Moreover, knockdown of HIF-1α alone without $CoCl_2$ treatment resulted in a 66% reduction in NS1 expression level (Figure 3.8F and 3.8G) and a 54% reduction in virus titer (Figure 3.8H).

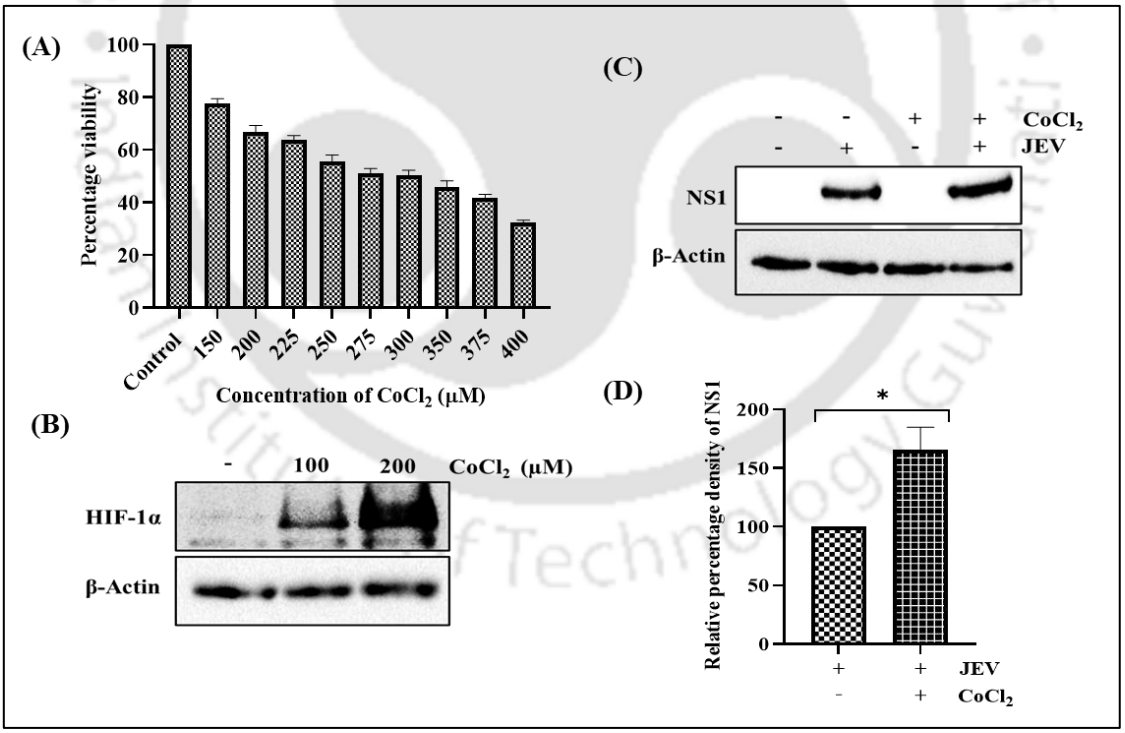

Figure 3.7 $CoCl_2$-induced stabilization of HIF-1α promotes JEV replication. Graph showing percentage cell viability upon treatment with different concentrations of $CoCl_2$ (A). Immunoblot showing CoCl2-mediated stabilization of HIF-1α (B). Immunoblot representing enhanced NS1

expression upon pre-treatment with 100 µM $CoCl_2$ compared to untreated infected cells (C). Graph depicting relative percentage density of NS1 upon $CoCl_2$ pre-treatment compared to untreated infected cells (D). Represented values are mean ± SD. Statistical analysis was performed using a student's t-test.

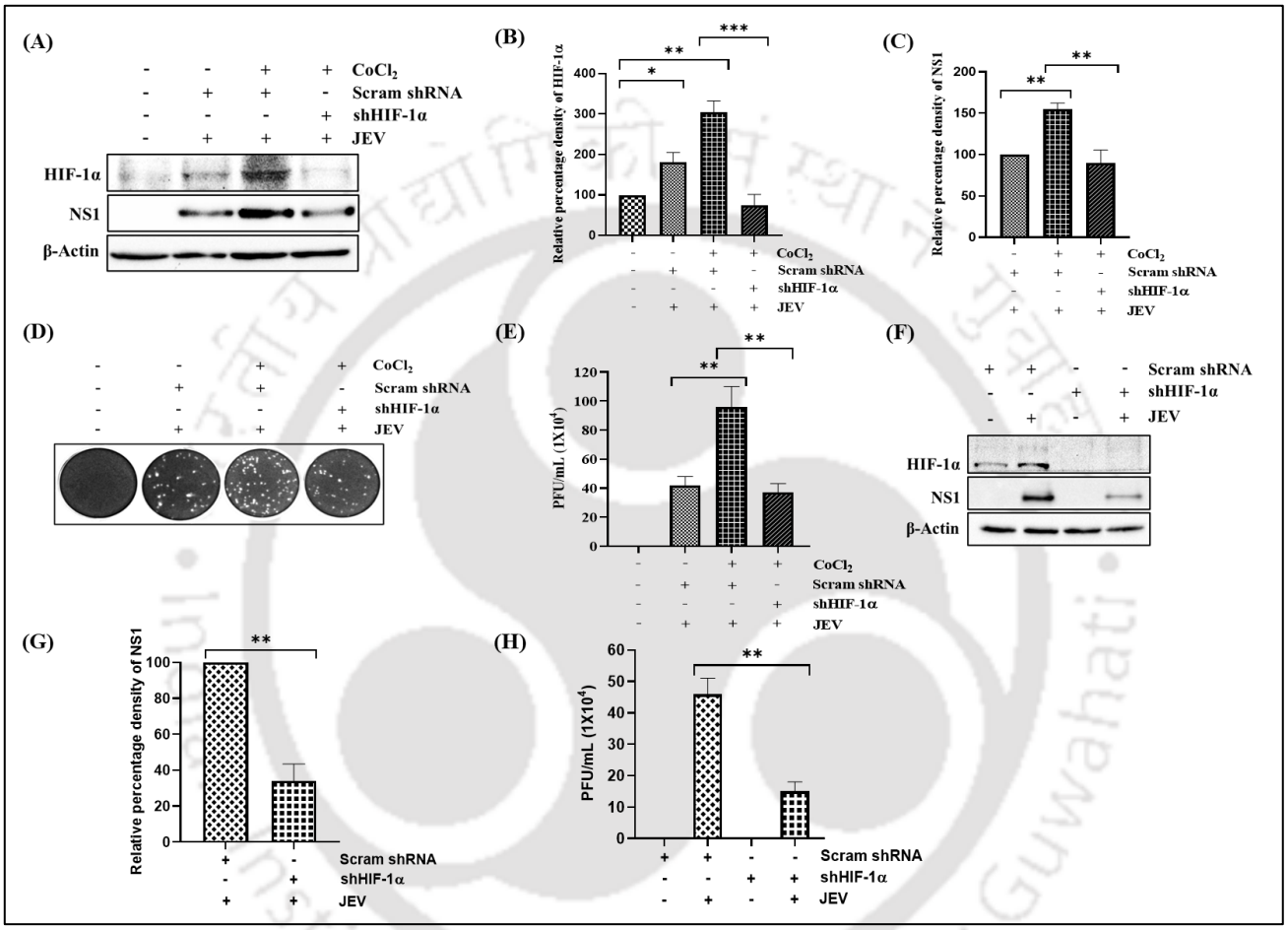

Figure 3.8 HIF-1α knockdown abrogated the effect of $CoCl_2$ on JEV replication. Immunoblot image showing NS1 expression upon transfection with HIF-1α-specific shRNA in $CoCl_2$ treated cells (A). Graph of relative percentage density of HIF-1α upon its knockdown in $CoCl_2$ treated infected cells compared to scrambled shRNA-transfected controls (B). Graph of relative percentage density of NS1 in HIF-1α knockdown $CoCl_2$-treated infected cells compared to scrambled shRNA-transfected controls (C). Plaque picture showing reduction in extracellular virus titer upon knockdown of HIF-1α in $CoCl_2$ treated infected cells (D). Graph showing virus titer in the supernatant collected from HIF-1α knockdown, $CoCl_2$ treated infected cells compared to scrambled shRNA-transfected controls (E). Immunoblot showing reduction in NS1 expression upon HIF-1α knockdown without $CoCl_2$ treatment

(F). Graph showing relative percentage density of NS1 upon HIF-1α knockdown (G). Graph showing reduction in virus titer in HIF-1α knockdown cells (H). Represented values are mean ± SD. Statistical analyses were performed using one-way ANOVA.

3.3.9 JEV infection induces ROS

To understand the mechanism by which HIF-1α expression is upregulated in JEV-infected Neuro-2a cells, we estimated the ROS production in JEV-infected Neuro-2a cells at 24-hour and 48-hours post-infection (Figure 3.9A and 3.9C). We observed a significant increase in ROS intensity at both 24-hours and 48-hours post-infection compared to the uninfected control (Figure 3.9B and 3.9D).

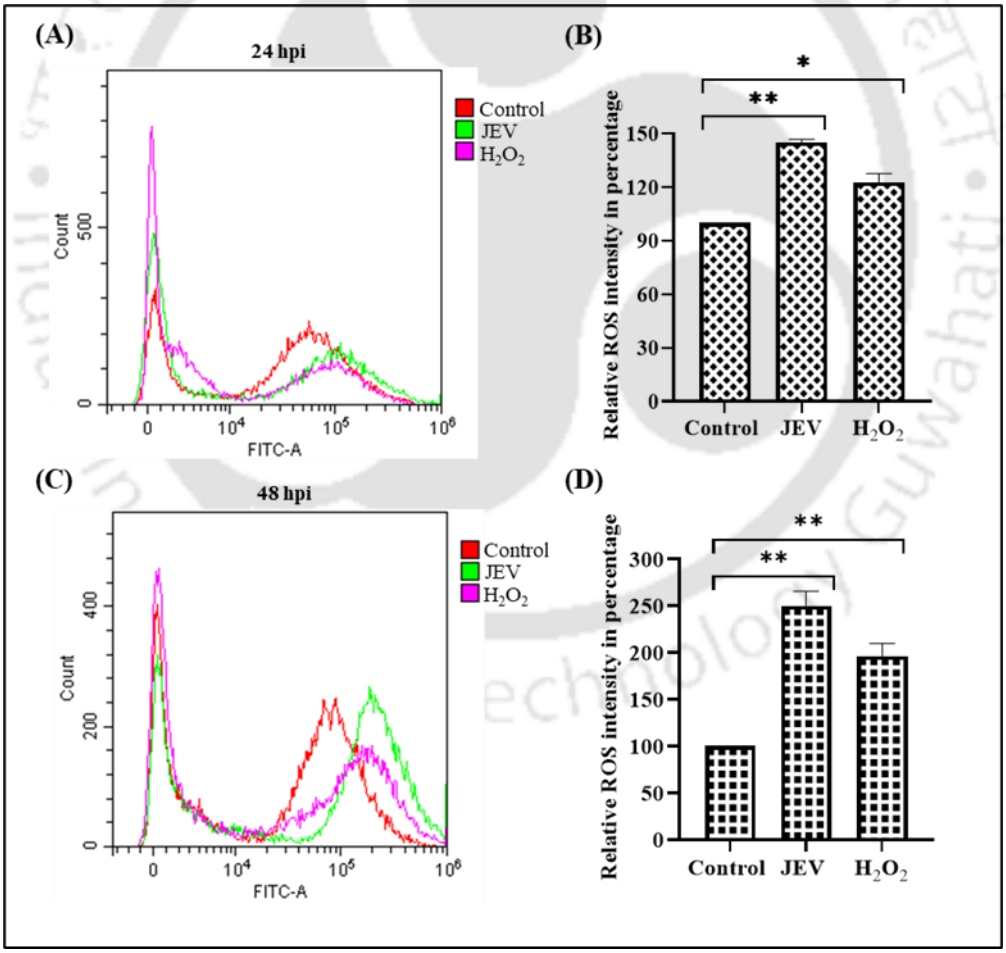

Figure 3.9 JEV infection induces ROS. Flow cytometric analysis of ROS 24-hours post-infection in JEV-infected, control and H_2O_2 treated cells (A). Graph showing relative percentage ROS intensity 24-

hours post-infection in JEV-infected, control and H_2O_2 treated cells (B). Flow cytometric analysis of ROS, 48-hours post-infection in JEV-infected, control and H_2O_2 treated cells (C). Graph showing relative percentage ROS intensity 48-hours post-infection in JEV-infected, control and H_2O_2 treated cells (D).

3.4 Discussion

Virus-infected cells synthesize additional nucleotides for their replication, lipids for their membrane formation, and genome-encoded proteins to support structural components of budding virions (Mayer et al., 2019a). Since glycolysis is a much faster process to generate ATP from a glucose molecule than oxidative phosphorylation (Shiratori et al., 2019). Perhaps, when energy demands are very high, most of the RNA viruses exploit glycolysis in the host cells to meet their energy requirements (Jaquet et al., 2024; Li et al., 2023b; Passalacqua et al., 2019; Qian et al., 2022). In the current study, we showed that JEV infection induces glycolysis in the Neuro-2a cells. This was demonstrated by time-dependent quantification of glucose and lactic acid in the supernatant of JEV-infected cells, which revealed lower glucose levels and higher lactic acid levels in the supernatant of the infected cells compared to the uninfected cells. Also, increased glucose concentration enhanced JEV replication. This was similar to other viruses belonging to the same genus, *Orthoflavivirus,* such as dengue virus, Zika virus and WNV, which have been shown to instigate glycolysis in the host cells (Fontaine et al., 2015b; Mingo-Casas et al., 2023; Rothan et al., 2019). Similar results were reported in the context of SARS-CoV-2 infection, where enhanced glycolysis supports the high energy demands of virus-producing cells (Krishnan et al., 2021b). Studies on HIV have also shown that glycolysis was enhanced in CD4+ T cells and monocytes (Datta et al., 2016; Hegedus et al., 2014). To show that glycolysis is essential for JEV replication, we inhibited glycolysis by treating cells with 2-DG and sodium oxamate. 2-DG and sodium oxamate are widely used pharmacological inhibitors of glycolysis. 2-DG inhibits glycolysis by targeting HK, while sodium oxamate inhibits glycolysis by targeting LDH. Treatment with glycolysis inhibitors reduced JEV replication significantly. The reduction in JEV

replication was much greater in 2-DG treated since it inhibits the first rate-limiting step of glycolysis. Previously, 2-DG was also shown to reduce the replication of the influenza virus, dengue virus and West Nile virus (Fontaine et al., 2015a; Mingo-Casas et al., 2023; Zhang et al., 2024c). Similarly, sodium oxamate was also shown to inhibit the replication of the influenza virus and the dengue virus (Fontaine et al., 2015a; Ren et al., 2021b).

Sodium pyruvate is very crucial under limiting glucose conditions when cellular energy demands are high, such as during rapid cell proliferation or metabolic stress, as it acts as an alternate energy substrate to glucose. Sodium pyruvate also acts as an antioxidant and protects cells against damage caused by reactive oxygen species. Virus infection induces metabolic stress, resulting in reactive oxygen species, which can damage cells and prevent further virus infection (Wang et al., 2007). Therefore, treatment with sodium pyruvate can not only act as an energy source but also protect cells from damage caused by virus-induced reactive oxygen species. When we supplemented the cell-culture media with additional sodium pyruvate, JEV replication was significantly enhanced, showing sodium pyruvate as a positive modulator of JEV replication.

Insulin enhances neuronal glucose uptake by inducing GLUT3 translocation to the cell surface (Uemura and Greenlee, 2006). This increased intracellular glucose promotes glycolysis, a process that many viruses modulate to meet the high energy and biosynthetic demands of virus-infected cells (Goyal and Rajala, 2023b). Therefore, insulin-treated cells can potentially support virus infection. In our study, JEV-infected cells were treated with insulin and enhanced JEV replication was observed in insulin-treated cells compared to uninfected cells, indicating that higher glucose levels support JEV replication.

Next, we performed the time-dependent expression analysis of glycolytic enzymes post-JEV infection. HK2, PKM and PDH were found to be upregulated at 24- and 48-hour post-infection as viral genome replication and protein synthesis mostly occur at early time points post-infection. This was similar to previous studies where HK2 was found to be upregulated in case of Zika virus-infected

HUVEC cells (Singh et al., 2020). In addition, dengue virus infection in suckling mice was also reported to induce glycolysis by inducing the expression of 2 (Fontaine et al., 2015b). Studies on other viruses, such as influenza and SARS-CoV-2 have also shown HK as a key modulator of virus replication (Bhatt et al., 2022a; Ren et al., 2021b). Past studies have also shown pyruvate kinase involvement in the replication of several viruses, such as CVB3, influenza virus and COVID-19 (McElvaney et al., 2020a; Qian et al., 2022; Ren et al., 2021b). Altogether, it can be concluded that increased glycolysis is facilitated by enhanced expression of glycolytic enzymes in JEV-infected cells.

Under hypoxic conditions, HIF-1 induces adaptive responses in the cell to support its survival by reducing its dependency on oxygen-dependent mechanisms of energy production. One such response is modulation of glucose metabolism. This regulation is achieved by HIF-1α-mediated upregulation of glycolytic enzymes (Papandreou et al., 2006). In the current study, we showed upregulation of HIF-1α in JEV-infected cells compared to uninfected cells, indicating that JEV replication induces hypoxia-like conditions, thereby stabilizing HIF-1α. Many past studies have reported that reactive oxygen species can stabilize HIF-1α, leading to its accumulation (Jung et al., 2008; Patten et al., 2010). Since JEV infection is known to induce ROS and mitochondrial damage, this can probably lead to excess HIF-1α in JEV-infected cells (Gupta et al., 2024a; Gupta et al., 2024b; Srivastava et al., 2009; Yang et al., 2012a; Yang et al., 2024). Similarly, the mitochondrial ROS in SARS-CoV-2 infected cells have also been found to induce HIF-1α stabilization. (Codo et al., 2020b; Tian et al., 2021). $CoCl_2$ is known to induce hypoxia-like conditions, stabilizing HIF-1α and resulting in its cytoplasmic accumulation (Rana et al., 2019). To understand whether HIF-1α positively or negatively regulates JEV replication, we treated the Neuro-2a cells with $CoCl_2$, followed by JEV infection and observed enhanced JEV replication in treated cells. The results showed that HIF-1α supports JEV replication in neuronal cells, which was consistent with the previous reports where the treatment with $CoCl_2$ was shown to promote the infection of SARS-CoV-2 in Caco2 cells (Tian et al., 2021). Further, when we transfected the Neuro-2a cells with HIF-1α-specific shRNA and then treated

them with $CoCl_2$, we did not observe an increase in JEV replication. This shows that the increase in JEV replication was due to $CoCl_2$-induced HIF-1α. The knockdown of HIF-1α alone without $CoCl_2$ treatment also resulted in a significant reduction in JEV replication. Similar results were observed for H5N1 influenza virus-infected A549 cells, where downregulation of HIF-1α resulted in inhibition of H1N1 influenza replication (Ren et al., 2021b). Other viruses, such as PRRSV, RCV, Zika virus, and SARS-CoV-2, have been reported to depend on HIF-1α for their replication (Chen et al., 2023b; de Farias et al., 2025a; Pang et al., 2022; Tian et al., 2021). Altogether, it can be concluded that JEV replication induces glycolysis to support its replication in neuronal cells by upregulating glycolytic enzymes through the activation of HIF-1α.

Chapter 4

Understanding the role of pyruvate kinase M2 in Japanese encephalitis virus replication

Brief overview of the chapter

PKM2 is a key modulator of glucose metabolism**.** The role of PKM2 in the autoimmune response and inflammatory processes is now increasingly being acknowledged. However, its role in modulating virus replication remains largely unexplored. This chapter investigates the role of PKM2 in JEV replication. The results demonstrate that JEV infection induces PKM2 expression in the infected cells. Both gain and loss-of-function studies substantiate the negative effect of PKM2 on JEV replication. Additionally, JEV infection induced STAT3 activation in the infected cells, which was enhanced by PKM2 overexpression and attenuated upon its knockdown. Moreover, elevated levels of PKM2 were associated with increased expression of proinflammatory cytokines such as TNF-α and IL-1β, whereas reduced PKM2 expression inhibited their expression in infected cells. This concludes that PKM2 negatively regulates JEV replication by inducing the expression of proinflammatory cytokines such as TNF-α and IL-1β through STAT3 activation, underscoring its potential as a host restriction factor.

4.1 Introduction

Several RNA viruses have been shown to modulate key glycolytic enzymes such as HK, PFK, PK and LDH (Fontaine et al., 2015b; Qian et al., 2022; Ren et al., 2024; Singh et al., 2020; Zhang et al., 2023). Some of these glycolytic enzymes also have non-metabolic roles, especially in regulating innate immune responses. The first rate-limiting enzyme of glycolysis, hexokinase, was found to be

upregulated in inflammatory diseases (Bao et al., 2022; Chen et al., 2024). Its inhibition by 2-DG has been shown to inhibit the expression of proinflammatory cytokines (Cai et al., 2021). In the case of Zika virus infection, it has been reported that treatment with 2-DG resulted in enhanced innate immune responses through the activation of AMPK, suppressing its replication (Singh et al., 2020). Furthermore, PRRSV infection was also found to induce glycolysis by upregulating hexokinase and LDH in the infected cells (Zhang et al., 2023). The LDH converts pyruvate into lactate, which in turn reduces RIG-I, MDA5 and MAVS-induced IFN-β promoter activity, thereby suppressing innate immune responses in PRRSV-infected cells (Zhang et al., 2023). LDH and aldolase were also found to modulate JEV replication (Tien et al., 2014; Zhou et al., 2024). PKM2 is one of the key glycolytic enzymes which has been well explored in terms of its non-metabolic roles in cancer; its role in virus replication remains unclear. While some studies do suggest its involvement in the replication of viruses (de Wit et al., 2016; Lo et al., 2015; Ma et al., 2015; Mazurek et al., 2001). However, there is currently no evidence suggesting its role in JEV replication.

PKM2 is a rate-limiting glycolytic enzyme, essential for tumour metabolism and development (Dong et al., 2016b). PKM2 plays a pivotal role in multiple cellular pathways, encompassing aerobic glycolysis, intranuclear signal transmission, protein synthesis, inflammation, and apoptosis (Liu et al., 2022). PKM2 enhances the expression of genes by activating HIF-1α, β-catenin (β-cat), insulin, signal STAT3, and other transcription factors that stimulate cell growth and proliferation (Azoitei et al., 2016; Iqbal et al., 2013; Li et al., 2015a). PKM2 also serves as a critical regulator in the apoptotic signaling pathways of several cancer types (He et al., 2017; Hu et al., 2015; Liang et al., 2017). BCL-2, a prominent anti-apoptotic protein and very well characterized for its anti-apoptotic properties, is a target of PKM2, both directly and indirectly (Liang et al., 2017). As part of the innate immune response, PKM2 stimulates the production of inflammatory cytokines such as IL-1β and TNF-α (Palsson-McDermott et al., 2015b). PKM2 also functions as a protein kinase, facilitating the phosphorylation of STAT3, leading to the production of IL-6 and IL-1β to initiate the inflammatory response (Shirai et

al., 2016). PKM2 activates and engages HIF-1α to regulate the release of HMGB1, an efficient proinflammatory cytokine that is released from activated macrophages (Andersson et al., 2000; Yang et al., 2014a). Recent studies have shown the role of PKM2 expression in autoimmune and inflammatory responses as well (Chung-Faye et al., 2007; Day et al., 2012; Tang et al., 2015).

PKM2 is one of the key glycolytic enzymes which performs several non-glycolytic tasks with far-reaching consequences, the extent of which has to be fully deciphered (Gupta and Bamezai, 2010). Hence, it is important to have a more comprehensive understanding of the metabolic and nonmetabolic roles of PKM2. PKM2 has been associated with several RNA virus infections. The expression of PKM2 was enhanced in mouse lung tissues infected with the H1N1 influenza virus (Ren et al., 2021a). PKM2 has also been shown to be elevated in individuals affected with severe coronavirus disease 2019 (COVID-19) (McElvaney et al., 2020b). Phosphorylation of PKM2 was also found to be enhanced upon dengue virus infection in U937 cells (Wongtrakul et al., 2020). Phosphorylation inhibits its catalytic activity and promotes its translocation to the nucleus (Alquraishi et al., 2019; Wongtrakul et al., 2020). Studies in CSFV and HCV have also shown PKM2 involvement in virus replication (Liu et al., 2024; Wu et al., 2008). Collectively, these studies suggest the potential involvement of PKM2 in RNA virus pathogenesis. However, there is no report about its role in JEV replication.

4.2 Materials and Methods

4.2.1 Plasmids and antibodies

The following plasmids were used in the current study: pEGFP.PKM2 (Addgene #64698) and pEGFP (Addgene #165830). The antibodies used are as follows: Anti-NS1 (GeneTex, USA), Anti-PKM2 (Cell Signaling Technology, USA), Anti-GAPDH (Cell Signaling Technology, USA), Anti-GFP (Bio Bharati, India), Goat anti-Rabbit (Invitrogen, USA) and anti-mouse (Cell Signaling Technology, USA) conjugated with horseradish peroxidase (HRP).

4.2.2 Gene expression analysis using quantitative RT-PCR

RNA lysate was prepared at different time points post-infection using RNAiso Plus reagent (TaKaRa, Japan). Total RNA was extracted using the phenol-chloroform extraction method and was quantified by measuring absorbance at 260 nm. The RNA was checked for purity by taking the ratio A260/280 (>1.8). A total of 1 µg of RNA was reverse transcribed to cDNA using a high-capacity cDNA reverse transcription kit (Thermo Fisher Scientific, USA). The quantitative real-time PCR was performed using PowerUp SYBR Green Master Mix (Applied Biosystems, USA). The fold change in mRNA level in infected versus mock-infected samples was calculated using the $2^{(-\Delta\Delta Ct)}$ method with GAPDH as an internal control for normalization.

4.2.3 Plasmid and siRNA transfection

The plasmid used in this study, pEGFP-PKM2 (Catalog No #64698), was a generous gift from Axel Ullrich's lab (Stetak et al., 2007). For overexpression experiments, Neuro-2a cells were cultured on 6-well plates and then transfected with 2 µg of an expression plasmid using Lipofectamine 2000 (Invitrogen, USA) as per the instructions provided by the manufacturer.

The knockdown of endogenous PKM2 was achieved by co-transfecting two siRNAs at a total concentration of 50 pmol. The following sense strand sequences of siRNA were used: GAUGUCGACCUUCGUGUAA[dT] and UCCUAUCAUUGCCGUGACU[dT][dT] (Zheng et al., 2020). Lipofectamine RNAiMAX (Invitrogen, USA) was used for transfection studies as per the manufacturer's protocol, and siRNA universal negative control (SIC001, Sigma-Aldrich, Germany).

4.2.4 Disuccinimidyl Suberate (DSS) cross-linking of PKM2

Neuro-2a cells were infected with JEV, and 48 hours post-infection, cells were washed with ice-cold PBS three times and treated with 500 µM of DSS crosslinker (Merck, Catalog No-S1885) for 30 min at 37 ˚C. The cross-linking reaction was quenched by treating cells with 10 mM Tris-HCl (pH

7.5) for 15 min. Cells were then lysed with RIPA buffer, followed by western blotting.

4.2.5 Statistical Analysis

All the data were statistically validated using GraphPad Prism software, and the results were shown as mean ± standard deviation. All the experiments were reproduced at least three times. The significance level among different groups was represented as *, **, ***, where * is for $P < 0.05$, ** for $P < 0.01$, and *** for $P < 0.001$. $P < 0.05$ was considered significant.

4.3 Results

4.3.1 JEV infection induces upregulation of PKM2 expression in Neuro-2a cells

The expression of PKM2 was investigated in Neuro-2a cells following JEV infection with different MOI. Quantitative analysis using real-time PCR at various MOI showed a gradual increase in JEV replication in infected cells compared to uninfected cells (Figure 4.1A). PKM2 mRNA also showed an increase in expression compared to the control with the increase in MOI, except at 0.001 (Figure 4.1B). However, the maximum increase in expression was at 0.1 MOI. At the protein level, there was a significant increase in PKM2 expression at both 0.01 and 0.1 MOI compared to the uninfected control. However, there was no change in PKM2 expression at 0.001 MOI compared to the uninfected control (Figure 4.1C and 4D). Furthermore, the time-dependent experiment was performed to investigate the progression of JEV replication over time (Figure 4.1E). The mRNA analysis revealed an upregulation of PKM2 expression at both 24- and 48-hours post-infection (Figure 4.1F). There was no significant difference in the PKM2 mRNA compared to the control at 72 hours post-infection. At the protein level, there was a significant increase in PKM2 expression in infected cells compared to uninfected controls (Figure 4.1G and 4H). Thus, JEV replication induces PKM2 expression in the infected cells.

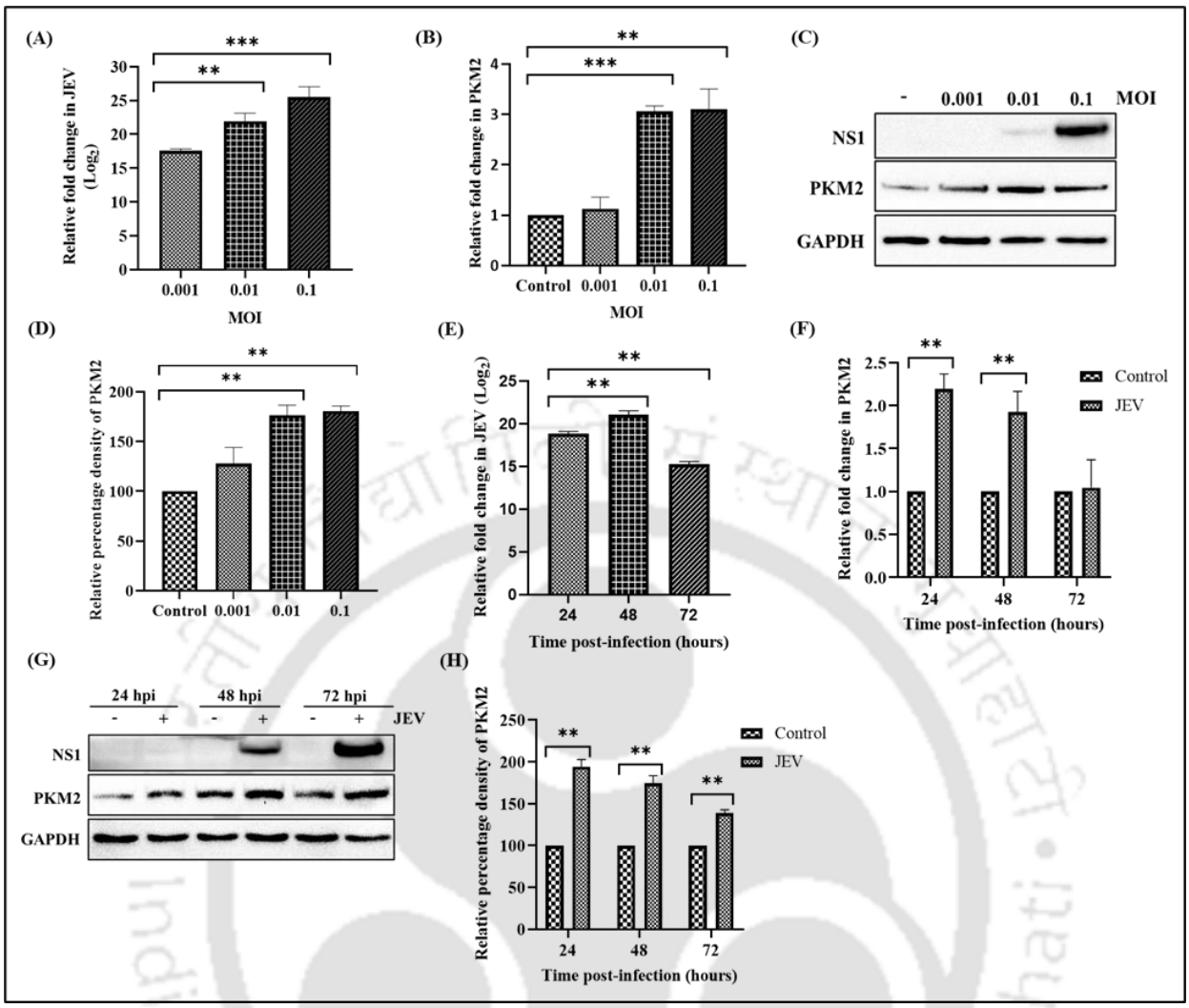

Figure 4.1 JEV infection leads to upregulation of PKM2. Real-time PCR analysis of JEV replication at different MOI (A). Fold-change in PKM2 mRNA at different MOI (B). Immunoblot showing MOI-dependent expression of PKM2 and NS1 at the protein level (C). Graph showing the relative percentage density of NS1 at different MOI (D). Time-dependent analysis of JEV replication (E). Time-dependent fold change in PKM2 mRNA expression post-infection (F). Immunoblot analysis of PKM2 and NS1 expression at different time points post-infection (G). Relative percentage density of PKM2 at different time intervals post-infection (H). GAPDH was used for the normalization of real-time PCR analysis. Values are shown as mean fold change ± standard deviation, validated with a one-way ANOVA statistical test.

4.3.2 PKM2 expression is responsible for inhibiting JEV replication

To investigate the function of PKM2 in the context of JEV infection, Neuro-2a cells were

transfected with the pEGFP-PKM2 plasmid (Figure 4.2A). Exogenous PKM2 expression was confirmed at both 24- and 48-hours post-transfection (Figure 4.2B). Next, the cells were infected with JEV at 0.1 MOI, 24 hours post-transfection, and protein lysate was prepared 48 hours post-infection. The western blot analysis revealed around 52% reduction in NS1 expression in cells with overexpressed exogenous PKM2 compared to GFP control (Figure 4.2C and 4.2D). This was further validated by an immunofluorescence experiment that showed a reduction (around 58%) in the number of cells expressing NS1 when exogenous PKM2 was overexpressed compared to GFP control (Figure 4.2E). Using the standard plaque assay, the virus titer in the supernatant collected from the infected cells was also quantified (Figure 4.2F). It was observed that there was about a 54% reduction in JEV titer in cells overexpressing PKM2 compared to the control (Figure 4.2G). In conclusion, the expression of exogenous PKM2 negatively regulates JEV replication.

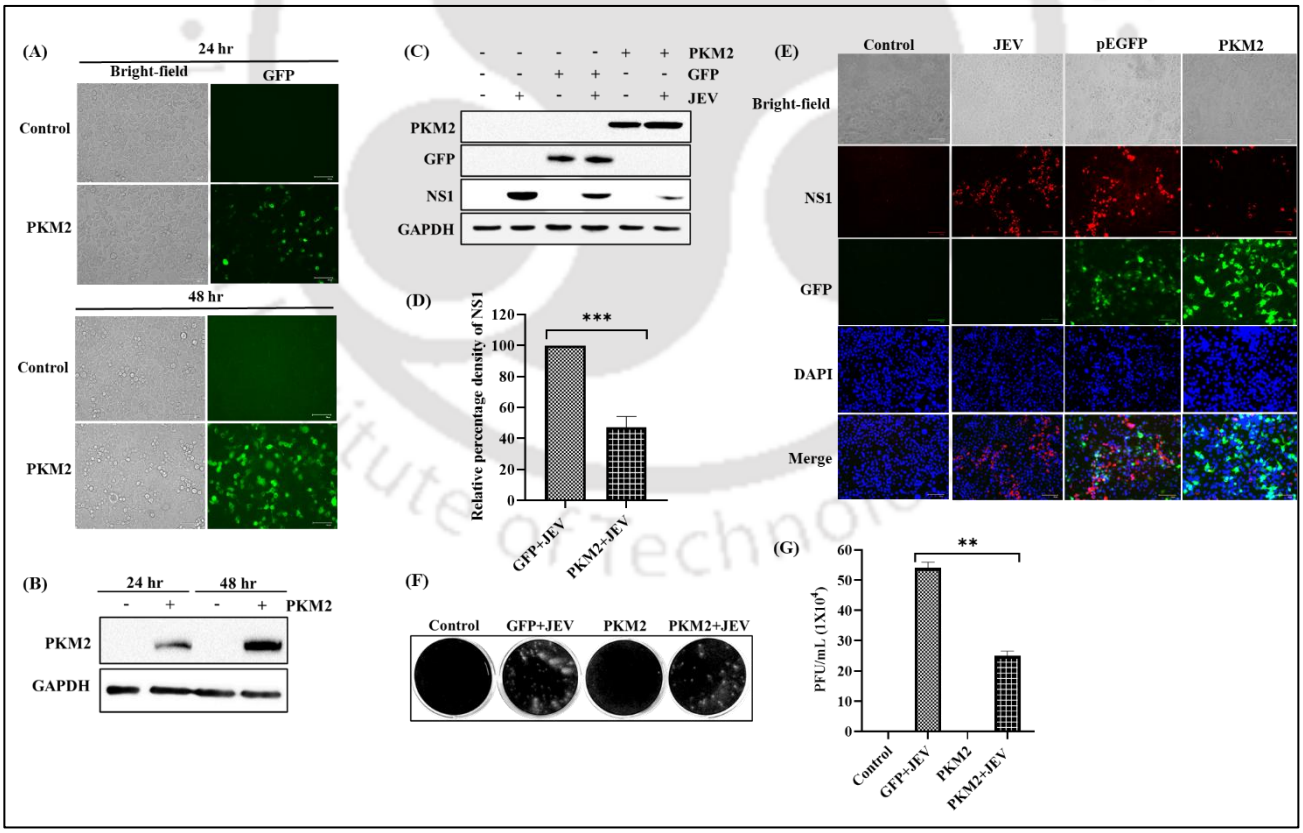

Figure 4.2 PKM2 overexpression inhibited JEV replication. Image shows expression of exogenous PKM2 24- and 48-hours post-transfection (A). Immunoblot analysis of time-dependent expression of

exogenous PKM2 post-transfection (B). Immunoblot analysis of NS1 expression upon overexpression of exogenous PKM2 in infected cells (C). Graph showing the relative percentage density of NS1 upon PKM2 overexpression (D). Immunofluorescence pictures of cells with exogenous PKM2 expression and JEV infection. Immunofluorescence labelling: red fluorescence indicates JEV-infected cells; blue fluorescence indicates DAPI-labelled nuclei; and green fluorescence represents PKM2 expression (E). Picture showing the reduction in extracellular viral titer in the form of plaques (F). Graph representing virus titer level measured in plaque-forming units per millilitre (PFU/ml) (G). Values are shown as mean ± standard deviation, validated with a one-way ANOVA statistical test.

4.3.3 PKM2 downregulation enhanced JEV replication

Endogenous PKM2 was knocked down via transfection of a cocktail consisting of two PKM2-specific siRNAs. At the mRNA level, around 84% reduction in PKM2 expression was observed compared to scRNA-transfected cells (Figure 4.3A). At the protein level, siRNA-mediated silencing resulted in approximately 99% reduction in PKM2 expression compared to scRNA-transfected cells (Figure 4.3B and 4.3C). The western blot analysis demonstrated about 80% increase in NS1 expression upon PKM2 silencing compared to control, indicating that PKM2 silencing positively modulates JEV replication (Figure 4.3D and 4.3E). This was further confirmed by immunofluorescence results, which showed around 62% of the number of cells expressing NS1 upon PKM2 downregulation (Figure 4.3F). We also quantified the extracellular virus titer in the supernatant by plaque assay (Figure 4.3G). The results showed that PKM2-silenced cells produced 2.56-fold higher JEV titer compared to scRNA control, and 2.1-fold higher titer compared to untransfected controls (Figure 4.3H).

4.3.4 Inhibition of PKM2 with metformin enhanced JEV infection

JEV-infected cells were treated with 100 µM of metformin post-infection. At the protein level, about 79% decrease in endogenous PKM2 expression was observed, while in JEV-infected cells, about 50.5% decrease was observed compared to the untreated control (Figure 4.4A and 4.4B). The amount of NS1 protein was also doubled (111% increase) in metformin-treated cells (Figure 4.4C). Plaque

assay also revealed about a 2.8-fold increase in virus titer in metformin-treated cells compared to untreated cells (Figure 4.4D and 4.4E).

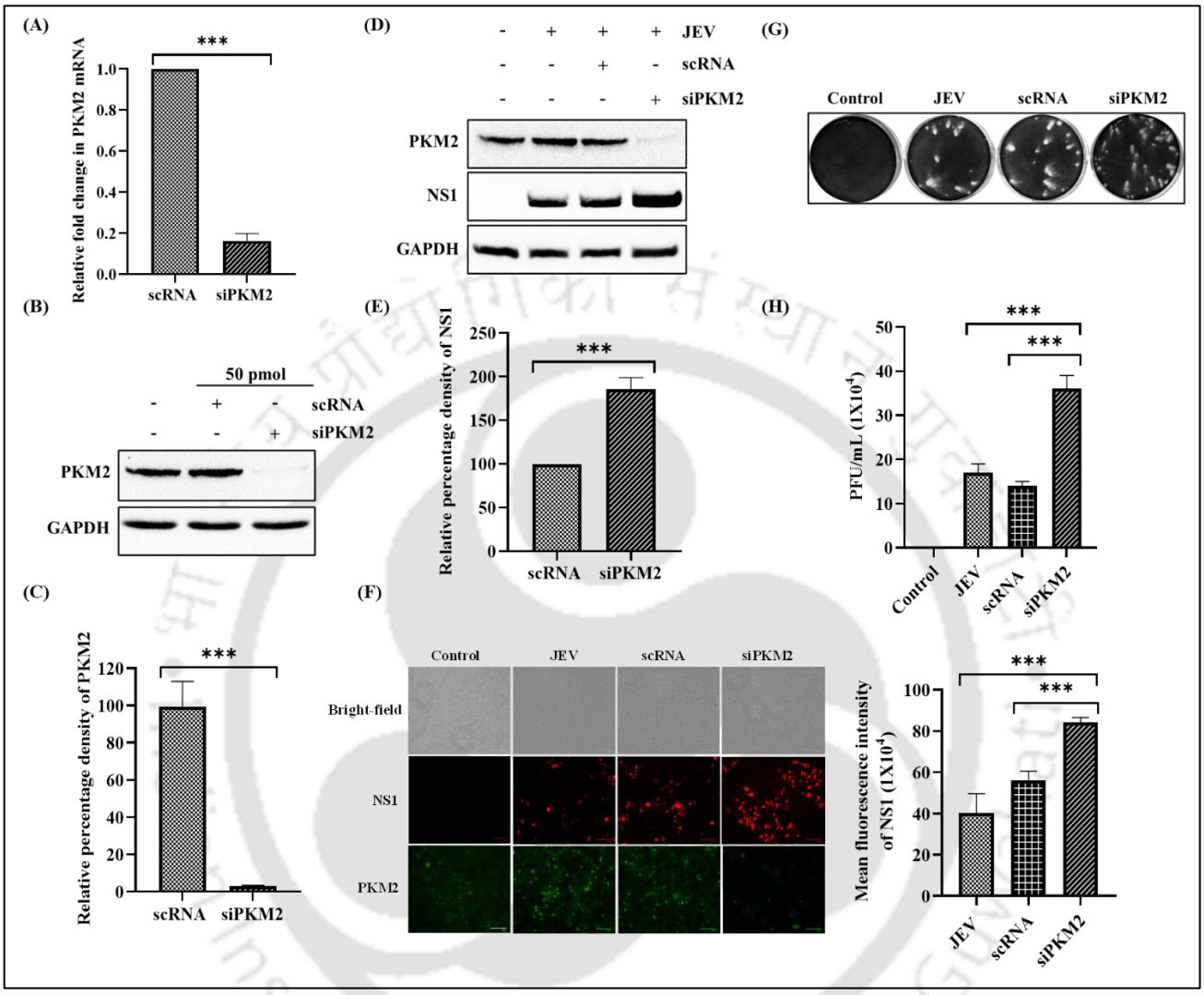

Figure 4.3 PKM2 knockdown enhanced JEV replication. Graph showing the reduction in PKM2 mRNA level upon treatment with PKM2 siRNA (A). Immunoblot showing a reduction in PKM2 expression upon treatment with PKM2 siRNA (B). Graph depicting the relative percentage density of PKM2 protein upon its knockdown (C). Immunoblot analysis of NS1 expression upon knockdown of PKM2 in infected cells (D). Graph representing the relative percentage density of NS1 protein upon its knockdown in infected cells (E). Immunofluorescence images showing enhanced JEV infection upon treatment with PKM2 siRNA. Red fluorescence images indicate JEV-infected cells, while green fluorescence indicates endogenous PKM2 expression (F). Plaque images showing the reduction in extracellular viral titer (G). Graph representing virus titer level in plaque-forming units per millilitre (PFU/ml) (H). Values are shown as mean ± standard deviation, validated with one-way ANOVA statistical test.

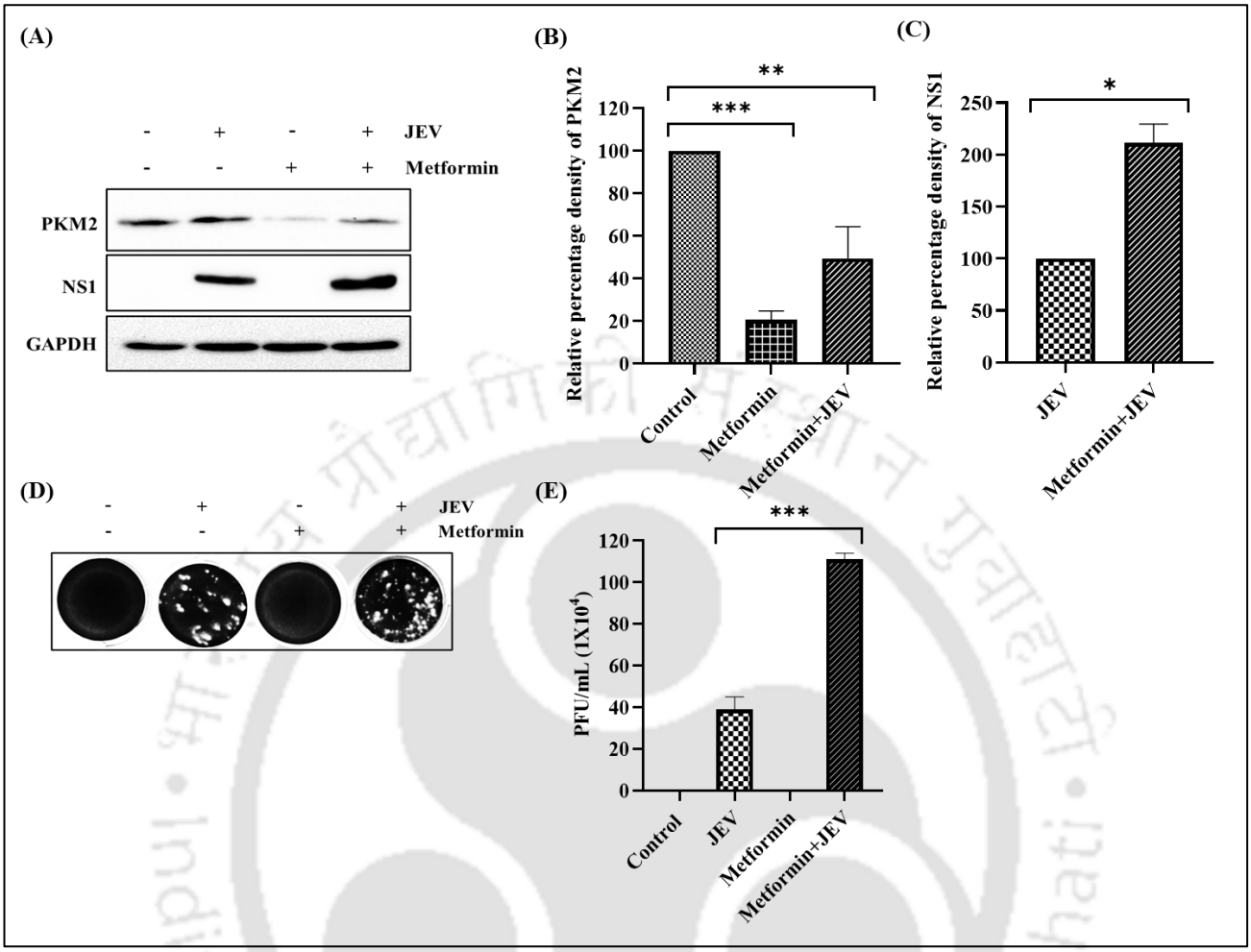

Figure 4.4 Inhibition of PKM2 with metformin enhanced JEV infection. Immunoblot indicates NS1 and PKM2 expression upon metformin treatment (A). Graph showing relative percentage density of PKM2 upon metformin treatment (B). Graph depicting relative percentage density of NS1 upon metformin treatment (C). Representative plaque image with enhanced JEV titer upon metformin treatment (D). Graph representing virus titer in PFU/mL (E). Values represent mean ± standard deviation, calculated from three independent experiments. Statistical analysis was performed using student's t-test.

4.3.5 JEV replication induces nuclear translocation of PKM2 and STAT3

To investigate the expression levels of different multimeric forms of PKM2 post-infection, protein lysates were collected from infected cells and subjected to chemical cross-linking followed by

Western blotting. The results revealed significantly enhanced expression of all three forms (monomer, dimer, and tetramer) of PKM2 post-infection compared to uninfected controls, suggesting that JEV infection promotes overall PKM2 abundance and multimerization (Figure 4.5A). We further analyzed the nuclear and cytoplasmic distribution of PKM2 and STAT3 post-infection, which showed significantly higher translocation of STAT3 to the nucleus in JEV-infected cells compared to the control (Figure 4.5B and 4.5C). Notably, a similar trend was observed for PKM2, which showed enhanced nuclear localization of PKM2 in infected cells compared to uninfected control (Figure 4.5B and 4.5D).

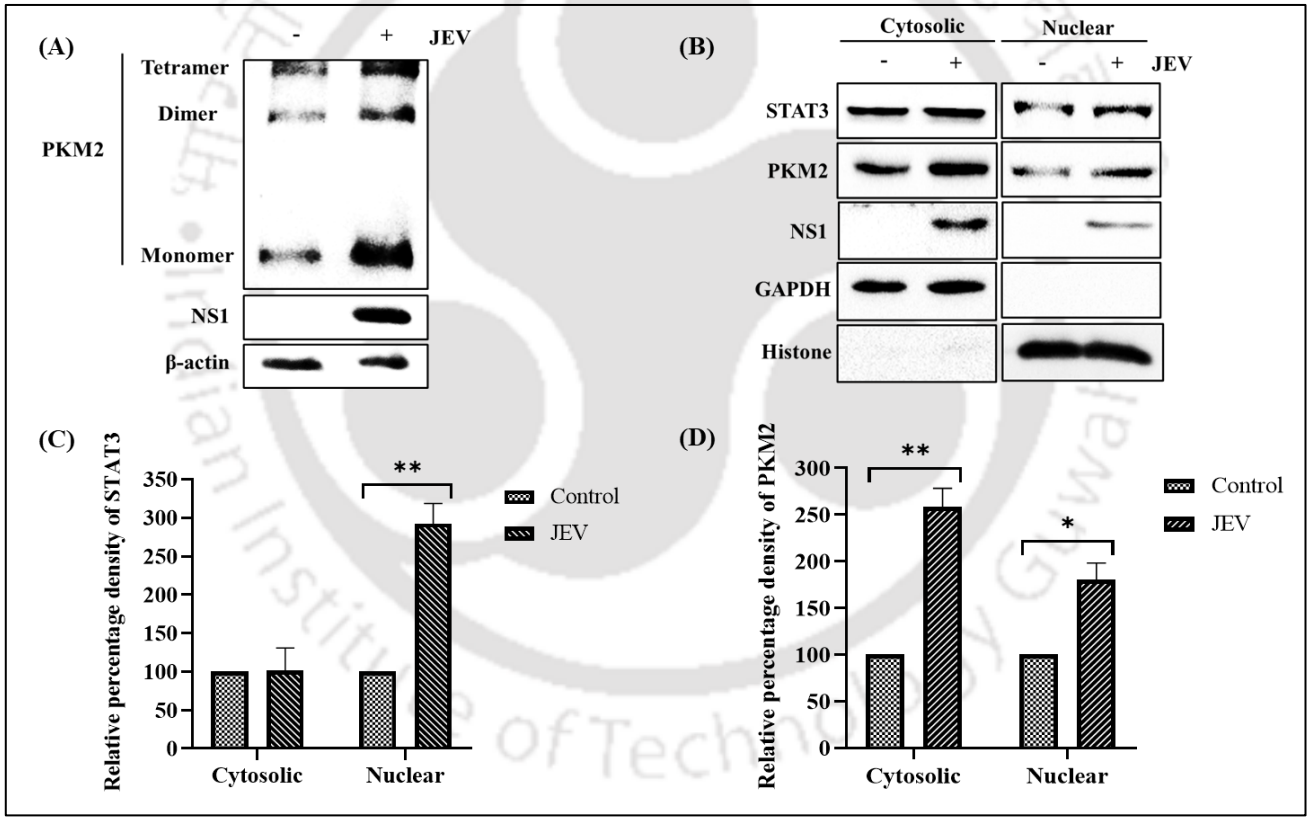

Figure 4.5 JEV replication induces nuclear translocation of PKM2 and STAT3. Immunoblot depicting different oligomers of PKM2 post-JEV infection (A). Western blot showing cytosolic and nuclear fraction of STAT3 and PKM2 upon JEV infection (B). Graph showing the relative percentage density of cytosolic and nuclear STAT3 upon JEV infection compared to control (C). Graph showing the relative percentage density of cytosolic and nuclear PKM2 upon JEV infection compared to control

(D). Values represent mean ± standard deviation, calculated from three independent experiments. Statistical analysis was performed using student's t-test.

4.3.6 PKM2 modulates JEV replication through STAT3 activation

To validate the role of PKM2 in mediating STAT3 translocation during JEV infection, both PKM2 overexpression and knockdown strategies were employed. In cells with overexpressed PKM2, a significant increase in nuclear localization of STAT3 was observed following JEV infection, as demonstrated by western blotting of nuclear and cytoplasmic fractions (Figure 4.6A, 4.6B and 4.6C). Conversely, downregulation of PKM2 substantially reduced STAT3 translocation to the nucleus post-infection (Figure 4.6D, 4.6E and 4.6F). Furthermore, knockdown of PKM2 also resulted in a substantial reduction of dimeric STAT3 in infected cells (Figure 4.6G and 4.6H). Collectively, these results demonstrate that JEV replication may induce the nuclear translocation of STAT3 by upregulating different forms of PKM2 in the infected cells.

4.3.7 PKM2 inhibits JEV replication by upregulating proinflammatory cytokines

To investigate the expression of proinflammatory cytokines such as TNF-α and IL-1β post-JEV infection, a time-dependent experiment was performed. It was observed that expression of TNF-α and IL-1β significantly enhanced at early time points (24- and 48-hours) post-infection (Figure 4.6A, 4.6B and 4.6C). The overexpression of PKM2 significantly upregulated the levels of TNF-α and IL-1β (Figure 4.6D, 4.6E and 4.6F), whereas the downregulation of PKM2 resulted in the significant reduction of these cytokines (Figure 4.6G, 4.6H and 4.6I). This indicates that PKM2 suppresses JEV infection by inducing the expression of TNF-α and IL-1β.

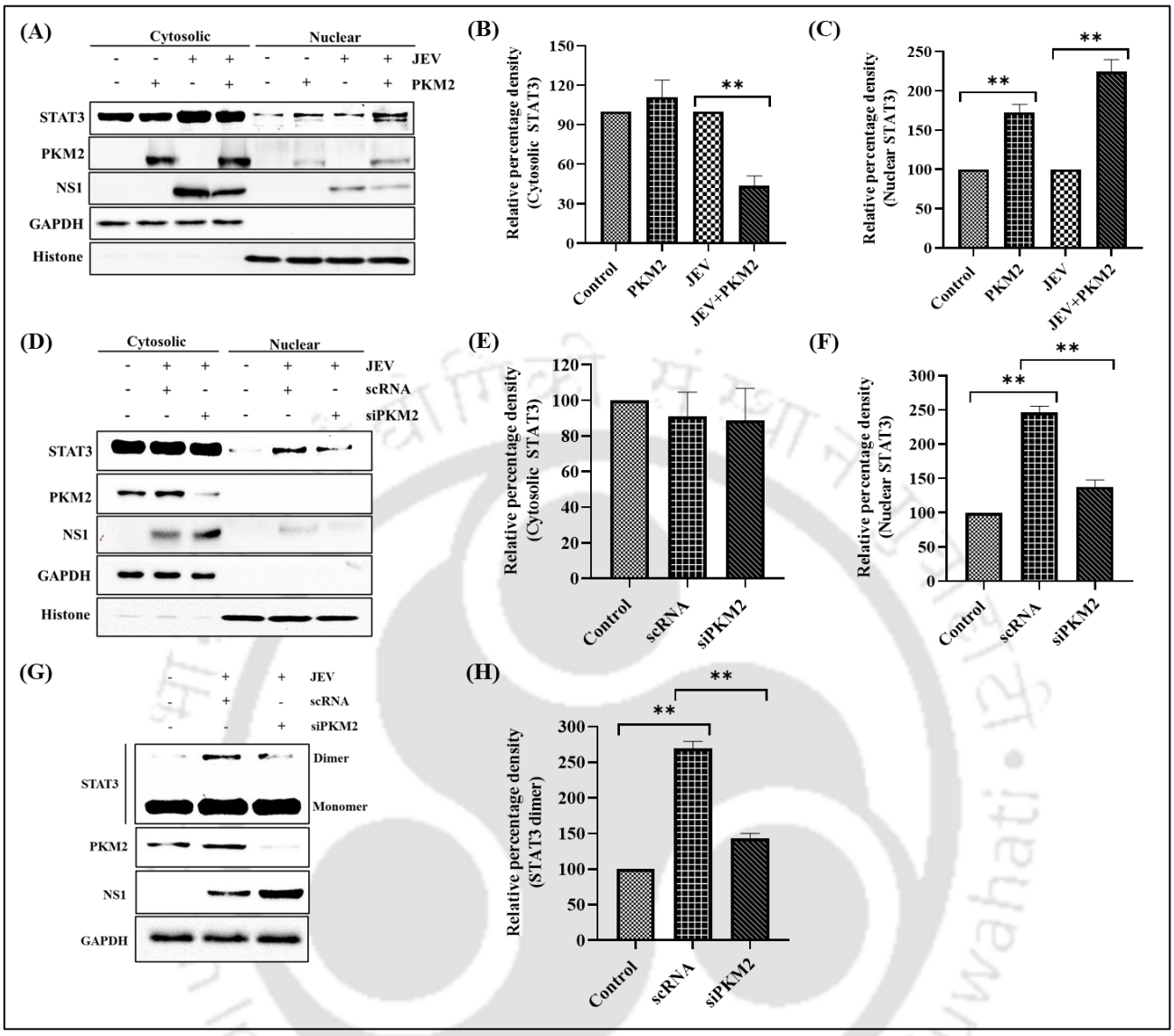

Figure 4.6 PKM2 modulates JEV replication through STAT3 activation. Western blot showing cytosolic and nuclear localization of STAT3 upon PKM2 overexpression (A). Graph showing relative percentage density of cytosolic STAT3 upon PKM2 overexpression (B). Graph showing relative percentage density of nuclear STAT3 upon PKM2 overexpression (C). Immunoblot showing cytosolic and nuclear translocation of STAT3 upon PKM2 knockdown in JEV-infected cells (D). Graph showing relative percentage density of cytosolic STAT3 upon PKM2 downregulation (E). Graph showing relative percentage density of nuclear STAT3 upon PKM2 downregulation (F). Immunoblot showing monomeric and dimeric forms of STAT3 upon PKM2 knockdown (G). Graphs showing the relative percentage density of STATE dimer (H). All the lysates were prepared 48 hours post-JEV infection.

Values represent mean ± standard deviation, calculated from three independent experiments. Statistical analysis was performed using student's t-test.

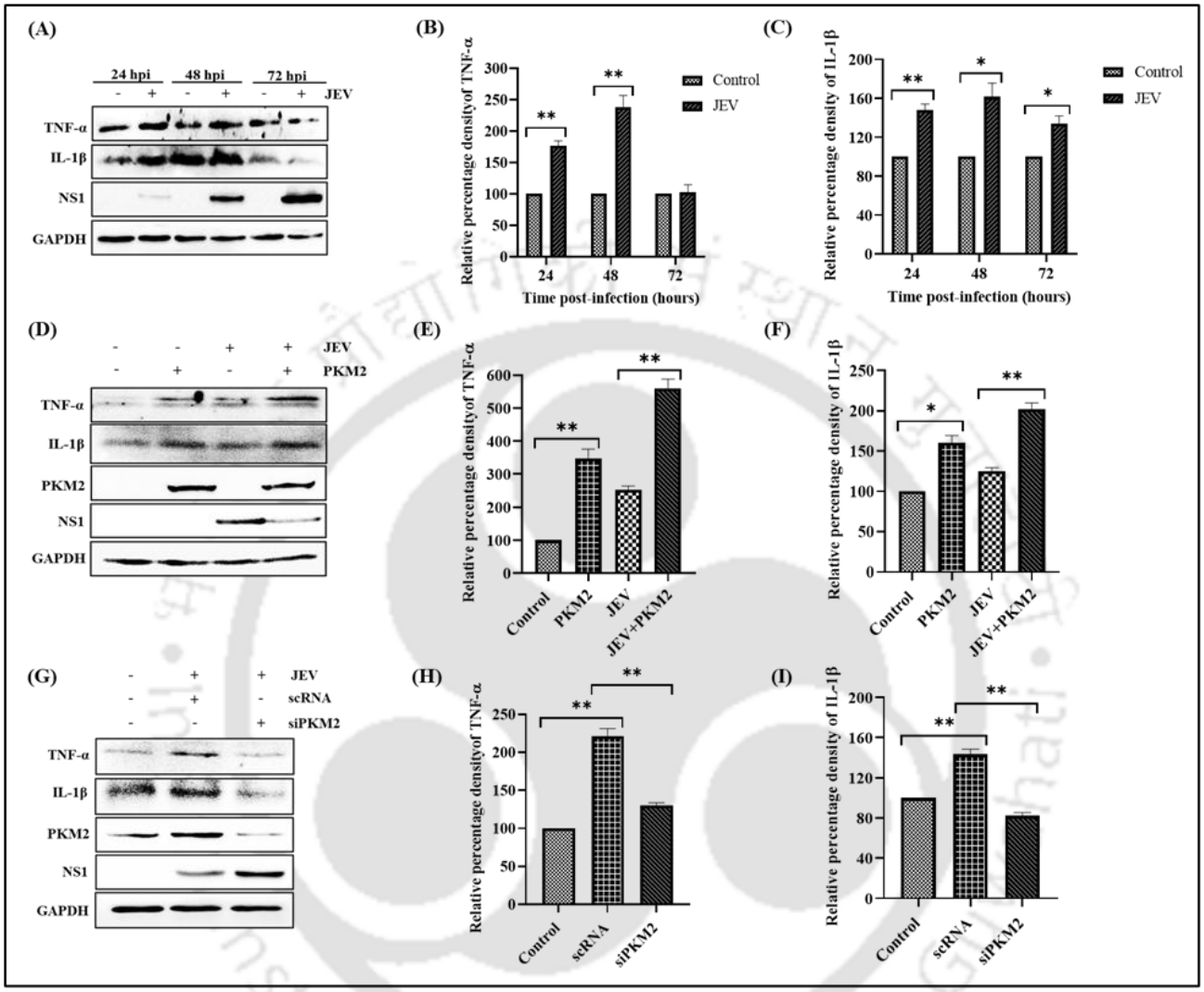

Figure 4.7. PKM2 inhibits JEV replication by upregulating pro-inflammatory cytokines. Western blot representing time-dependent analysis of TNF-α and IL-1β post-JEV infection (A). Graph showing relative percentage density of TNF-α at different time points post-infection (B). Graph showing relative percentage density of IL-1β at different time points post-infection (C). Immunoblot depicting effect of PKM2 overexpression on TNF-α and IL-1β (D). Graph showing relative percentage density of TNF-α upon PKM2 overexpression (E). Graph showing relative percentage density of IL-1β upon PKM2 overexpression (F). Immunoblot analysis of TNF-α and IL-1β expression upon PKM2 down-regulation (G). Graph showing relative percentage density of TNF-α upon PKM2 knockdown (H). Graph showing relative percentage density of IL-1β upon PKM2 knockdown (I). Values represent mean± SD

calculated from three independent experiments. Statistical analysis was performed using student's t-test considering P < 005 as significant. (* for P < 0.05, ** for P < 0.01, and *** for P < 0.001).

4.4 Discussion

PKM2 is a glycolytic enzyme catalyzing the rate-limiting, last step of glycolysis (Dong et al., 2016b). PKM2 is a multifunctional protein involved in several critical functions like apoptosis, mitosis, hypoxia, inflammation, and metabolic reprogramming (Liu et al., 2022; Mucaj et al., 2012). The role of PKM2 in several cancers has been well-explored (Bluemlein et al., 2011; Cairns et al., 2011; Chen et al., 2020a; Christofk et al., 2008b). Furthermore, PKM2's participation in numerous cellular pathways, protein-protein interactions, and nuclear transport indicates that it performs several non-glycolytic functions (Dong et al., 2016b). Perhaps, PKM2 might also be involved directly or indirectly in regulating virus replication and pathogenesis through multiple pathways. Since the role of PKM2 in JEV pathogenesis has not been studied. The present study aims to understand the role of PKM2 in JEV replication. The results collectively show that PKM2 negatively regulates JEV replication.

We performed MOI and time-dependent analysis of PKM2 expression in JEV-infected and uninfected Neuro-2a cells. The results revealed enhanced endogenous PKM2 expression in infected cells. Studies performed on other RNA viruses, such as CSFV and SARS-CoV-2, have also shown higher expression of PKM2 in infected cells (Liu et al., 2024; McElvaney et al., 2020b). To investigate the potential role of PKM2 in JEV replication, we conducted overexpression and knockdown experiments. We observed that JEV infection was significantly reduced in cells with overexpressed PKM2, while JEV replication was enhanced in cells with silenced PKM2. Similar results were observed upon treatment with metformin, which is a known inhibitor of PKM2 (Shang et al., 2017; Su et al., 2018). Altogether, these studies show that PKM2 plays a negative role in JEV replication.

PKM2 exists in two functional states: the active tetrameric state and the inactive dimeric state (Nandi et al., 2020). The affinity of dimeric PKM2 for PEP is low, contrary to that of tetrameric PKM2

(Christofk et al., 2008b). PKM2 transforms into its dimeric form within cancer cells, enhancing glucose absorption and promoting the buildup of glycolytic intermediates essential for anabolic activities, including the production of nucleic acids, amino acids, and lipids (Christofk et al., 2008c; Israelsen and Vander Heiden, 2015; Mazurek, 2011). Multiple molecules regulate the transition between the dimeric and tetrameric forms of PKM2. E7 oncoproteins, tyrosine kinase-mediated phosphorylation, acetylation, and oxidation promote the development of the low-activity dimeric PKM2. Conversely, FBP, serine, and SAICAR facilitate the assembly of a highly active tetramer (Anastasiou et al., 2012). We investigated the expression level of different forms of PKM2 in JEV-infected neurons and observed an increase in all multimeric forms of PKM2 in JEV-infected cells relative to uninfected cells. It has been reported that tetrameric PKM2 mostly resides in the cytoplasm to perform glycolytic functions, whereas dimeric PKM2 frequently translocates to the nucleus to regulate gene transcription (Qian et al., 2024). In JEV-infected neuronal cells, we observed higher PKM2 expression in both cytosolic and nuclear fractions compared to uninfected cells. This indicates the multifaceted role of all PKM2 isomers in JEV replication kinetics. It has been shown that dimeric nuclear PKM2 directly phosphorylates STAT3 at Tyr705, independent of the JAK2 and c-Src pathways, activating the transcription of MEK5 (Gao et al., 2012). Tyr705 phosphorylation promotes the dimerization of STAT3, inducing its translocation to the nucleus and DNA binding (Guadagnin et al., 2015). Prior work has also shown that PKM2 interacts with STAT3, facilitating its activation by phosphorylating it at Tyr705, which subsequently promotes Th17 cell development (Damasceno et al., 2020). Furthermore, it has been shown that the mutation of PKM2 at position Arg399 stabilizes its dimeric conformation, hence increasing its ability to phosphorylate STAT3 (Gao et al., 2012). In the present study, we observed increased levels of both STAT3 and PKM2 in the nucleus of infected neuronal cells compared to uninfected ones. Further, silencing of PKM2 reduced STAT3 dimerization and its translocation to the nucleus in infected cells compared to untreated infected cells. Altogether, these results indicated that PKM2 induces STAT3 activation to regulate JEV replication.

Several studies have linked PKM2 with the expression of proinflammatory cytokines (Shirai et al., 2016; Shu et al., 2024; Sun et al., 2024; Yuan et al., 2023). LPS has been shown to increase the PKM2 expression and STAT3 promoter binding, leading to TNF-α and IL-1β production in colorectal cancer (Yang et al., 2015). Several proinflammatory cytokines are induced by neurotropic viruses and are responsible for neuronal death (Cheng et al., 2016; Gupta et al., 2024b; Kumar et al., 2010; Plociennikowska et al., 2021). Consistent with the previous studies, we observed that neuronal cells infected with JEV resulted in enhanced proinflammatory cytokines expression during the early stages of infection. Moreover, overexpression of PKM2 enhanced the cellular antiviral response by inducing the expression of TNF-α and IL-1β, resulting in decreased viral multiplication and reduced its release in the culture supernatant. Conversely, siRNA-mediated knockdown diminished the cellular antiviral response, facilitating JEV multiplication in neurons. This aligns with the previous research showing enhanced replication of JEV because of decreased levels of proinflammatory cytokines (IL-6 and TNF-α) in SOCS5 overexpressing microglial cells following JEV infection (Sharma et al., 2016). Taken together, we concluded that PKM2 negatively modulates JEV replication by inducing the expression of proinflammatory cytokines in neurons.

Chapter 5

Investigating the interaction and cellular co-localization of JEV NS1 and PKM2 in JEV-infected neuronal cells

Brief overview of the chapter

In this chapter, we have investigated the potential interaction between NS1 and PKM2. Molecular docking was used to identify PKM2–NS1 complexes. Out of five complexes, we selected the most stable complex based on the binding free energies. Next, we performed the molecular dynamics simulations to analyze the stability of the complex. Molecular dynamics simulation results confirmed the structural stability and rigidity of the complex, validated by consistent Root mean square deviation (RMSD), Root mean square fluctuation (RMSF), radius of gyration (Rg), and Solvent-accessible surface area (SASA) profiles. Using *in silico* studies, the interacting residues were also identified. Later, we performed the microscopic studies, which revealed the co-localization of PKM2 and NS1 in the endoplasmic reticulum (ER) of the JEV-infected cells. Subsequently, we validated the PKM2-NS1 interaction by co-immunoprecipitation (Co-IP) assay. Altogether, the study identifies PKM2 as a binding partner of NS1.

5.1 Introduction

NS1 protein is a highly conserved protein with a molecular weight ranging from 46 to 55 kDa, depending on the extent of glycosylation (Rosales Ramirez and Ludert, 2019). It exists in three forms: monomeric, dimeric, and hexameric. The hydrophobic dimeric form is membrane-associated and is transported to viral replication sites to participate in viral replication. Dimeric NS1 is further processed into hexameric NS1, which is secreted from the cell (Zhang et al., 2024a). Secreted NS1 has an immune

evasion function as it directly interacts with several complement proteins such as C1q, C1s and C4, antagonizing their functions (Avirutnan et al., 2010; Edeling et al., 2014; Silva et al., 2013). NS1 forms a structural role, potentially contributing to the attachment of the viral replication complex to the membrane, alongside transmembrane replicase components (Muller and Young, 2013). Additionally, the NS1 protein interacts with SLC25A12, which results in enhanced type I interferon expression, inhibiting JEV replication (Yin et al., 2024). Furthermore, NS1 and NS1' proteins promote JEV replication by binding to CDK1, which translocates them from the nucleus to the cytoplasm, where they phosphorylate vimentin and remodel its network (Xie et al., 2024). NS1 also interacts with several ribosomal proteins constituting the 60S ribosomal subunit, such as RPL18, RL18a, and RPL7, re-localizing these proteins to the viral replication sites (Cervantes-Salazar et al., 2015). These ribosomal proteins are not only crucial components of the host translational machinery but also perform several extra-ribosomal tasks by facilitating interaction with IRES and supporting ribosomes to the ER membrane. Silencing of these proteins has shown a negative effect on flavivirus replication (Rastogi et al., 2016). It has been reported that the NS1 protein of dengue virus interacts and co-localizes with GAPDH in the perinuclear region, where it enhances GAPDH activity and supports viral replication (Allonso et al., 2015).

PKM2 is a multifunctional protein known for its sticky nature and extensive interactome, encompassing both host and viral proteins. Beyond its traditional role in glycolysis, PKM2 is involved in non-glycolytic functions through direct interactions with viral proteins. Notably, PKM2 has been shown to interact with the oncogenic E7 protein of HPV, leading to activation of its non-glycolytic functions{Lee, 2021 #207}. Additionally, PKM2 interacts with several viral non-structural proteins. For instance, it associates with NS4A and NS5A of CSFV, promoting their expression in the infected cells (Liu et al., 2024). It also binds with the NS5B protein of the HCV and CSFV, enhancing its RNA polymerase activity (Mazurek et al., 2001; Song et al., 2025; Wu et al., 2008; Zwerschke et al., 1999). Furthermore, influenza virus RNA polymerase is another target of PKM2 (Miyake et al., 2017). These

diverse interactions suggest that PKM2 can modulate virus replication either positively or negatively, depending on the context and virus involved. In this chapter, we have explored the potential interaction between NS1 and PKM2 utilizing both *in silico* and *in vitro* approaches. We have also examined the cellular localization of PKM2 in JEV-infected cells.

5.2 Materials and Methods

5.2.1 Structure modeling

The amino acid sequences of JEV NS1 and mouse PKM2 proteins were retrieved from GenBank accession numbers, QCZ42158 and NP_001365797, respectively. The three-dimensional structures of the proteins were predicted and generated by I-TASSER (Iterative Threading ASSEmbly Refinement) protein structure and function prediction software as experimentally validated complete structures were not available for the proteins. The tool constructs 3D structure models by threading the query protein sequence through a library of known structures in the Protein Data Bank (PDB), followed by iterative template-based fragment assembly simulation (Roy et al., 2010; Yang and Zhang, 2015; Zhang, 2008). Further, the predicted models were subsequently subjected to energy minimization using YASARA software to enhance the structural stability and reduce steric clashes. Thereafter, the models were validated by Ramachandran plot using PROCHECK, which assesses their stereochemical stability based on dihedral angle distributions (Laskowski et al., 1993). All three-dimensional structures were visualized using PyMOL.

5.2.2 Molecular docking

To study the possible interaction between the predicted structure of JEV NS1 and mouse PKM2 protein, molecular docking was performed using Cluspro 2.0 protein-protein docking software. ClusPro 2.0 generates multiple docking conformations (clusters) based on rigid-body docking, followed by energy-based filtering and clustering to identify the most probable binding models

(Kozakov et al., 2017). The top-ranked docked complexes from ClusPro 2.0 were further analyzed for binding affinity using the HawkDock server scoring function, which is based on Molecular Mechanics/Generalized Born Surface Area (MM/GBSA) free energy decomposition (Liu et al., 2019; Zhang et al., 2025c). The MM/GBSA method provides a more rigorous estimation of binding free energy for protein-protein complexes, where lower binding energy values indicate higher stability of the complex (Chen et al., 2016; Gohlke and Case, 2004). Finally, the PDB sum generator tool was used to get insights into the amino acid residues involved in binding, over the molecular interface spanning both proteins (de Beer et al., 2014).

5.2.3 Molecular dynamics simulations

To study the conformational stability, the docked protein-protein complex was subjected to all-atom molecular dynamics simulations using the GROMACS v2020.1 software (Hess et al., 2008; Van Der Spoel et al., 2005). The system consisted of the protein-protein complex in a solvated dodecahedron box with a minimum distance of 1.2 nm from the boundary. The system was solvated with the TIP3P water model and subsequently neutralized by adding countercations (Na^+) or anions (Cl^-). The solvated system was then energy minimized using the steepest descent algorithm of 50,000 steps and further equilibrated for NPT (constant number, pressure, and temperature) and NVT (constant number, volume, and temperature) at 300 K, 1 bar pressure, and 100 ps to optimize the orientation and system density. The final equilibrated system was used as a starting conformation for the simulation run of 50 ns with a 2 fs time step. Long-range electrostatic interactions were defined by the Particle Mesh Ewald approach, and the cut-offs for Coulomb and van der Waals interactions were set to 1.2 nm. Finally, the output trajectory was obtained, and the estimation of RMSD, RMSF, SASA, and Rg were performed using GROMACS packages. The graphs were analyzed and plotted using GraphPad Prism software.

5.2.4 Confocal microscopy

Neuro-2a cells were grown on coverslips and subsequently transfected with pEGFP-PKM2. The cells were infected with JEV 24 hours post-transfection and 48 hours post-infection, cells were fixed with 4% formaldehyde in PBS for 15 minutes at room temperature. Following fixation, cells were washed with PBS at least 3 times and permeabilized with 0.3% Triton X-100 in PBS. Subsequently, the fixed cells were rinsed using 1X PBS and then incubated in a blocking buffer (5% BSA). For JEV protein detection, cells were incubated with 1/100 dilution of mouse monoclonal antibody against NS1 (GeneTex, USA), followed by incubation with a 1/500 dilution of goat Alexa-fluor 594 (Invitrogen, USA) anti-mouse IgG secondary antibody. After the final wash with PBS, cells were stained with DAPI, and slides were mounted using Prolong Gold Antifade Reagent (Invitrogen, USA) and examined under a 63X objective using the confocal microscope (Zeiss LSM 880, Germany).

5.2.5 Co-immunoprecipitation (Co-IP) assay

Capturem Co-IP kit was procured from TaKaRa (Japan). The Neuro-2a cells were transfected with pEGFP-PKM2, and the cells were infected with JEV 24 hours post-transfection. Infected cells were harvested and lysed after 48 hours in the 200 µl lysis buffer per 1 x 10^6 cells. An appropriate amount of the protease inhibitor cocktail was added to the lysis buffer to yield a 1X final concentration. The collected lysate was centrifuged at 17,000g for 10 minutes at 4 ˚C. The clear supernatant was collected and incubated with the recommended amount of anti-GFP (Bio Bharati, India) and anti-NS1 (GeneTex, USA) antibodies for 3 hours at 4 ˚C. Pre-incubated samples were loaded onto the Capturem protein A columns (TaKaRa) and centrifuged at 1000g for 1 minute at room temperature. Flowthrough was discarded, and spin columns were washed with wash buffer (provided in the kit). Bound samples were eluted from spin columns in elution buffer by centrifugation at 1000g for 1 minute at room temperature and analyzed by Western blot.

5.2.6 Cloning of JEV NS1 in eukaryotic expression vector

Neuro-2a cells were infected with JEV at 0.1 MOI, and 72 hours later, RNA lysate was prepared using RNAiso Plus reagent (TaKaRa, Japan). Total RNA was extracted using the phenol-chloroform extraction method, 1µg of total RNA was reverse transcribed to cDNA using a high-capacity cDNA reverse transcription kit (Thermo Fisher Scientific, USA). The NS1 gene was amplified using specific primer forward primer: 5'CTAGCTAGCATGGACACTGGATGTGCCATTG3' and reverse primer: 5'CGGAATTCCTAAGCAGCGACTAGCAC3. The amplified product was digested with *Nhe*I and *Eco*RI and was ligated using ligase (TaKaRa, Japan) to pre-digested (with the same restriction enzymes) pcDNA3.1 mammalian expression vector (Invitrogen, USA). The positive clone was confirmed by restriction enzyme digestion, and the expression was confirmed by immunoblotting using NS1-specific antibody (GeneTex, USA).

5.2.7 Co-overexpression of PKM2 and NS1

Neuro2a cells were seeded in 35 mm culture dishes, and 12 hours later cells were transfected with pCDNA.NS1 and pEGFP.PKM2 using Lipofectamine 2000 (Invitrogen, USA). 48-hours post-transfection, whole cell lysate was prepared and analyzed using non-reducing SDS-PAGE followed by western blotting.

5.3 Results

5.3.1 Structure modeling of JEV NS1 and mouse PKM2 protein

PKM2 is known to regulate virus infection by directly interacting with viral proteins involved in the replication (Mazurek et al., 2001; Miyake et al., 2017; Wu et al., 2008). NS1 is a key non-structural protein involved in the replication of flavivirus (Rastogi et al., 2016). Therefore, we first investigated the possible PKM2 and JEV NS1 interaction *in silico*. For this, the three-dimensional structure of the mouse PKM2 protein was modeled using I-TASSER (Figure 5.1A). The modeled

structure that was found to be most similar to human PKM2 (PDB ID-3GR4) with RMSD value 0.74 was selected and analyzed for stereochemical stability using a Ramachandran plot, which showed 90.8% residues in most favoured regions, 7.5% in additional allowed regions, 0.9% in generously allowed regions, and only 0.9% in disallowed regions (Figure 5.1B). Similarly, the three-dimensional model of the JEV NS1 protein was predicted (Figure 5.1C). The predicted model was found to be most similar in structure to Zika virus NS1 (PDB ID-5K6K) with RMSD value 0.50, and was subsequently analyzed using a Ramachandran plot which showed 87.8% residues in most favoured regions, 11.6% in additional allowed regions, 0.3% in generously allowed regions, and only 0.3% in disallowed regions (Figure 5.1D).

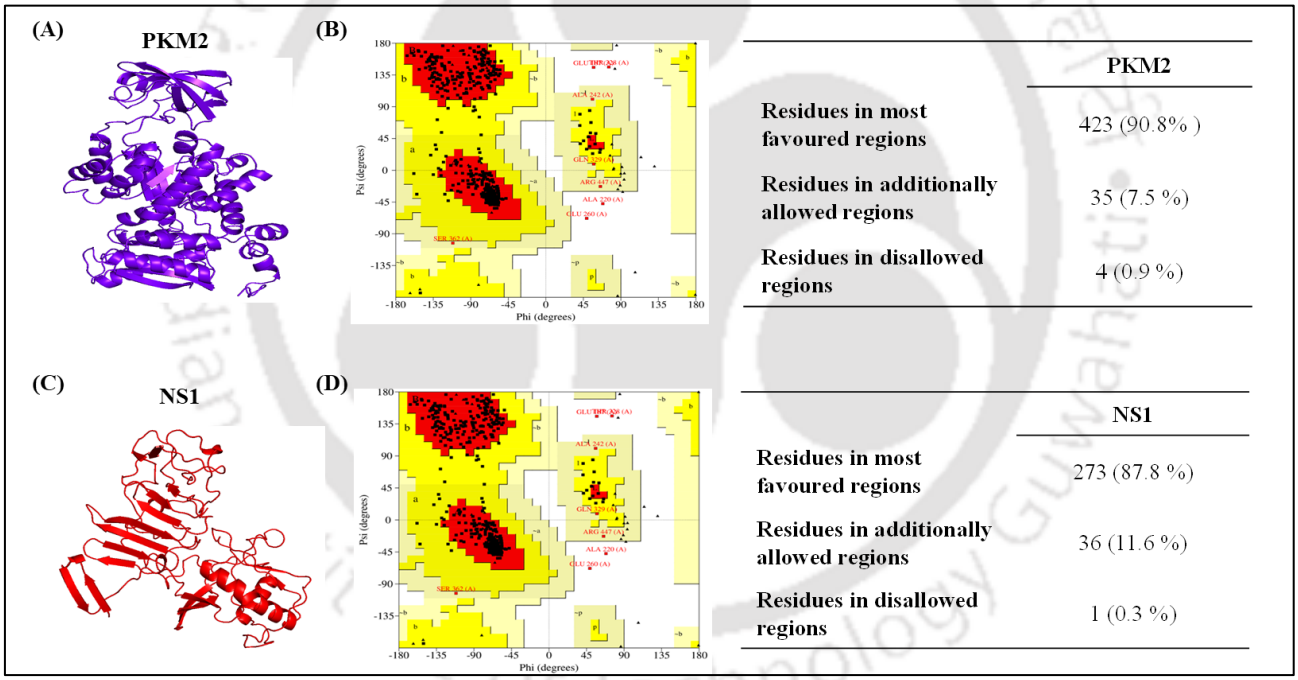

	PKM2
Residues in most favoured regions	423 (90.8%)
Residues in additionally allowed regions	35 (7.5 %)
Residues in disallowed regions	4 (0.9 %)

	NS1
Residues in most favoured regions	273 (87.8 %)
Residues in additionally allowed regions	36 (11.6 %)
Residues in disallowed regions	1 (0.3 %)

Figure 5.1 Structure modeling of JEV NS1 and mouse PKM2 protein. Figures depicting the three-dimensional model of Mouse PKM2 protein (A) with its analyzed Ramachandran plot (B) and the three-dimensional structure of JEV NS1 protein (C) with its analyzed Ramachandran plot (D).

5.3.2 PKM2-NS1 Docking studies

Docking between the predicted structure of the mouse PKM2 protein and the NS1 protein of

JEV was performed (Figure 5.2A). The most stable complex out of the top 5 predicted models of PKM2-NS1 complex was determined using MM/GBSA-based binding free energy values. The most stable PKM2-NS1 complex (M1) with the lowest binding free energy of -150.85 kcal/mol was selected for further analysis. The stereochemical stability of the most stable PKM2-NS1complex was analyzed by Ramachandran plot, which showed 647 residues (83.3%) in the most favourable regions, 112 residues (14.4%) in additionally allowed regions, 10 residues (1.3%) in the generously allowed regions, and 8 residues (1.0%) in the disallowed regions (Figure 5.2B). The interface residues of the complex were also analysed. The 33 residues of PKM2 interacted with 33 residues of NS1 (Figure 5.2C). The number of salt bridges was 6, hydrogen bonds were 24, and non-bonded contacts were 372 (Table 1). These results indicate the potential PKM2 and NS1 interaction.

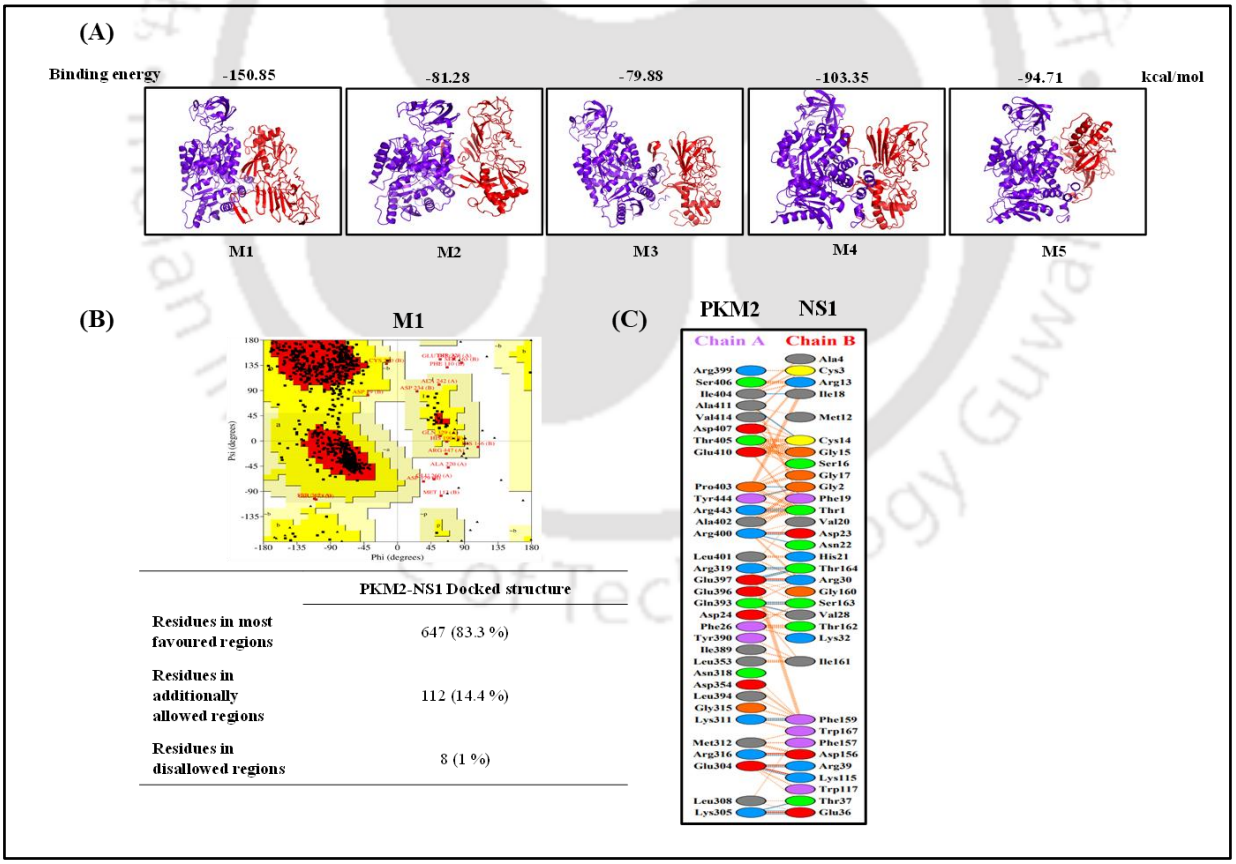

Figure 5.2 PKM2-NS1 Docking studies. Pictures of the predicted docking models (M1, M2, M3, M4 and M5) along with their binding free energies (A). Image representing Ramachandran plot of model

M1 (B). Diagrammatic representation of interacting amino acid residues involved in model M1 (C).

Table 3: The number of interface residues, interface area, salt bridges, H-bonds, and non-bonded contacts involved in PKM2-NS1 interaction.

Interactions	**PKM2 and NS1**
No. of interface residues	33:33:00
Interface area (A^2)	1711:1847
No. of salt bridges	6
No. of H-bonds	24
No. of non-bonded contacts	372

5.3.3 Molecular dynamics simulation studies

MD simulations were performed to test whether the PKM2-NS1 complex was stable over time in a simulated physiological environment, such as a solvated system and appropriate temperature. It rules out false docking results based on the strength and stability of the complex in comparison to the interacting proteins. Several parameters, such as RMSD, RMSF, Rg, and SASA, were analyzed for PKM2, NS1 and PKM2-NS1 complex over a 50 ns time scale. The RMSD plot analysis is crucial in understanding the structural stability of the protein and protein-protein complex. It denotes conformational changes in the structure over a time. Stable RMSD values over a time represent more stable structures (Rastogi et al., 2016). The PKM2, NS1 and PKM2-NS1 complex achieved steadiness at 12 ns, 22 ns, and 17 ns, respectively and remained in equilibrium with only minor changes. The average RMSD values for PKM2, NS1 and PKM2-NS1 complex were 0.35 nm, 0.385 nm, and 0.325 nm, respectively (Figure 5.3A). RMSF evaluates the rigidity and flexibility of a complex. RMSF represents the flexibility of individual atoms or residues within a molecule over a time (Martinez,

2015). C-alpha atoms of the residues of the bound complexes were analyzed to identify the fluctuations of each atom across the backbone. The PKM2, NS1 and PKM2-NS1 complex were stable throughout except for minor fluctuations around the 110 residue region for NS1 and the 500 residue region for PKM2 and PKM2-NS1 complex (Figure 5.3B). The average RMSF values for PKM2, NS1 and PKM2-NS1 complex were 0.119 nm, 0.152 nm, and 0.154 nm, respectively. The rigidity and compactness of the complex were characterized using Rg values. A stable protein or protein-protein complex usually has constant Rg values throughout the simulation (Rastogi et al., 2016). Therefore, it is one of the important parameters to assess the stability of the complex. Rg values for PKM2 acquired equilibrium at 10 ns and maintained it till the end, except for minor fluctuations around 20 ns and 30 ns, while NS1 achieved equilibrium at 6 ns and maintained it till the end, except for minor fluctuations at around 20-26 ns timeframe. The Rg values for the PKM2-NS1 complex showed minor fluctuations in the beginning. However, it achieved equilibrium at around 14 ns and maintained it till the end except for minor fluctuations at around 33–38 ns timeframe (Figure 5.3C). The average Rg values for PKM2, NS1, and PKM2-NS1 complex were 2.58 nm, 2.34 nm, and 3.20 nm, respectively. Additionally, the SASA values were also analyzed to assess the solvent behaviour and examine the folding/unfolding of the PKM2, NS1 and PK2-NS1 complex. Overall SASA values for PKM2, NS1, and the PKM2-NS1 complex remained in equilibrium over the course of the simulation. The average SASA values obtained for the proteins PKM2, NS1 and PKM2-NS1 complex were 248.249 nm^2, 194.187 nm^2 and 403.759 nm^2 respectively (Figure 5.3D). Overall, these parameters show that the PKM2-NS1 complex is stable and rigid.

5.3.4 Cellular localization and interaction studies

Confocal microscopy was performed to study the cellular localization of PKM2 and NS1. Cells were transfected with a PKM2-expressing plasmid and infected with JEV. Immunofluorescence results showed the cellular co-localization of PKM2 with NS1 protein (Figure 5.3A). JEV NS1 protein

localizes in the ER of infected cells (Figure 5.3B). PKM2 showed a strong correlation with NS1 (Pearson correlation coefficient 0.72), and NS1 showed a strong correlation with ER (Pearson correlation coefficient 0.82) in the infected cells (Figure 5.3C). The Co-IP experiment was performed to study the potential interaction between PKM2 and NS1. PKM2 was detected after the pull-down with NS1, while NS1 was detected after the pull-down with GFP. This validated the interaction between PKM2 and NS1 protein (Figure 5.3D). From these microscopic studies, we conclude that PKM2 and NS1 interact with each other, possibly in the ER of infected cells.

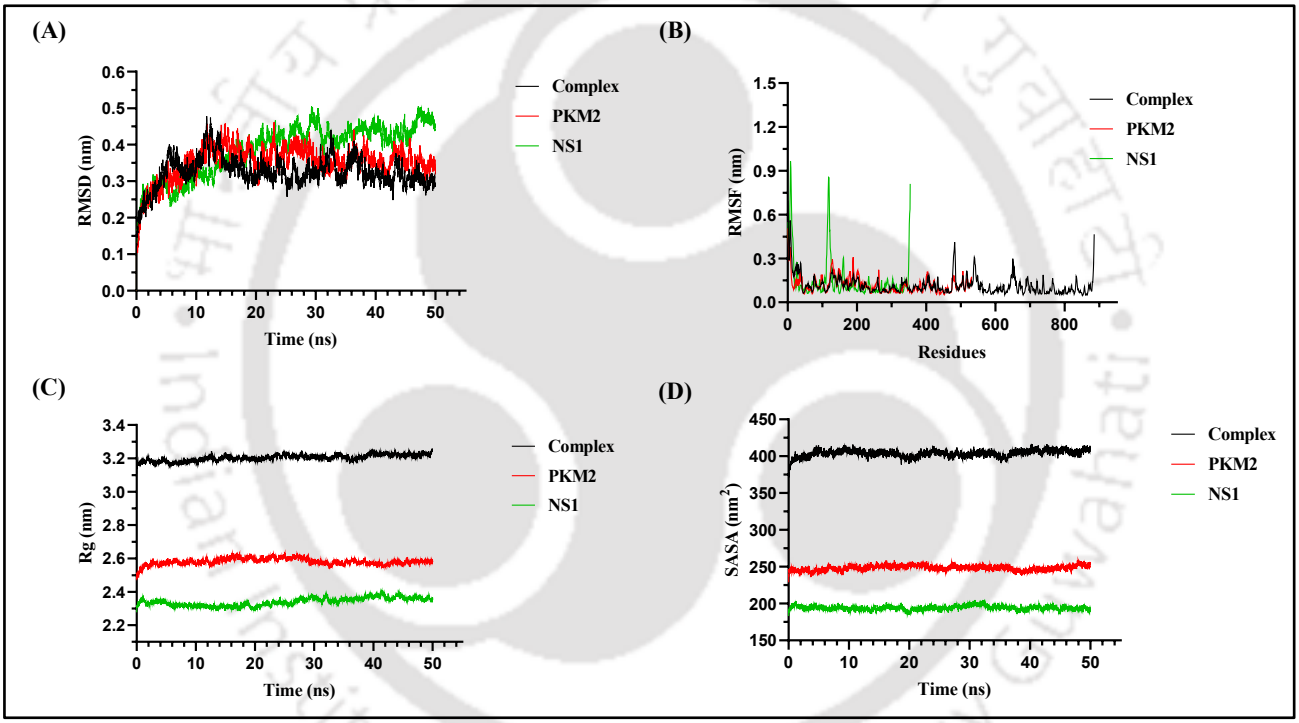

Figure 5.3 Molecular dynamics simulations. Graphs showing results after Root Mean Square Deviation (RMSD) analysis (A), Root Mean Square Fluctuations (RMSF) analysis (B), Radius of Gyration (Rg) analysis (C), and Solvent Accessible Surface Area (SASA) analysis (D).

5.3.5 Effect of PKM2 binding on oligomerization of NS1.

To check the effect of PKM2 on NS1 oligomerization. NS1 was cloned into the eukaryotic expression vector pCDNA3.1. Cloning was confirmed using restriction digestion (Figures 5.5A).

Further, we also analyzed the multimeric form of overexpressed NS1 using non-reducing SDS-PAGE (Figure 5.5B). Next, we co-overexpressed PKM2 and NS1, which did not show any effect of PKM2 on NS1 oligomerization (Figure 5.5C).

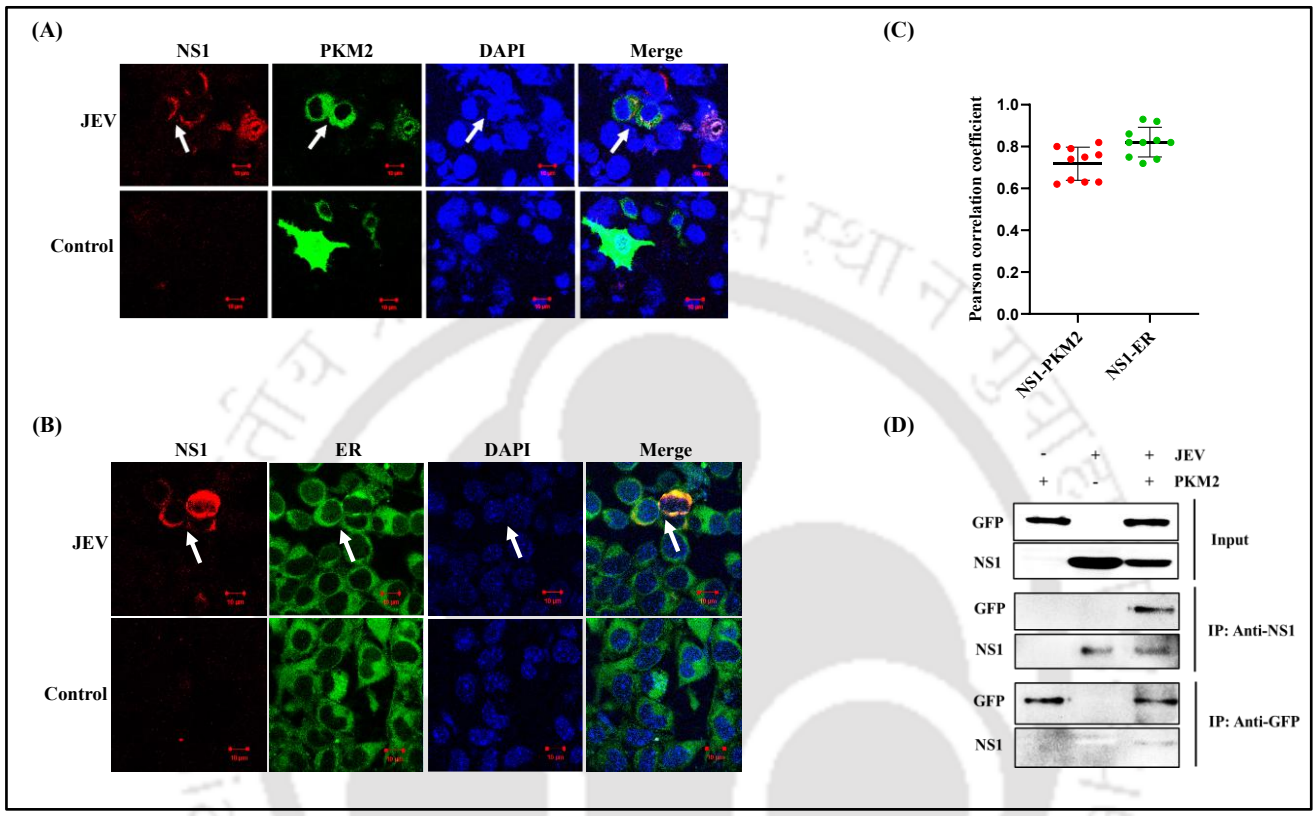

Figure 5.4 Cellular localization and interaction studies**.** Confocal images showing cellular co-localization of PKM2 with NS1 in JEV-infected cells (A). Representative images showing red fluorescence indicate NS1 expression while green fluorescence indicates PKM2 expression. The merge panel shows both PKM2 and NS1 proteins. Cell nuclei were stained with DAPI (blue channel). Arrows indicate cells showing co-localization of PKM2 and NS1 (A). Confocal images showing localization of NS1 (red channel) and ER (green channel) in the JEV-infected cells (B). ER was stained with ER tracker dye while the nucleus was stained with DAPI. Arrows indicate the localization of NS1 in the ER of the infected cells. The graph shows the average Pearson correlation coefficient of PKM2-NS1 and NS1-ER calculated from 10 individual cells (C). The interaction of PKM2 with the NS1 protein of JEV was examined by co-immunoprecipitation assay (co-IP). The cell lysates were immunoprecipitated by anti-NS1 and anti-GFP antibodies and interactions were detected using immunoblot (D). Statistical analysis was performed using student's t-test. `

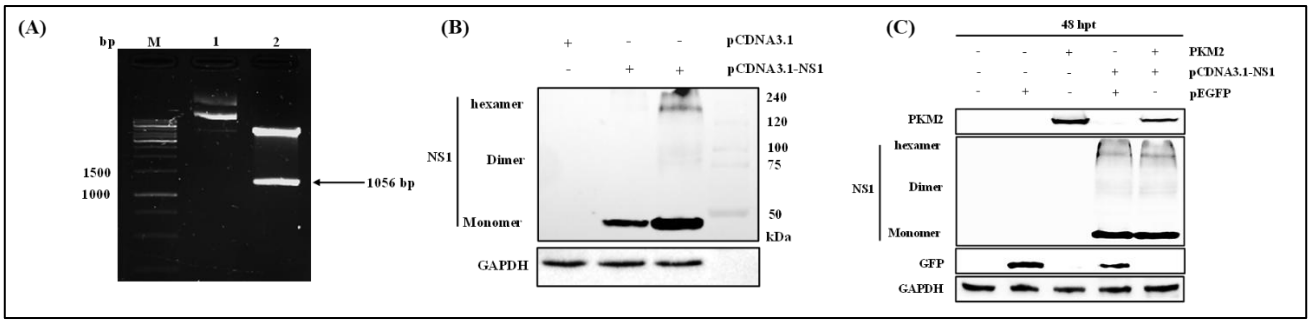

Figure 5.5 Effect of PKM2 binding on oligomerization of NS1. Restriction digestion confirmation image of NS1 cloned in pCDNA3.1 (M: size marker, Lane 1: undigested pCDNA3.1, Lane 2: digested pCDNA3.1-NS1 (NheI and EcoRI) (A). Western blot showing oligomers of NS1 (B). Immunoblot showing oligomers of NS1 in cells overexpressing PKM2 (C).

5.4 Discussion

The present study elucidated the potential interaction between PKM2 and NS1 using both *in silico* and *in vitro* studies. The molecular docking studies yielded the top five PKM2-NS1 complexes, all of which exhibited negative binding free energies, indicating a favorable binding interaction. The most stable PKM2-NS1 complex was found to have a binding free energy of -150.85 kcal/mol. The analysis of the residues involved in the interaction further supported the binding of PKM2 with the NS1 protein of JEV, involving several salt bridges and hydrogen bond linkages. We also analyzed the rigidity and stability of PKM2, NS1 and the PKM2-NS1 complex with the help of molecular dynamics simulations, and comparisons were made using parameters such as RMSD, RMSF, Rg and SASA. The RMSD and RMSF patterns did not show any substantial shifts, which suggested the stability of the PKM2, NS1 and PKM2-NS1 complex. Further, the increase in Rg and SASA values after NS1 binding with PKM2 is because of the increase in the size of the complex compared to individual proteins. Also, the Rg and SASA patterns were overall consistent and suggested a stable complex. Microscopic studies also showed cellular co-localization of PKM2 and NS1 protein with a strong positive correlation between them, suggesting their probable interaction. Also, we observed NS1 to be localized in the ER

of the JEV-infected cells, as indicated by a strong positive correlation coefficient. This was consistent with the previous reports of NS1 reported to be concentrated in the ER membranes to facilitate viral replication (Ci et al., 2020; Xie et al., 2025). PKM2 was also found to be localized in the ER, where it interacts with valosin-containing protein (VCP) and regulates the expression of ER membrane-associated proteins such as TMEM33 (Liu et al., 2021a). It also regulates calcium signaling by interacting directly with IP_3 in the ER (Lavik et al., 2022). Therefore, we concluded that PKM2 probably interacts with NS1 in the ER of infected cells. Further, the interaction of PKM2 with NS1 was validated by the Co-IP assay. Since NS1 localizes in the ER of the infected cells, where it anchors the replication complex and facilitates replication (Sarkar et al., 2024; Xie et al., 2025). Therefore, it can be suggested that both might co-localize in the ER of the infected cells, where PKM2 may interfere with the formation of the replication complex. However, this remains to be experimentally validated. Studies on the dengue virus and influenza A virus have shown that the NS1 protein is phosphorylated (Dechtawewat et al., 2021; Kathum et al., 2016). In the influenza virus, phosphorylation of NS1 at Thr49 was shown to suppress its interferon antagonist activity, whereas phosphorylation at Ser205 was found to be essential for its polymerase-enhancing function (Kathum et al., 2016; Patil et al., 2021). Since dimeric PKM2 acts as a protein kinase, its interaction with NS1 could induce phosphorylation of NS1. Although, depending on the position and type of phosphorylated residues, it can have both positive and negative effects on JEV replication. PKM2 also undergoes several post-translational modifications, one of which is O-GlcNAcylation, the attachment of O-linked N-acetylglucosamine to Ser and Thr residues (Prakasam et al., 2018; Wang et al., 2017c). *O*-GlcNAcylation of PKM2 at Thr405 and Ser406 promotes the Warburg effect by enhancing the translocation of PKM2 to the nucleus (Wang et al., 2017c; Yang and Qian, 2017). Several RNA viruses are known to induce glycolysis to support their replication (Codo et al., 2020a; Fontaine et al., 2015b; Mingo-Casas et al., 2023). We have also shown that Thr405 and Ser406 are interacting residues of PKM2 with NS1. This can affect the *O*-GlcNAcylation of PKM2, thereby regulating glycolysis and JEV replication in the infected cells.

However, further extensive investigation is required to authenticate it. NS1 consists of 6 pairs of cysteine residues, which form disulfide linkages, resulting in the formation of dimeric NS1 (Rastogi et al., 2016). The dimeric NS1, together with other non-structural proteins, forms a replication complex (RC) where replication of the virus genome occurs (Hall et al., 1999; van de Wetering et al., 2020). The cellular dimeric NS1 protein is heavily glycosylated. Its carbohydrate moieties are trimmed off in the trans-Golgi network by glycosidases, resulting in the formation of a soluble hexamer, which is secreted from the cells (Rastogi et al., 2016). We hypothesized that one of the implications of PKM-NS1 interaction could be interference with the formation of NS1 dimers and hexamers, resulting in negative regulation of JEV replication. However, PKM2 and NS1 co-transfection experiments, which did not show any effect of PKM2 on NS1 dimerization, ruled out this possibility, suggesting an alternative way by which PKM2-NS1 interaction impedes JEV replication.

Chapter 6
Conclusion and future prospects

Virus-infected cells have been shown to reprogram glycolysis to fuel the biosynthesis of additional biomacromolecules required for sustained production of new progeny virions. However, the molecular mechanisms involved in the reprogramming of glycolysis differ with viruses (Jaquet et al., 2024; Li et al., 2023b; Passalacqua et al., 2019; Qian et al., 2022).

The present study confirmed the regulation of glycolysis in JEV-infected neurons. In the normal cells, HIF-1α is degraded by ubiquitin-mediated proteasomal degradation (Salceda and Caro, 1997). However, our findings showed that rapid JEV replication in neurons induces ROS accumulation, which prevents the HIF-1α degradation, leading to its stabilization. The increased HIF-1α then translocates to the nucleus and binds to the promoter of glycolytic genes, leading to the overexpression of glycolytic enzymes. The increased expression of glycolytic enzymes supports rapid glycolysis, enhancing glucose utilization in the infected cells compared to uninfected cells.

Although JEV exploits glycolysis for its replication, the specific metabolic changes induced are context-dependent and can vary with the host-cell type (Goyal and Rajala, 2023b). Moreover, there could be multiple strategies simultaneously involved in the regulation of glycolysis by JEV. The current study establishes HIF-1α as a crucial host-transcription factor that modulates the expression of glycolytic enzymes in JEV-infected neuronal cells. Being a multifunctional transcription factor, it has to interact with many other cellular proteins to regulate cellular processes other than glycolysis (Liu et al., 2012). Therefore, there is a possibility that it can modulate JEV replication through multiple other mechanisms simultaneously. Further studies are required for deeper insights into the cross-talk between HIF-1α and JEV infection, which can extend beyond the metabolism. The study also identified glycolytic enzyme PKM2 as a crucial modulator of JEV replication in neuronal cells. From the study,

we concluded that enhanced PKM2 expression in JEV-infected activated STAT3, which in turn modulated the expression of proinflammatory cytokines such as TNF-α and IL-1β, thereby negatively regulating JEV replication in neurons. Beyond its well-known function in metabolism, PKM2 also influences key cellular processes such as cell-cycle regulation, cell migration, apoptosis, and autophagy (Hamza et al., 2023; Jiang et al., 2014a; Luo et al., 2021; Wang et al., 2017a). Exploring these functions in the context of JEV neuropathogenesis could shed more light on the broader impact of PKM2 in JEV replication and uncover potential therapeutic targets. In addition, *in vivo* studies will help in better assessing the effect of PKM2 modulation on viral load, neuroinflammation, and overall disease progression in a complex biological system. Although we have confirmed physical interaction between PKM2 and NS1, and shown the potential interacting residues, further site-directed mutagenesis of specific residues would help in identifying critical residues involved in the interaction and their effect on the overall binding affinity and functionality of the interacting proteins.

Bibliography

Akhtar, K., Gupta, V., Koul, A., Alam, N., Bhat, R., Bamezai, R.N., 2009. Differential behavior of missense mutations in the intersubunit contact domain of the human pyruvate kinase M2 isozyme. J Biol Chem 284, 11971-11981.

Allison, S.L., Schalich, J., Stiasny, K., Mandl, C.W., Kunz, C., Heinz, F.X., 1995. Oligomeric rearrangement of tick-borne encephalitis virus envelope proteins induced by an acidic pH. J Virol 69, 695-700.

Allonso, D., Andrade, I.S., Conde, J.N., Coelho, D.R., Rocha, D.C., da Silva, M.L., Ventura, G.T., Silva, E.M., Mohana-Borges, R., 2015. Dengue Virus NS1 Protein Modulates Cellular Energy Metabolism by Increasing Glyceraldehyde-3-Phosphate Dehydrogenase Activity. J Virol 89, 11871-11883.

Alquraishi, M., Puckett, D.L., Alani, D.S., Humidat, A.S., Frankel, V.D., Donohoe, D.R., Whelan, J., Bettaieb, A., 2019. Pyruvate kinase M2: A simple molecule with complex functions. Free Radic Biol Med 143, 176-192.

Altenberg, B., Greulich, K.O., 2004. Genes of glycolysis are ubiquitously overexpressed in 24 cancer classes. Genomics 84, 1014-1020.

Anastasiou, D., Poulogiannis, G., Asara, J.M., Boxer, M.B., Jiang, J.K., Shen, M., Bellinger, G., Sasaki, A.T., Locasale, J.W., Auld, D.S., Thomas, C.J., Vander Heiden, M.G., Cantley, L.C., 2011. Inhibition of pyruvate kinase M2 by reactive oxygen species contributes to cellular antioxidant responses. Science 334, 1278-1283.

Anastasiou, D., Yu, Y., Israelsen, W.J., Jiang, J.K., Boxer, M.B., Hong, B.S., Tempel, W., Dimov, S., Shen, M., Jha, A., Yang, H., Mattaini, K.R., Metallo, C.M., Fiske, B.P., Courtney, K.D., Malstrom, S., Khan, T.M., Kung, C., Skoumbourdis, A.P., Veith, H., Southall, N., Walsh, M.J., Brimacombe, K.R., Leister, W., Lunt, S.Y., Johnson, Z.R., Yen, K.E., Kunii, K., Davidson, S.M., Christofk, H.R., Austin, C.P., Inglese, J., Harris, M.H., Asara, J.M., Stephanopoulos, G., Salituro, F.G., Jin, S., Dang, L., Auld, D.S., Park, H.W., Cantley, L.C., Thomas, C.J., Vander Heiden, M.G., 2012. Pyruvate kinase M2 activators promote tetramer formation and suppress tumorigenesis. Nat Chem Biol 8, 839-847.

Andersson, U., Wang, H., Palmblad, K., Aveberger, A.C., Bloom, O., Erlandsson-Harris, H., Janson, A., Kokkola, R., Zhang, M., Yang, H., Tracey, K.J., 2000. High mobility group 1 protein (HMG-1) stimulates proinflammatory cytokine synthesis in human monocytes. J Exp Med 192, 565-570.

Argade, S.P., Banerjee, K., 1990. Plasma lactic dehydrogenase in mice infected with Japanese encephalitis & West Nile viruses. Indian J Med Res 91, 307-314.

Armilla, J., 1967. Predicting self-assessed social leadership in a new culture with the MMPI. J Soc Psychol 73, 219-225.

Armstrong, T.D., Pulaski, B.A., Ostrand-Rosenberg, S., 1998. Tumor antigen presentation: changing the rules. Cancer Immunol Immunother 46, 70-74.

Avirutnan, P., Fuchs, A., Hauhart, R.E., Somnuke, P., Youn, S., Diamond, M.S., Atkinson, J.P., 2010. Antagonism of the complement component C4 by flavivirus nonstructural protein NS1. J Exp Med 207, 793-806.

Azoitei, N., Becher, A., Steinestel, K., Rouhi, A., Diepold, K., Genze, F., Simmet, T., Seufferlein, T., 2016. PKM2 promotes tumor angiogenesis by regulating HIF-1α through NF-κB activation. Molecular Cancer 15, 3.

Bao, C., Zhu, S., Song, K., He, C., 2022. HK2: a potential regulator of osteoarthritis via glycolytic and non-glycolytic pathways. Cell Commun Signal 20, 132.

Barban, S., Schulze, H.O., 1961. The effects of 2-deoxyglucose on the growth and metabolism of cultured human cells. J Biol Chem 236, 1887-1890.

Bennaceur, K., Chapman, J., Brikci-Nigassa, L., Sanhadji, K., Touraine, J.L., Portoukalian, J., 2008. Dendritic cells dysfunction in tumour environment. Cancer Lett 272, 186-196.
Berra, E., Benizri, E., Ginouves, A., Volmat, V., Roux, D., Pouyssegur, J., 2003. HIF prolyl-hydroxylase 2 is the key oxygen sensor setting low steady-state levels of HIF-1alpha in normoxia. EMBO J 22, 4082-4090.
Bertrand, J., Marion-Letellier, R., Azhar, S., Chan, P., Legrand, R., Goichon, A., Ghouzali, I., Aziz, M., Vaudry, D., Savoye, G., Dechelotte, P., Coeffier, M., 2015. Glutamine enema regulates colonic ubiquitinated proteins but not proteasome activities during TNBS-induced colitis leading to increased mitochondrial activity. Proteomics 15, 2198-2210.
Bessaud, M., Pastorino, B.A., Peyrefitte, C.N., Rolland, D., Grandadam, M., Tolou, H.J., 2006. Functional characterization of the NS2B/NS3 protease complex from seven viruses belonging to different groups inside the genus Flavivirus. Virus Res 120, 79-90.
Bhatt, A.N., Kumar, A., Rai, Y., Kumari, N., Vedagiri, D., Harshan, K.H., Chinnadurai, V., Chandna, S., 2022a. Glycolytic inhibitor 2-deoxy-D-glucose attenuates SARS-CoV-2 multiplication in host cells and weakens the infective potential of progeny virions. Life Sci 295.
Bhatt, A.N., Kumar, A., Rai, Y., Kumari, N., Vedagiri, D., Harshan, K.H., Chinnadurai, V., Chandna, S., 2022b. Glycolytic inhibitor 2-deoxy-d-glucose attenuates SARS-CoV-2 multiplication in host cells and weakens the infective potential of progeny virions. Life Sci 295, 120411.
Bichler, K.H., Fluchter, S.H., Steimann, J., Strohmaier, W.L., 1989. Combination of hyperthermia and cytostatics in the treatment of bladder cancer. Urol Int 44, 10-14.
Bilz, N.C., Jahn, K., Lorenz, M., Ludtke, A., Hubschen, J.M., Geyer, H., Mankertz, A., Hubner, D., Liebert, U.G., Claus, C., 2018. Rubella Viruses Shift Cellular Bioenergetics to a More Oxidative and Glycolytic Phenotype with a Strain-Specific Requirement for Glutamine. J Virol 92.
Bluemlein, K., Grüning, N.M., Feichtinger, R.G., Lehrach, H., Kofler, B., Ralser, M., 2011. No evidence for a shift in pyruvate kinase PKM1 to PKM2 expression during tumorigenesis. Oncotarget 2, 393-400.
Bose, S., Zhang, C., Le, A., 2021. Glucose Metabolism in Cancer: The Warburg Effect and Beyond. Adv Exp Med Biol 1311, 3-15.
Bratthauer, G.L., 1994. The avidin-biotin complex (ABC) method. Methods Mol Biol 34, 175-184.
Bressanelli, S., Stiasny, K., Allison, S.L., Stura, E.A., Duquerroy, S., Lescar, J., Heinz, F.X., Rey, F.A., 2004. Structure of a flavivirus envelope glycoprotein in its low-pH-induced membrane fusion conformation. EMBO J 23, 728-738.
Bruick, R.K., McKnight, S.L., 2001. A conserved family of prolyl-4-hydroxylases that modify HIF. Science 294, 1337-1340.
Cai, W., Cheng, J., Zong, S., Yu, Y., Wang, Y., Song, Y., He, R., Yuan, S., Chen, T., Hu, M., Pan, Y., Ma, R., Liu, H., Wei, F., 2021. The glycolysis inhibitor 2-deoxyglucose ameliorates adjuvant-induced arthritis by regulating macrophage polarization in an AMPK-dependent manner. Mol Immunol 140, 186-195.
Cairns, R.A., Harris, I.S., Mak, T.W., 2011. Regulation of cancer cell metabolism. Nature reviews. Cancer 11, 85-95.
Carter, C.C., Mast, F.D., Olivier, J.P., Bourgeois, N.M., Kaushansky, A., Aitchison, J.D., 2022. Dengue activates mTORC2 signaling to counteract apoptosis and maximize viral replication. Front Cell Infect Microbiol 12, 979996.
Cervantes-Salazar, M., Angel-Ambrocio, A.H., Soto-Acosta, R., Bautista-Carbajal, P., Hurtado-Monzon, A.M., Alcaraz-Estrada, S.L., Ludert, J.E., Del Angel, R.M., 2015. Dengue virus NS1 protein interacts with the ribosomal protein RPL18: this interaction is required for viral translation and replication in Huh-7 cells. Virology 484, 113-126.
Chan, J.F., Zhu, Z., Chu, H., Yuan, S., Chik, K.K., Chan, C.C., Poon, V.K., Yip, C.C., Zhang, X., Tsang, J.O., Zou, Z., Tee, K.M., Shuai, H., Lu, G., Yuen, K.Y., 2018. The celecoxib derivative kinase

inhibitor AR-12 (OSU-03012) inhibits Zika virus via down-regulation of the PI3K/Akt pathway and protects Zika virus-infected A129 mice: A host-targeting treatment strategy. Antiviral Res 160, 38-47.
Chaneton, B., Hillmann, P., Zheng, L., Martin, A.C.L., Maddocks, O.D.K., Chokkathukalam, A., Coyle, J.E., Jankevics, A., Holding, F.P., Vousden, K.H., Frezza, C., O'Reilly, M., Gottlieb, E., 2012. Serine is a natural ligand and allosteric activator of pyruvate kinase M2. Nature 491, 458-462.
Chen, B., Cepko, C.L., 2009. HDAC4 regulates neuronal survival in normal and diseased retinas. Science 323, 256-259.
Chen, F., Liu, H., Sun, H., Pan, P., Li, Y., Li, D., Hou, T., 2016. Assessing the performance of the MM/PBSA and MM/GBSA methods. 6. Capability to predict protein-protein binding free energies and re-rank binding poses generated by protein-protein docking. Phys Chem Chem Phys 18, 22129-22139.
Chen, J., Li, G., Sun, D., Li, H., Chen, L., 2024. Research progress of hexokinase 2 in inflammatory-related diseases and its inhibitors. Eur J Med Chem 264, 115986.
Chen, L., Shi, Y., Liu, S., Cao, Y., Wang, X., Tao, Y., 2014. PKM2: the thread linking energy metabolism reprogramming with epigenetics in cancer. Int J Mol Sci 15, 11435-11445.
Chen, L.F., Cai, J.X., Zhang, J.J., Tang, Y.J., Chen, J.Y., Xiong, S., Li, Y.L., Zhang, H., Liu, Z., Li, M.M., 2023a. Respiratory syncytial virus co-opts hypoxia-inducible factor-1alpha-mediated glycolysis to favor the production of infectious virus. mBio 14, e0211023.
Chen, L.F., Cai, J.X., Zhang, J.J., Tang, Y.J., Chen, J.Y., Xiong, S., Li, Y.L., Zhang, H., Liu, Z., Li, M.M., 2023b. Respiratory syncytial virus co-opts hypoxia-inducible factor-1α-mediated glycolysis to favor the production of infectious virus. Mbio 14.
Chen, X., Chen, S., Yu, D., 2020a. Protein kinase function of pyruvate kinase M2 and cancer. Cancer Cell International 20, 523.
Chen, X., Chen, S., Yu, D., 2020b. Protein kinase function of pyruvate kinase M2 and cancer. Cancer Cell Int 20, 523.
Cheng, T.Y., Yang, Y.C., Wang, H.P., Tien, Y.W., Shun, C.T., Huang, H.Y., Hsiao, M., Hua, K.T., 2018. Pyruvate kinase M2 promotes pancreatic ductal adenocarcinoma invasion and metastasis through phosphorylation and stabilization of PAK2 protein. Oncogene 37, 1730-1742.
Cheng, Y.L., Lin, Y.S., Chen, C.L., Tsai, T.T., Tsai, C.C., Wu, Y.W., Ou, Y.D., Chu, Y.Y., Wang, J.M., Yu, C.Y., Lin, C.F., 2016. Activation of Nrf2 by the dengue virus causes an increase in CLEC5A, which enhances TNF-alpha production by mononuclear phagocytes. Sci Rep 6, 32000.
Chi, P.I., Huang, W.R., Chiu, H.C., Li, J.Y., Nielsen, B.L., Liu, H.J., 2018. Avian reovirus sigmaA-modulated suppression of lactate dehydrogenase and upregulation of glutaminolysis and the mTOC1/eIF4E/HIF-1alpha pathway to enhance glycolysis and the TCA cycle for virus replication. Cell Microbiol 20, e12946.
Christofk, H.R., Vander Heiden, M.G., Harris, M.H., Ramanathan, A., Gerszten, R.E., Wei, R., Fleming, M.D., Schreiber, S.L., Cantley, L.C., 2008a. The M2 splice isoform of pyruvate kinase is important for cancer metabolism and tumour growth. Nature 452, 230-233.
Christofk, H.R., Vander Heiden, M.G., Harris, M.H., Ramanathan, A., Gerszten, R.E., Wei, R., Fleming, M.D., Schreiber, S.L., Cantley, L.C., 2008b. The M2 splice isoform of pyruvate kinase is important for cancer metabolism and tumour growth. Nature 452, 230-233.
Christofk, H.R., Vander Heiden, M.G., Wu, N., Asara, J.M., Cantley, L.C., 2008c. Pyruvate kinase M2 is a phosphotyrosine-binding protein. Nature 452, 181-186.
Chung-Faye, G., Hayee, B., Maestranzi, S., Donaldson, N., Forgacs, I., Sherwood, R., 2007. Fecal M2-pyruvate kinase (M2-PK): a novel marker of intestinal inflammation. Inflamm Bowel Dis 13, 1374-1378.
Ci, Y., Liu, Z.Y., Zhang, N.N., Niu, Y., Yang, Y., Xu, C., Yang, W., Qin, C.F., Shi, L., 2020. Zika NS1-induced ER remodeling is essential for viral replication. J Cell Biol 219.
Clayton, S.A., Lockwood, C., O'Neil, J.D., Daley, K.K., Hain, S., Abdelmottaleb, D., Bolimowska, O.O., Tennant, D.A., Clark, A.R., 2023. The glucocorticoid dexamethasone inhibits HIF-1alpha

stabilization and metabolic reprogramming in lipopolysaccharide-stimulated primary macrophages. Discov Immunol 2, kyad027.
Clower, C.V., Chatterjee, D., Wang, Z., Cantley, L.C., Vander Heiden, M.G., Krainer, A.R., 2010. The alternative splicing repressors hnRNP A1/A2 and PTB influence pyruvate kinase isoform expression and cell metabolism. Proc Natl Acad Sci U S A 107, 1894-1899.
Codo, A.C., Davanzo, G.G., Monteiro, L.B., de Souza, G.F., Muraro, S.P., Virgilio-da-Silva, J.V., Prodonoff, J.S., Carregari, V.C., de Biagi Junior, C.A.O., Crunfli, F., Jimenez Restrepo, J.L., Vendramini, P.H., Reis-de-Oliveira, G., Bispo Dos Santos, K., Toledo-Teixeira, D.A., Parise, P.L., Martini, M.C., Marques, R.E., Carmo, H.R., Borin, A., Coimbra, L.D., Boldrini, V.O., Brunetti, N.S., Vieira, A.S., Mansour, E., Ulaf, R.G., Bernardes, A.F., Nunes, T.A., Ribeiro, L.C., Palma, A.C., Agrela, M.V., Moretti, M.L., Sposito, A.C., Pereira, F.B., Velloso, L.A., Vinolo, M.A.R., Damasio, A., Proenca-Modena, J.L., Carvalho, R.F., Mori, M.A., Martins-de-Souza, D., Nakaya, H.I., Farias, A.S., Moraes-Vieira, P.M., 2020a. Elevated Glucose Levels Favor SARS-CoV-2 Infection and Monocyte Response through a HIF-1alpha/Glycolysis-Dependent Axis. Cell Metab 32, 498-499.
Codo, A.C., Davanzo, G.G., Monteiro, L.B., de Souza, G.F., Muraro, S.P., Virgilio-da-Silva, J.V., Prodonoff, J.S., Carregari, V.C., de Biagi Junior, C.A.O., Crunfli, F., Jimenez Restrepo, J.L., Vendramini, P.H., Reis-de-Oliveira, G., Bispo Dos Santos, K., Toledo-Teixeira, D.A., Parise, P.L., Martini, M.C., Marques, R.E., Carmo, H.R., Borin, A., Coimbra, L.D., Boldrini, V.O., Brunetti, N.S., Vieira, A.S., Mansour, E., Ulaf, R.G., Bernardes, A.F., Nunes, T.A., Ribeiro, L.C., Palma, A.C., Agrela, M.V., Moretti, M.L., Sposito, A.C., Pereira, F.B., Velloso, L.A., Vinolo, M.A.R., Damasio, A., Proenca-Modena, J.L., Carvalho, R.F., Mori, M.A., Martins-de-Souza, D., Nakaya, H.I., Farias, A.S., Moraes-Vieira, P.M., 2020b. Elevated Glucose Levels Favor SARS-CoV-2 Infection and Monocyte Response through a HIF-1alpha/Glycolysis-Dependent Axis. Cell Metab 32, 437-446 e435.
Coloff, J.L., Mason, E.F., Altman, B.J., Gerriets, V.A., Liu, T., Nichols, A.N., Zhao, Y., Wofford, J.A., Jacobs, S.R., Ilkayeva, O., Garrison, S.P., Zambetti, G.P., Rathmell, J.C., 2011. Akt requires glucose metabolism to suppress puma expression and prevent apoptosis of leukemic T cells. J Biol Chem 286, 5921-5933.
Damasceno, L.E.A., Prado, D.S., Veras, F.P., Fonseca, M.M., Toller-Kawahisa, J.E., Rosa, M.H., Publio, G.A., Martins, T.V., Ramalho, F.S., Waisman, A., Cunha, F.Q., Cunha, T.M., Alves-Filho, J.C., 2020. PKM2 promotes Th17 cell differentiation and autoimmune inflammation by fine-tuning STAT3 activation. J Exp Med 217.
Datta, P.K., Deshmane, S., Khalili, K., Merali, S., Gordon, J.C., Fecchio, C., Barrero, C.A., 2016. Glutamate metabolism in HIV-1 infected macrophages: Role of HIV-1 Vpr. Cell Cycle 15, 2288-2298.
Day, A.S., Judd, T., Lemberg, D.A., Leach, S.T., 2012. Fecal M2-PK in children with Crohn's disease: a preliminary report. Dig Dis Sci 57, 2166-2170.
Dayan, F., Roux, D., Brahimi-Horn, M.C., Pouyssegur, J., Mazure, N.M., 2006. The oxygen sensor factor-inhibiting hypoxia-inducible factor-1 controls expression of distinct genes through the bifunctional transcriptional character of hypoxia-inducible factor-1alpha. Cancer Res 66, 3688-3698.
de Beer, T.A., Berka, K., Thornton, J.M., Laskowski, R.A., 2014. PDBsum additions. Nucleic Acids Res 42, D292-296.
de Farias, I.S., Ribeiro, G., Noronha, I.H., Lucena, V.W.L., Peron, J.P.S., Moraes-Vieira, P.M., Alves-Filho, J.C., Bortoluci, K.R., 2025a. Caspase-1/11 controls Zika virus replication in astrocytes by inhibiting glycolytic metabolism. FEBS J 292, 3113-3128.
de Farias, I.S., Ribeiro, G., Noronha, I.H., Lucena, V.W.L., Peron, J.P.S., Moraes-Vieira, P.M., Alves-Filho, J.C., Bortoluci, K.R., 2025b. Caspase-1/11 controls Zika virus replication in astrocytes by inhibiting glycolytic metabolism. FEBS J.
De Wied, D., De Kloet, E.R., 1987. Pro-opiomelanocortin (POMC) as homeostatic control system. Ann N Y Acad Sci 512, 328-337.

de Wit, R.H., Mujic-Delic, A., van Senten, J.R., Fraile-Ramos, A., Siderius, M., Smit, M.J., 2016. Human cytomegalovirus encoded chemokine receptor US28 activates the HIF-1alpha/PKM2 axis in glioblastoma cells. Oncotarget 7, 67966-67985.
Dechtawewat, T., Roytrakul, S., Yingchutrakul, Y., Charoenlappanit, S., Siridechadilok, B., Limjindaporn, T., Mangkang, A., Prommool, T., Puttikhunt, C., Songprakhon, P., Kongmanas, K., Kaewjew, N., Avirutnan, P., Yenchitsomanus, P.T., Malasit, P., Noisakran, S., 2021. Potential Phosphorylation of Viral Nonstructural Protein 1 in Dengue Virus Infection. Viruses 13.
Deming, S.N., 1991. Proficiency testing of clinical chemistry laboratories: the role of the reference laboratory. Clin Chem 37, 483.
Deshmane, S.L., Mukerjee, R., Fan, S., Del Valle, L., Michiels, C., Sweet, T., Rom, I., Khalili, K., Rappaport, J., Amini, S., Sawaya, B.E., 2009. Activation of the oxidative stress pathway by HIV-1 Vpr leads to induction of hypoxia-inducible factor 1alpha expression. J Biol Chem 284, 11364-11373.
Dey, D., Poudyal, S., Rehman, A., Hasan, S.S., 2021. Structural and biochemical insights into flavivirus proteins. Virus Res 296, 198343.
Dong, G., Mao, Q., Xia, W., Xu, Y., Wang, J., Xu, L., Jiang, F., 2016a. PKM2 and cancer: The function of PKM2 beyond glycolysis. Oncol Lett 11, 1980-1986.
Dong, G., Mao, Q., Xia, W., Xu, Y., Wang, J., Xu, L., Jiang, F., 2016b. PKM2 and cancer: The function of PKM2 beyond glycolysis (Review). Oncol Lett 11, 1980-1986.
Dong, H., Fink, K., Zust, R., Lim, S.P., Qin, C.F., Shi, P.Y., 2014. Flavivirus RNA methylation. J Gen Virol 95, 763-778.
Dunn, D.M., Rodriguez-Sanchez, I., Schafer, X., Munger, J., 2021. Human Cytomegalovirus Induces the Expression of the AMPKa2 Subunit to Drive Glycolytic Activation and Support Productive Viral Infection. J Virol 95.
Edeling, M.A., Diamond, M.S., Fremont, D.H., 2014. Structural basis of Flavivirus NS1 assembly and antibody recognition. Proc Natl Acad Sci U S A 111, 4285-4290.
El-Bacha, T., Menezes, M.M., Azevedo e Silva, M.C., Sola-Penna, M., Da Poian, A.T., 2004. Mayaro virus infection alters glucose metabolism in cultured cells through activation of the enzyme 6-phosphofructo 1-kinase. Mol Cell Biochem 266, 191-198.
Elshuber, S., Allison, S.L., Heinz, F.X., Mandl, C.W., 2003. Cleavage of protein prM is necessary for infection of BHK-21 cells by tick-borne encephalitis virus. J Gen Virol 84, 183-191.
Epstein, T., Xu, L., Gillies, R.J., Gatenby, R.A., 2014. Separation of metabolic supply and demand: aerobic glycolysis as a normal physiological response to fluctuating energetic demands in the membrane. Cancer Metab 2, 7.
Erbel, P.J.A., Card, P.B., Karakuzu, O., Bruick, R.K., Gardner, K.H., 2003. Structural basis for PAS domain heterodimerization in the basic helix-loop-helix-PAS transcription factor hypoxia-inducible factor. P Natl Acad Sci USA 100, 15504-15509.
Fan, L., Liang, Z., Ren, J., Chen, Y., Zhu, H., Chen, Y., Xiang, B., Lin, Q., Ding, C., Chen, L., Ren, T., 2024. Newcastle disease virus activates the PI3K/AKT signaling pathway by targeting PHLPP2 degradation to delay cell apoptosis and promote viral replication. Vet Microbiol 289, 109949.
Fan, W., Qian, P., Wang, D., Zhi, X., Wei, Y., Chen, H., Li, X., 2017. Integrin alphavbeta3 promotes infection by Japanese encephalitis virus. Res Vet Sci 111, 67-74.
Faubert, B., Boily, G., Izreig, S., Griss, T., Samborska, B., Dong, Z., Dupuy, F., Chambers, C., Fuerth, B.J., Viollet, B., Mamer, O.A., Avizonis, D., DeBerardinis, R.J., Siegel, P.M., Jones, R.G., 2013. AMPK is a negative regulator of the Warburg effect and suppresses tumor growth in vivo. Cell Metab 17, 113-124.
Findlay, J.S., Ulaeto, D., 2015. Semliki Forest virus and Sindbis virus, but not vaccinia virus, require glycolysis for optimal replication. J Gen Virol 96, 2693-2696.
Flamand, M., Megret, F., Mathieu, M., Lepault, J., Rey, F.A., Deubel, V., 1999. Dengue virus type 1 nonstructural glycoprotein NS1 is secreted from mammalian cells as a soluble hexamer in a glycosylation-dependent fashion. J Virol 73, 6104-6110.

Fontaine, K.A., Sanchez, E.L., Camarda, R., Lagunoff, M., 2015a. Dengue Virus Induces and Requires Glycolysis for Optimal Replication. Journal of Virology 89, 2358-2366.
Fontaine, K.A., Sanchez, E.L., Camarda, R., Lagunoff, M., 2015b. Dengue virus induces and requires glycolysis for optimal replication. J Virol 89, 2358-2366.
Gao, X., Wang, H., Yang, J.J., Liu, X., Liu, Z.R., 2012. Pyruvate kinase M2 regulates gene transcription by acting as a protein kinase. Mol Cell 45, 598-609.
Gohlke, H., Case, D.A., 2004. Converging free energy estimates: MM-PB(GB)SA studies on the protein-protein complex Ras-Raf. J Comput Chem 25, 238-250.
Gong, Y., Tang, N., Liu, P., Sun, Y., Lu, S., Liu, W., Tan, L., Song, C., Qiu, X., Liao, Y., Yu, S., Liu, X., Lin, S.H., Ding, C., 2022. Newcastle disease virus degrades SIRT3 via PINK1-PRKN-dependent mitophagy to reprogram energy metabolism in infected cells. Autophagy 18, 1503-1521.
Goyal, P., Rajala, M.S., 2023a. Reprogramming of glucose metabolism in virus infected cells. Mol Cell Biochem 478, 2409-2418.
Goyal, P., Rajala, M.S., 2023b. Reprogramming of glucose metabolism in virus infected cells. Mol Cell Biochem 478, 2409-2418.
Gratton, R., Agrelli, A., Tricarico, P.M., Brandao, L., Crovella, S., 2019. Autophagy in Zika Virus Infection: A Possible Therapeutic Target to Counteract Viral Replication. Int J Mol Sci 20.
Greer, E.L., Oskoui, P.R., Banko, M.R., Maniar, J.M., Gygi, M.P., Gygi, S.P., Brunet, A., 2007. The energy sensor AMP-activated protein kinase directly regulates the mammalian FOXO3 transcription factor. J Biol Chem 282, 30107-30119.
Guadagnin, E., Narola, J., Bonnemann, C.G., Chen, Y.W., 2015. Tyrosine 705 Phosphorylation of STAT3 Is Associated with Phenotype Severity in TGFbeta1 Transgenic Mice. Biomed Res Int 2015, 843743.
Gualdoni, G.A., Mayer, K.A., Kapsch, A.M., Kreuzberg, K., Puck, A., Kienzl, P., Oberndorfer, F., Fruhwirth, K., Winkler, S., Blaas, D., Zlabinger, G.J., Stockl, J., 2018. Rhinovirus induces an anabolic reprogramming in host cell metabolism essential for viral replication. Proc Natl Acad Sci U S A 115, E7158-E7165.
Guarnieri, J.W., Dybas, J.M., Fazelinia, H., Kim, M.S., Frere, J., Zhang, Y., Soto Albrecht, Y., Murdock, D.G., Angelin, A., Singh, L.N., Weiss, S.L., Best, S.M., Lott, M.T., Zhang, S., Cope, H., Zaksas, V., Saravia-Butler, A., Meydan, C., Foox, J., Mozsary, C., Bram, Y., Kidane, Y., Priebe, W., Emmett, M.R., Meller, R., Demharter, S., Stentoft-Hansen, V., Salvatore, M., Galeano, D., Enguita, F.J., Grabham, P., Trovao, N.S., Singh, U., Haltom, J., Heise, M.T., Moorman, N.J., Baxter, V.K., Madden, E.A., Taft-Benz, S.A., Anderson, E.J., Sanders, W.A., Dickmander, R.J., Baylin, S.B., Wurtele, E.S., Moraes-Vieira, P.M., Taylor, D., Mason, C.E., Schisler, J.C., Schwartz, R.E., Beheshti, A., Wallace, D.C., 2023. Core mitochondrial genes are down-regulated during SARS-CoV-2 infection of rodent and human hosts. Sci Transl Med 15, eabq1533.
Guo, M., Zhao, X., Yuan, X., Jiang, J., Li, P., 2017. MiR-let-7a inhibits cell proliferation, migration, and invasion by down-regulating PKM2 in cervical cancer. Oncotarget 8, 28226-28236.
Gupta, A., Bohara, V.S., Chauhan, A.S., Mohapatra, A., Kaur, H., Sharma, A., Chaudhary, N., Kumar, S., 2024a. Alpha-synuclein expression in neurons modulates Japanese encephalitis virus infection. J Virol 98, e0041824.
Gupta, A., Bohara, V.S., Siddegowda, Y.B., Chaudhary, N., Kumar, S., 2024b. Alpha-synuclein and RNA viruses: Exploring the neuronal nexus. Virology 597, 110141.
Gupta, V., Bamezai, R.N., 2010. Human pyruvate kinase M2: a multifunctional protein. Protein Sci 19, 2031-2044.
Gupta, V., Kalaiarasan, P., Faheem, M., Singh, N., Iqbal, M.A., Bamezai, R.N., 2010. Dominant negative mutations affect oligomerization of human pyruvate kinase M2 isozyme and promote cellular growth and polyploidy. J Biol Chem 285, 16864-16873.
Haas, R., Smith, J., Rocher-Ros, V., Nadkarni, S., Montero-Melendez, T., D'Acquisto, F., Bland, E.J., Bombardieri, M., Pitzalis, C., Perretti, M., Marelli-Berg, F.M., Mauro, C., 2015. Lactate Regulates

Metabolic and Pro-inflammatory Circuits in Control of T Cell Migration and Effector Functions. PLoS Biol 13, e1002202.
Hajari, N., Knoll, M., Lu, A., Barber-Axthelm, I., Gale, M., Jr., 2025. The Zika virus NS5 protein binds HSP90 to suppress EGF-induced Akt signaling and trophoblast cell migration. Virology 603, 110370.
Hall, R.A., Khromykh, A.A., Mackenzie, J.M., Scherret, J.H., Khromykh, T.I., Mackenzie, J.S., 1999. Loss of dimerisation of the nonstructural protein NS1 of Kunjin virus delays viral replication and reduces virulence in mice, but still allows secretion of NS1. Virology 264, 66-75.
Hamabe, A., Konno, M., Tanuma, N., Shima, H., Tsunekuni, K., Kawamoto, K., Nishida, N., Koseki, J., Mimori, K., Gotoh, N., Yamamoto, H., Doki, Y., Mori, M., Ishii, H., 2014. Role of pyruvate kinase M2 in transcriptional regulation leading to epithelial-mesenchymal transition. Proc Natl Acad Sci U S A 111, 15526-15531.
Hamza, A., Cho, J.Y., Cap, K.C., Hossain, A.J., Kim, J.G., Park, J.B., 2023. Extracellular pyruvate kinase M2 induces cell migration through p-Tyr42 RhoA-mediated superoxide generation and epithelial-mesenchymal transition. Free Radic Biol Med 208, 614-629.
He, X., Du, S., Lei, T., Li, X., Liu, Y., Wang, H., Tong, R., Wang, Y., 2017. PKM2 in carcinogenesis and oncotherapy. Oncotarget 8, 110656-110670.
Hegedus, A., Williamson, M.K., Huthoff, H., 2014. HIV-1 pathogenicity and virion production are dependent on the metabolic phenotype of activated CD4+T cells. Retrovirology 11.
Hess, B., Kutzner, C., van der Spoel, D., Lindahl, E., 2008. GROMACS 4: Algorithms for Highly Efficient, Load-Balanced, and Scalable Molecular Simulation. J Chem Theory Comput 4, 435-447.
Heyward, P., Eisenhofer, G., 1985. Ethanol-induced inhibition of the drinking response to hypertonic saline in the rat. Pharmacol Biochem Behav 22, 493-496.
Hitosugi, T., Kang, S., Vander Heiden, M.G., Chung, T.W., Elf, S., Lythgoe, K., Dong, S., Lonial, S., Wang, X., Chen, G.Z., Xie, J., Gu, T.L., Polakiewicz, R.D., Roesel, J.L., Boggon, T.J., Khuri, F.R., Gilliland, D.G., Cantley, L.C., Kaufman, J., Chen, J., 2009. Tyrosine phosphorylation inhibits PKM2 to promote the Warburg effect and tumor growth. Sci Signal 2, ra73.
Holbrook, M.R., 2017. Historical Perspectives on Flavivirus Research. Viruses 9.
Hon, W.C., Wilson, M.I., Harlos, K., Claridge, T.D., Schofield, C.J., Pugh, C.W., Maxwell, P.H., Ratcliffe, P.J., Stuart, D.I., Jones, E.Y., 2002. Structural basis for the recognition of hydroxyproline in HIF-1 alpha by pVHL. Nature 417, 975-978.
Hsu, C.Y., Huang, J.W., Huang, W.R., Chen, I.C., Chen, M.S., Liao, T.L., Chang, Y.K., Munir, M., Liu, H.J., 2023. Oncolytic Avian Reovirus sigmaA-Modulated Upregulation of the HIF-1alpha/C-myc/glut1 Pathway to Produce More Energy in Different Cancer Cell Lines Benefiting Virus Replication. Viruses 15.
Hu, M., Bogoyevitch, M.A., Jans, D.A., 2023. Respiratory Syncytial Virus Matrix Protein Is Sufficient and Necessary to Remodel Host Mitochondria in Infection. Cells 12.
Hu, T., Wu, Z., Wu, S., Chen, S., Cheng, A., 2021. The key amino acids of E protein involved in early flavivirus infection: viral entry. Virol J 18, 136.
Hu, W., Lu, S.X., Li, M., Zhang, C., Liu, L.L., Fu, J., Jin, J.T., Luo, R.Z., Zhang, C.Z., Yun, J.P., 2015. Pyruvate kinase M2 prevents apoptosis via modulating Bim stability and associates with poor outcome in hepatocellular carcinoma. Oncotarget 6, 6570-6583.
Huang, A.Y., Golumbek, P., Ahmadzadeh, M., Jaffee, E., Pardoll, D., Levitsky, H., 1994. Bone marrow-derived cells present MHC class I-restricted tumour antigens in priming of antitumour immune responses. Ciba Found Symp 187, 229-240; discussion 240-224.
Hung, Y.P., Teragawa, C., Kosaisawe, N., Gillies, T.E., Pargett, M., Minguet, M., Distor, K., Rocha-Gregg, B.L., Coloff, J.L., Keibler, M.A., Stephanopoulos, G., Yellen, G., Brugge, J.S., Albeck, J.G., 2017. Akt regulation of glycolysis mediates bioenergetic stability in epithelial cells. Elife 6.
Iansante, V., Choy, P.M., Fung, S.W., Liu, Y., Chai, J.G., Dyson, J., Del Rio, A., D'Santos, C., Williams, R., Chokshi, S., Anders, R.A., Bubici, C., Papa, S., 2015. PARP14 promotes the Warburg

effect in hepatocellular carcinoma by inhibiting JNK1-dependent PKM2 phosphorylation and activation. Nat Commun 6, 7882.
Iqbal, M.A., Siddiqui, F.A., Gupta, V., Chattopadhyay, S., Gopinath, P., Kumar, B., Manvati, S., Chaman, N., Bamezai, R.N., 2013. Insulin enhances metabolic capacities of cancer cells by dual regulation of glycolytic enzyme pyruvate kinase M2. Mol Cancer 12, 72.
Israelsen, W.J., Vander Heiden, M.G., 2015. Pyruvate kinase: Function, regulation and role in cancer. Semin Cell Dev Biol 43, 43-51.
Jaquet, M., Bengue, M., Lambert, K., Carnac, G., Missé, D., Bisbal, C., 2024. Human muscle cells sensitivity to chikungunya virus infection relies on their glycolysis activity and differentiation stage. Biochimie 218, 85-95.
Jiang, Y., Li, X., Yang, W., Hawke, D.H., Zheng, Y., Xia, Y., Aldape, K., Wei, C., Guo, F., Chen, Y., Lu, Z., 2014a. PKM2 regulates chromosome segregation and mitosis progression of tumor cells. Mol Cell 53, 75-87.
Jiang, Y., Wang, Y., Wang, T., Hawke, D.H., Zheng, Y., Li, X., Zhou, Q., Majumder, S., Bi, E., Liu, D.X., Huang, S., Lu, Z., 2014b. PKM2 phosphorylates MLC2 and regulates cytokinesis of tumour cells. Nat Commun 5, 5566.
Jung, G.S., Jeon, J.H., Choi, Y.K., Jang, S.Y., Park, S.Y., Kim, S.W., Byun, J.K., Kim, M.K., Lee, S., Shin, E.C., Lee, I.K., Kang, Y.N., Park, K.G., 2016a. Pyruvate dehydrogenase kinase regulates hepatitis C virus replication. Sci Rep-Uk 6.
Jung, G.S., Jeon, J.H., Choi, Y.K., Jang, S.Y., Park, S.Y., Kim, S.W., Byun, J.K., Kim, M.K., Lee, S., Shin, E.C., Lee, I.K., Kang, Y.N., Park, K.G., 2016b. Pyruvate dehydrogenase kinase regulates hepatitis C virus replication. Sci Rep 6, 30846.
Jung, S.N., Yang, W.K., Kim, J., Kim, H.S., Kim, E.J., Yun, H., Park, H., Kim, S.S., Choe, W., Kang, I., Ha, J., 2008. Reactive oxygen species stabilize hypoxia-inducible factor-1 alpha protein and stimulate transcriptional activity via AMP-activated protein kinase in DU145 human prostate cancer cells. Carcinogenesis 29, 713-721.
Jurica, M.S., Mesecar, A., Heath, P.J., Shi, W., Nowak, T., Stoddard, B.L., 1998. The allosteric regulation of pyruvate kinase by fructose-1,6-bisphosphate. Structure 6, 195-210.
Kathum, O.A., Schrader, T., Anhlan, D., Nordhoff, C., Liedmann, S., Pande, A., Mellmann, A., Ehrhardt, C., Wixler, V., Ludwig, S., 2016. Phosphorylation of influenza A virus NS1 protein at threonine 49 suppresses its interferon antagonistic activity. Cell Microbiol 18, 784-791.
Kavanagh Williamson, M., Coombes, N., Juszczak, F., Athanasopoulos, M., Khan, M.B., Eykyn, T.R., Srenathan, U., Taams, L.S., Dias Zeidler, J., Da Poian, A.T., Huthoff, H., 2018. Upregulation of Glucose Uptake and Hexokinase Activity of Primary Human CD4+ T Cells in Response to Infection with HIV-1. Viruses 10.
Keller, K.E., Doctor, Z.M., Dwyer, Z.W., Lee, Y.S., 2014. SAICAR induces protein kinase activity of PKM2 that is necessary for sustained proliferative signaling of cancer cells. Mol Cell 53, 700-709.
Kim, J.K., Kim, J.M., Song, B.H., Yun, S.I., Yun, G.N., Byun, S.J., Lee, Y.M., 2015. Profiling of viral proteins expressed from the genomic RNA of Japanese encephalitis virus using a panel of 15 region-specific polyclonal rabbit antisera: implications for viral gene expression. PLoS One 10, e0124318.
Kleinehr, J., Schofbanker, M., Daniel, K., Gunl, F., Mohamed, F.F., Janowski, J., Brunotte, L., Boergeling, Y., Liebmann, M., Behrens, M., Gerdemann, A., Klotz, L., Esselen, M., Humpf, H.U., Ludwig, S., Hrincius, E.R., 2023. Glycolytic interference blocks influenza A virus propagation by impairing viral polymerase-driven synthesis of genomic vRNA. PLoS Pathog 19, e1010986.
Kohio, H.P., Adamson, A.L., 2013. Glycolytic control of vacuolar-type ATPase activity: a mechanism to regulate influenza viral infection. Virology 444, 301-309.
Kolesnik, D.L., Prokhorova, I.V., Pyaskovskaya, O.N., Solyanik, G.I., 2023. Effect of Lactate Dehydrogenase Inhibition by Oxamate on Lewis Lung Carcinoma Cells with Different Metastatic Potential. Exp Oncol 45, 242-251.

Kong, W., Mao, J., Yang, Y., Yuan, J., Chen, J., Luo, Y., Lai, T., Zuo, L., 2020. Mechanisms of mTOR and Autophagy in Human Endothelial Cell Infected with Dengue Virus-2. Viral Immunol 33, 61-70.
Konishi, E., Mason, P.W., 1993. Proper maturation of the Japanese encephalitis virus envelope glycoprotein requires cosynthesis with the premembrane protein. J Virol 67, 1672-1675.
Kozakov, D., Hall, D.R., Xia, B., Porter, K.A., Padhorny, D., Yueh, C., Beglov, D., Vajda, S., 2017. The ClusPro web server for protein-protein docking. Nat Protoc 12, 255-278.
Kraut, H., Lipps, H.J., Prescott, D.M., 1986. The genome of hypotrichous ciliates. Int Rev Cytol 99, 1-28.
Krishnan, S., Nordqvist, H., Ambikan, A.T., Gupta, S., Sperk, M., Svensson-Akusjarvi, S., Mikaeloff, F., Benfeitas, R., Saccon, E., Ponnan, S.M., Rodriguez, J.E., Nikouyan, N., Odeh, A., Ahlen, G., Asghar, M., Sallberg, M., Vesterbacka, J., Nowak, P., Vegvari, A., Sonnerborg, A., Treutiger, C.J., Neogi, U., 2021a. Metabolic Perturbation Associated With COVID-19 Disease Severity and SARS-CoV-2 Replication. Mol Cell Proteomics 20, 100159.
Krishnan, S., Nordqvist, H., Ambikan, A.T., Gupta, S., Sperk, M., Svensson-Akusjärvi, S., Mikaeloff, F., Benfeitas, R., Saccon, E., Ponnan, S.M., Rodriguez, J.E., Nikouyan, N., Odeh, A., Ahlén, G., Asghar, M., Sällberg, M., Vesterbacka, J., Nowak, P., Végvári, A., Sönnerborg, A., Treutiger, C.J., Neogi, U., 2021b. Metabolic Perturbation Associated With COVID-19 Disease Severity and SARS-CoV-2 Replication. Molecular & Cellular Proteomics 20.
Kulkarni, P., Padmanabhan, S., 2022. A novel property of hexokinase inhibition by Favipiravir and proposed advantages over Molnupiravir and 2 Deoxy D glucose in treating COVID-19. Biotechnol Lett 44, 831-843.
Kulkarni, R., Sapkal, G.N., Kaushal, H., Mourya, D.T., 2018. Japanese Encephalitis: A Brief Review on Indian Perspectives. Open Virol J 12, 121-130.
Kumar, M., Verma, S., Nerurkar, V.R., 2010. Pro-inflammatory cytokines derived from West Nile virus (WNV)-infected SK-N-SH cells mediate neuroinflammatory markers and neuronal death. J Neuroinflammation 7, 73.
Kumar, S., Verma, A., Yadav, P., Dubey, S.K., Azhar, E.I., Maitra, S.S., Dwivedi, V.D., 2022. Molecular pathogenesis of Japanese encephalitis and possible therapeutic strategies. Arch Virol 167, 1739-1762.
Lahon, A., Arya, R.P., Banerjea, A.C., 2021. Dengue Virus Dysregulates Master Transcription Factors and PI3K/AKT/mTOR Signaling Pathway in Megakaryocytes. Front Cell Infect Microbiol 11, 715208.
Lai, C.Y., Tsai, W.Y., Lin, S.R., Kao, C.L., Hu, H.P., King, C.C., Wu, H.C., Chang, G.J., Wang, W.K., 2008. Antibodies to envelope glycoprotein of dengue virus during the natural course of infection are predominantly cross-reactive and recognize epitopes containing highly conserved residues at the fusion loop of domain II. J Virol 82, 6631-6643.
Lan, D., Tang, C., Li, M., Yue, H., 2010. Screening and identification of differentially expressed genes from chickens infected with Newcastle disease virus by suppression subtractive hybridization. Avian Pathol 39, 151-159.
Laskowski, R.A., Macarthur, M.W., Moss, D.S., Thornton, J.M., 1993. Procheck - a Program to Check the Stereochemical Quality of Protein Structures. J Appl Crystallogr 26, 283-291.
Lavik, A.R., McColl, K.S., Lemos, F.O., Kerkhofs, M., Zhong, F., Harr, M., Schlatzer, D., Hamada, K., Mikoshiba, K., Crea, F., Bultynck, G., Bootman, M.D., Parys, J.B., Distelhorst, C.W., 2022. A non-canonical role for pyruvate kinase M2 as a functional modulator of Ca(2+) signalling through IP(3) receptors. Biochim Biophys Acta Mol Cell Res 1869, 119206.
Lee, J.W., Bae, S.H., Jeong, J.W., Kim, S.H., Kim, K.W., 2004. Hypoxia-inducible factor (HIF-1)α:: its protein stability and biological functions. Exp Mol Med 36, 1-12.
Lee, S.A., Ho, C., Troxler, M., Lin, C.Y., Chung, S.H., 2021. Non-Metabolic Functions of PKM2 Contribute to Cervical Cancer Cell Proliferation Induced by the HPV16 E7 Oncoprotein. Viruses 13.
Lee, Y.R., Wu, S.Y., Chen, R.Y., Lin, Y.S., Yeh, T.M., Liu, H.S., 2020. Regulation of autophagy, glucose uptake, and glycolysis under dengue virus infection. Kaohsiung J Med Sci 36, 911-919.

Levy, G., Habib, N., Guzzardi, M.A., Kitsberg, D., Bomze, D., Ezra, E., Uygun, B.E., Uygun, K., Trippler, M., Schlaak, J.F., Shibolet, O., Sklan, E.H., Cohen, M., Timm, J., Friedman, N., Nahmias, Y., 2016. Nuclear receptors control pro-viral and antiviral metabolic responses to hepatitis C virus infection. Nat Chem Biol 12, 1037-1045.
Leyssen, P., De Clercq, E., Neyts, J., 2000. Perspectives for the treatment of infections with Flaviviridae. Clin Microbiol Rev 13, 67-82, table of contents.
Li, F., Li, J., Wang, P.H., Yang, N., Huang, J., Ou, J., Xu, T., Zhao, X., Liu, T., Huang, X., Wang, Q., Li, M., Yang, L., Lin, Y., Cai, Y., Chen, H., Zhang, Q., 2021a. SARS-CoV-2 spike promotes inflammation and apoptosis through autophagy by ROS-suppressed PI3K/AKT/mTOR signaling. Biochim Biophys Acta Mol Basis Dis 1867, 166260.
Li, G., Li, X., Chen, J., Lemey, P., Vrancken, B., Su, S., Dellicour, S., Gambaro, F., 2025. Tracing more than two decades of Japanese encephalitis virus circulation in mainland China. J Virol 99, e0157524.
Li, H., Lin, C., Qi, W., Sun, Z., Xie, Z., Jia, W., Ning, Z., 2023a. Senecavirus A-induced glycolysis facilitates virus replication by promoting lactate production that attenuates the interaction between MAVS and RIG-I. PLoS Pathog 19, e1011371.
Li, H.Z., Lin, C.H., Qi, W.B., Sun, Z.Z., Xie, Z.X., Jia, W.X., Ning, Z.Y., 2023b. Senecavirus A-induced glycolysis facilitates virus replication by promoting lactate production that attenuates the interaction between MAVS and RIG-I. Plos Pathogens 19.
Li, L., Lok, S.M., Yu, I.M., Zhang, Y., Kuhn, R.J., Chen, J., Rossmann, M.G., 2008. The flavivirus precursor membrane-envelope protein complex: structure and maturation. Science 319, 1830-1834.
Li, M., Yang, J., Ye, C., Bian, P., Yang, X., Zhang, H., Luo, C., Xue, Z., Lei, Y., Lian, J., 2021b. Integrated Metabolomics and Transcriptomics Analyses Reveal Metabolic Landscape in Neuronal Cells during JEV Infection. Virol Sin 36, 1554-1565.
Li, Q., Zhang, D., Chen, X., He, L., Li, T., Xu, X., Li, M., 2015a. Nuclear PKM2 contributes to gefitinib resistance via upregulation of STAT3 activation in colorectal cancer. Sci Rep 5, 16082.
Li, X.D., Deng, C.L., Ye, H.Q., Zhang, H.L., Zhang, Q.Y., Chen, D.D., Zhang, P.T., Shi, P.Y., Yuan, Z.M., Zhang, B., 2016. Transmembrane Domains of NS2B Contribute to both Viral RNA Replication and Particle Formation in Japanese Encephalitis Virus. J Virol 90, 5735-5749.
Li, X.J., Xu, M., Zhao, X.Q., Zhao, J.N., Chen, F.F., Yu, W., Gao, D.Y., Luo, B., 2013. Proteomic analysis of synovial fibroblast-like synoviocytes from rheumatoid arthritis. Clin Exp Rheumatol 31, 552-558.
Li, Y., Li, Q., Wong, Y.L., Liew, L.S., Kang, C., 2015b. Membrane topology of NS2B of dengue virus revealed by NMR spectroscopy. Biochim Biophys Acta 1848, 2244-2252.
Li, Z., Yang, P., Li, Z., 2014. The multifaceted regulation and functions of PKM2 in tumor progression. Biochim Biophys Acta 1846, 285-296.
Liang, J., Cao, R., Wang, X., Zhang, Y., Wang, P., Gao, H., Li, C., Yang, F., Zeng, R., Wei, P., Li, D., Li, W., Yang, W., 2017. Mitochondrial PKM2 regulates oxidative stress-induced apoptosis by stabilizing Bcl2. Cell Res 27, 329-351.
Liang, Q., Luo, Z., Zeng, J., Chen, W., Foo, S.S., Lee, S.A., Ge, J., Wang, S., Goldman, S.A., Zlokovic, B.V., Zhao, Z., Jung, J.U., 2016. Zika Virus NS4A and NS4B Proteins Deregulate Akt-mTOR Signaling in Human Fetal Neural Stem Cells to Inhibit Neurogenesis and Induce Autophagy. Cell Stem Cell 19, 663-671.
Liao, M., Yao, D., Wu, L., Luo, C., Wang, Z., Zhang, J., Liu, B., 2024. Targeting the Warburg effect: A revisited perspective from molecular mechanisms to traditional and innovative therapeutic strategies in cancer. Acta Pharm Sin B 14, 953-1008.
Lin, R.J., Chang, B.L., Yu, H.P., Liao, C.L., Lin, Y.L., 2006. Blocking of interferon-induced Jak-Stat signaling by Japanese encephalitis virus NS5 through a protein tyrosine phosphatase-mediated mechanism. J Virol 80, 5908-5918.
Lindenbach, B.D., Rice, C.M., 2003. Molecular biology of flaviviruses. Adv Virus Res 59, 23-61.

Liu, C., Liu, C., Fu, R., 2022. Research progress on the role of PKM2 in the immune response. Front Immunol 13, 936967.
Liu, F., Ma, M., Gao, A., Ma, F., Ma, G., Liu, P., Jia, C., Wang, Y., Donahue, K., Zhang, S., Ong, I.M., Keles, S., Li, L., Xu, W., 2021a. PKM2-TMEM33 axis regulates lipid homeostasis in cancer cells by controlling SCAP stability. EMBO J 40, e108065.
Liu, H., Liu, Y., Wang, S., Zhang, Y., Zu, X., Zhou, Z., Zhang, B., Xiao, G., 2015. Structure-based mutational analysis of several sites in the E protein: implications for understanding the entry mechanism of Japanese encephalitis virus. J Virol 89, 5668-5686.
Liu, W., Shen, S.M., Zhao, X.Y., Chen, G.Q., 2012. Targeted genes and interacting proteins of hypoxia inducible factor-1. Int J Biochem Mol Biol 3, 165-178.
Liu, W.J., Chen, H.B., Khromykh, A.A., 2003. Molecular and functional analyses of Kunjin virus infectious cDNA clones demonstrate the essential roles for NS2A in virus assembly and for a nonconservative residue in NS3 in RNA replication. J Virol 77, 7804-7813.
Liu, X., Peng, L., Zhang, J.Z.H., 2019. Accurate and Efficient Calculation of Protein-Protein Binding Free Energy-Interaction Entropy with Residue Type-Specific Dielectric Constants. J Chem Inf Model 59, 272-281.
Liu, X., Yan, Q., Liu, X., Wei, W., Zou, L., Zhao, F., Zeng, S., Yi, L., Ding, H., Zhao, M., Chen, J., Fan, S., 2024. PKM2 induces mitophagy through the AMPK-mTOR pathway promoting CSFV proliferation. J Virol 98, e0175123.
Liu, Z., Le, Y., Chen, H., Zhu, J., Lu, D., 2021b. Role of PKM2-Mediated Immunometabolic Reprogramming on Development of Cytokine Storm. Front Immunol 12, 748573.
Lo, A.K., Dawson, C.W., Young, L.S., Ko, C.W., Hau, P.M., Lo, K.W., 2015. Activation of the FGFR1 signalling pathway by the Epstein-Barr virus-encoded LMP1 promotes aerobic glycolysis and transformation of human nasopharyngeal epithelial cells. J Pathol 237, 238-248.
Locasale, J.W., Cantley, L.C., 2011. Metabolic flux and the regulation of mammalian cell growth. Cell Metab 14, 443-451.
Loisel-Meyer, S., Swainson, L., Craveiro, M., Oburoglu, L., Mongellaz, C., Costa, C., Martinez, M., Cosset, F.L., Battini, J.L., Herzenberg, L.A., Herzenberg, L.A., Atkuri, K.R., Sitbon, M., Kinet, S., Verhoeyen, E., Taylor, N., 2012. Glut1-mediated glucose transport regulates HIV infection. Proc Natl Acad Sci U S A 109, 2549-2554.
Long, Y.C., Zierath, J.R., 2006. AMP-activated protein kinase signaling in metabolic regulation. J Clin Invest 116, 1776-1783.
Lorenz, I.C., Allison, S.L., Heinz, F.X., Helenius, A., 2002. Folding and dimerization of tick-borne encephalitis virus envelope proteins prM and E in the endoplasmic reticulum. J Virol 76, 5480-5491.
Lu, Z., 2012. Nonmetabolic functions of pyruvate kinase isoform M2 in controlling cell cycle progression and tumorigenesis. Chin J Cancer 31, 5-7.
Luca, V.C., AbiMansour, J., Nelson, C.A., Fremont, D.H., 2012. Crystal structure of the Japanese encephalitis virus envelope protein. J Virol 86, 2337-2346.
Luo, D., Vasudevan, S.G., Lescar, J., 2015. The flavivirus NS2B-NS3 protease-helicase as a target for antiviral drug development. Antiviral Res 118, 148-158.
Luo, D., Xu, T., Hunke, C., Gruber, G., Vasudevan, S.G., Lescar, J., 2008. Crystal structure of the NS3 protease-helicase from dengue virus. J Virol 82, 173-183.
Luo, H., Yanagawa, B., Zhang, J., Luo, Z., Zhang, M., Esfandiarei, M., Carthy, C., Wilson, J.E., Yang, D., McManus, B.M., 2002. Coxsackievirus B3 replication is reduced by inhibition of the extracellular signal-regulated kinase (ERK) signaling pathway. J Virol 76, 3365-3373.
Luo, J., Zhang, L., Guo, L., Yang, S., 2021. PKM2 regulates proliferation and apoptosis through the Hippo pathway in oral tongue squamous cell carcinoma. Oncol Lett 21, 461.
Luo, W., Hu, H., Chang, R., Zhong, J., Knabel, M., O'Meally, R., Cole, R.N., Pandey, A., Semenza, G.L., 2011. Pyruvate kinase M2 is a PHD3-stimulated coactivator for hypoxia-inducible factor 1. Cell 145, 732-744.

Luo, W., Semenza, G.L., 2011. Pyruvate kinase M2 regulates glucose metabolism by functioning as a coactivator for hypoxia-inducible factor 1 in cancer cells. Oncotarget 2, 551-556.
Ma, T., Patel, H., Babapoor-Farrokhran, S., Franklin, R., Semenza, G.L., Sodhi, A., Montaner, S., 2015. KSHV induces aerobic glycolysis and angiogenesis through HIF-1-dependent upregulation of pyruvate kinase 2 in Kaposi's sarcoma. Angiogenesis 18, 477-488.
Markoff, L., 1989. In vitro processing of dengue virus structural proteins: cleavage of the pre-membrane protein. J Virol 63, 3345-3352.
Markoff, L., Chang, A., Falgout, B., 1994. Processing of flavivirus structural glycoproteins: stable membrane insertion of premembrane requires the envelope signal peptide. Virology 204, 526-540.
Martínez-Betancur, V., Martínez-Gutierrez, M., 2016. Proteomic profile of human monocytic cells infected with dengue virus. Asian Pac J Trop Bio 6, 914-923.
Martinez, L., 2015. Automatic identification of mobile and rigid substructures in molecular dynamics simulations and fractional structural fluctuation analysis. PLoS One 10, e0119264.
Mathupala, S.P., Rempel, A., Pedersen, P.L., 2001. Glucose catabolism in cancer cells: identification and characterization of a marked activation response of the type II hexokinase gene to hypoxic conditions. J Biol Chem 276, 43407-43412.
Matsuzawa, A., Yamamoto, T., 1975. Response of a pregnancy-dependent mouse mammary tumor to hormones. J Natl Cancer Inst 55, 447-453.
Maxwell, P.H., Pugh, C.W., Ratcliffe, P.J., 2001. The pVHL-hIF-1 system. A key mediator of oxygen homeostasis. Adv Exp Med Biol 502, 365-376.
Mayer, K.A., Stöckl, J., Ziabinger, G.J., Gualdoni, G.A., 2019a. Hijacking the Supplies: Metabolism as a Novel Facet of Virus-Host Interaction. Front Immunol 10.
Mayer, K.A., Stockl, J., Zlabinger, G.J., Gualdoni, G.A., 2019b. Hijacking the Supplies: Metabolism as a Novel Facet of Virus-Host Interaction. Front Immunol 10, 1533.
Mazurek, S., 2007. Pyruvate kinase type M2: a key regulator within the tumour metabolome and a tool for metabolic profiling of tumours. Ernst Schering Found Symp Proc, 99-124.
Mazurek, S., 2011. Pyruvate kinase type M2: a key regulator of the metabolic budget system in tumor cells. Int J Biochem Cell Biol 43, 969-980.
Mazurek, S., Zwerschke, W., Jansen-Dürr, P., Eigenbrodt, E., 2001. Effects of the human papilloma virus HPV-16 E7 oncoprotein on glycolysis and glutaminolysis: role of pyruvate kinase type M2 and the glycolytic-enzyme complex. Biochem J 356, 247-256.
Mazzoni, A., Gambetta, R.A., Trave, F., Zunino, F., 1986. Comparative distribution of free doxorubicin and poly-L-aspartic acid linked doxorubicin in MS-2 sarcoma bearing mice. Cancer Drug Deliv 3, 163-172.
McElvaney, O.J., McEvoy, N.L., McElvaney, O.F., Carroll, T.P., Murphy, M.P., Dunlea, D.M., Ni Choileain, O., Clarke, J., O'Connor, E., Hogan, G., Ryan, D., Sulaiman, I., Gunaratnam, C., Branagan, P., O'Brien, M.E., Morgan, R.K., Costello, R.W., Hurley, K., Walsh, S., de Barra, E., McNally, C., McConkey, S., Boland, F., Galvin, S., Kiernan, F., O'Rourke, J., Dwyer, R., Power, M., Geoghegan, P., Larkin, C., O'Leary, R.A., Freeman, J., Gaffney, A., Marsh, B., Curley, G.F., McElvaney, N.G., 2020a. Characterization of the Inflammatory Response to Severe COVID-19 Illness. Am J Respir Crit Care Med 202, 812-821.
McElvaney, O.J., McEvoy, N.L., McElvaney, O.F., Carroll, T.P., Murphy, M.P., Dunlea, D.M., O, N.C., Clarke, J., O'Connor, E., Hogan, G., Ryan, D., Sulaiman, I., Gunaratnam, C., Branagan, P., O'Brien, M.E., Morgan, R.K., Costello, R.W., Hurley, K., Walsh, S., de Barra, E., McNally, C., McConkey, S., Boland, F., Galvin, S., Kiernan, F., O'Rourke, J., Dwyer, R., Power, M., Geoghegan, P., Larkin, C., O'Leary, R.A., Freeman, J., Gaffney, A., Marsh, B., Curley, G.F., McElvaney, N.G., 2020b. Characterization of the Inflammatory Response to Severe COVID-19 Illness. Am J Respir Crit Care Med 202, 812-821.
Mingo-Casas, P., Blazquez, A.B., Gomez de Cedron, M., San-Felix, A., Molina, S., Escribano-Romero, E., Calvo-Pinilla, E., Jimenez de Oya, N., Ramirez de Molina, A., Saiz, J.C., Perez-Perez,

M.J., Martin-Acebes, M.A., 2023. Glycolytic shift during West Nile virus infection provides new therapeutic opportunities. J Neuroinflammation 20, 217.
Mishra, S., Goyal, P., Kumar, D., Chaudhari, R., Rajala, M.S., 2020. Experimental validation of influenza A virus matrix protein (M1) interaction with host cellular alpha enolase and pyruvate kinase. Virology 549, 59-67.
Miyake, Y., Ishii, K., Honda, A., 2017. Influenza Virus Infection Induces Host Pyruvate Kinase M Which Interacts with Viral RNA-Dependent RNA Polymerase. Frontiers in microbiology 8, 162.
Modis, Y., Ogata, S., Clements, D., Harrison, S.C., 2004. Structure of the dengue virus envelope protein after membrane fusion. Nature 427, 313-319.
Mohsin, F., Suleman, S., Anzar, N., Narang, J., Wadhwa, S., 2022. A review on Japanese Encephalitis virus emergence, pathogenesis and detection: From conventional diagnostics to emerging rapid detection techniques. Int J Biol Macromol 217, 435-448.
Moreno, I., Jr., Rodriguez-Sanchez, I., Schafer, X., Munger, J., 2022. Human cytomegalovirus induces neuronal enolase to support virally mediated metabolic remodeling. Proc Natl Acad Sci U S A 119, e2205789119.
Morgan, H.P., O'Reilly, F.J., Wear, M.A., O'Neill, J.R., Fothergill-Gilmore, L.A., Hupp, T., Walkinshaw, M.D., 2013. M2 pyruvate kinase provides a mechanism for nutrient sensing and regulation of cell proliferation. Proc Natl Acad Sci U S A 110, 5881-5886.
Morris, D.R., Qu, Y., Agrawal, A., Garofalo, R.P., Casola, A., 2020. HIF-1alpha Modulates Core Metabolism and Virus Replication in Primary Airway Epithelial Cells Infected with Respiratory Syncytial Virus. Viruses 12.
Mucaj, V., Shay, J.E.S., Simon, M.C., 2012. Effects of hypoxia and HIFs on cancer metabolism. International Journal of Hematology 95, 464-470.
Muller, D.A., Young, P.R., 2013. The flavivirus NS1 protein: molecular and structural biology, immunology, role in pathogenesis and application as a diagnostic biomarker. Antiviral Res 98, 192-208.
Nandi, S., Razzaghi, M., Srivastava, D., Dey, M., 2020. Structural basis for allosteric regulation of pyruvate kinase M2 by phosphorylation and acetylation. J Biol Chem 295, 17425-17440.
Noguchi, T., Inoue, H., Tanaka, T., 1986. The M1- and M2-type isozymes of rat pyruvate kinase are produced from the same gene by alternative RNA splicing. J Biol Chem 261, 13807-13812.
Noguchi, T., Yamada, K., Inoue, H., Matsuda, T., Tanaka, T., 1987. The L- and R-type isozymes of rat pyruvate kinase are produced from a single gene by use of different promoters. J Biol Chem 262, 14366-14371.
Ogire, E., Perrin-Cocon, L., Figl, M., Kundlacz, C., Jacquemin, C., Hubert, S., Aublin-Gex, A., Toesca, J., Ramiere, C., Vidalain, P.O., Mathieu, C., Lotteau, V., Diaz, O., 2024. Dengue Virus dependence on glucokinase activity and glycolysis Confers Sensitivity to NAD(H) biosynthesis inhibitors. Antiviral Res 228, 105939.
Palmer, C.S., Ostrowski, M., Gouillou, M., Tsai, L., Yu, D., Zhou, J., Henstridge, D.C., Maisa, A., Hearps, A.C., Lewin, S.R., Landay, A., Jaworowski, A., McCune, J.M., Crowe, S.M., 2014. Increased glucose metabolic activity is associated with CD4+ T-cell activation and depletion during chronic HIV infection. AIDS 28, 297-309.
Palsson-McDermott, E.M., Curtis, A.M., Goel, G., Lauterbach, M.A., Sheedy, F.J., Gleeson, L.E., van den Bosch, M.W., Quinn, S.R., Domingo-Fernandez, R., Johnston, D.G., Jiang, J.K., Israelsen, W.J., Keane, J., Thomas, C., Clish, C., Vander Heiden, M., Xavier, R.J., O'Neill, L.A., 2015a. Pyruvate kinase M2 regulates Hif-1alpha activity and IL-1beta induction and is a critical determinant of the warburg effect in LPS-activated macrophages. Cell Metab 21, 65-80.
Palsson-McDermott, E.M., Curtis, A.M., Goel, G., Lauterbach, M.A., Sheedy, F.J., Gleeson, L.E., van den Bosch, M.W., Quinn, S.R., Domingo-Fernandez, R., Johnston, D.G., Jiang, J.K., Israelsen, W.J., Keane, J., Thomas, C., Clish, C., Vander Heiden, M., Xavier, R.J., O'Neill, L.A., 2015b. Pyruvate

kinase M2 regulates Hif-1α activity and IL-1β induction and is a critical determinant of the warburg effect in LPS-activated macrophages. Cell Metab 21, 65-80.
Panasyuk, G., Espeillac, C., Chauvin, C., Pradelli, L.A., Horie, Y., Suzuki, A., Annicotte, J.S., Fajas, L., Foretz, M., Verdeguer, F., Pontoglio, M., Ferre, P., Scoazec, J.Y., Birnbaum, M.J., Ricci, J.E., Pende, M., 2012. PPARgamma contributes to PKM2 and HK2 expression in fatty liver. Nat Commun 3, 672.
Pando-Robles, V., Oses-Prieto, J.A., Rodriguez-Gandarilla, M., Meneses-Romero, E., Burlingame, A.L., Batista, C.V., 2014. Quantitative proteomic analysis of Huh-7 cells infected with Dengue virus by label-free LC-MS. J Proteomics 111, 16-29.
Pang, Y., Zhou, Y., Wang, Y., Sun, Z., Liu, J., Li, C., Xiao, S., Fang, L., 2022. Porcine Reproductive and Respiratory Syndrome Virus nsp1beta Stabilizes HIF-1alpha to Enhance Viral Replication. Microbiol Spectr 10, e0317322.
Papandreou, I., Cairns, R.A., Fontana, L., Lim, A.L., Denko, N.C., 2006. HIF-1 mediates adaptation to hypoxia by actively downregulating mitochondrial oxygen consumption. Cell Metab 3, 187-197.
Passalacqua, K.D., Lu, J., Goodfellow, I., Kolawole, A.O., Arche, J.R., Maddox, R.J., Carnahan, K.E., O'Riordan, M.X.D., Wobus, C.E., 2019. Glycolysis Is an Intrinsic Factor for Optimal Replication of a Norovirus. Mbio 10.
Pathria, G., Scott, D.A., Feng, Y., Sang Lee, J., Fujita, Y., Zhang, G., Sahu, A.D., Ruppin, E., Herlyn, M., Osterman, A.L., Ronai, Z.A., 2018. Targeting the Warburg effect via LDHA inhibition engages ATF4 signaling for cancer cell survival. EMBO J 37.
Patil, A., Anhlan, D., Ferrando, V., Mecate-Zambrano, A., Mellmann, A., Wixler, V., Boergeling, Y., Ludwig, S., 2021. Phosphorylation of Influenza A Virus NS1 at Serine 205 Mediates Its Viral Polymerase-Enhancing Function. J Virol 95.
Patten, D.A., Lafleur, V.N., Robitaille, G.A., Chan, D.A., Giaccia, A.J., Richard, D.E., 2010. Hypoxia-inducible factor-1 activation in nonhypoxic conditions: the essential role of mitochondrial-derived reactive oxygen species. Mol Biol Cell 21, 3247-3257.
Paul, R., Herbert, J.M., Maffrand, J.P., Lansen, J., Modat, G., Pereillo, J.M., Gordon, J.L., 1987. Inhibition of vascular smooth muscle cell proliferation in culture by pentosan polysulphate and related compounds. Thromb Res 46, 793-801.
Pierson, T.C., Kielian, M., 2013. Flaviviruses: braking the entering. Curr Opin Virol 3, 3-12.
Pinapati, K.K., Tandon, R., Tripathi, P., Srivastava, N., 2023. Recent advances to overcome the burden of Japanese encephalitis: A zoonotic infection with problematic early detection. Rev Med Virol 33, e2383.
Plociennikowska, A., Frankish, J., Moraes, T., Del Prete, D., Kahnt, F., Acuna, C., Slezak, M., Binder, M., Bartenschlager, R., 2021. TLR3 activation by Zika virus stimulates inflammatory cytokine production which dampens the antiviral response induced by RIG-I-like receptors. J Virol 95.
Poonsiri, T., Wright, G.S.A., Solomon, T., Antonyuk, S.V., 2019. Crystal Structure of the Japanese Encephalitis Virus Capsid Protein. Viruses 11.
Prakasam, G., Iqbal, M.A., Bamezai, R.N.K., Mazurek, S., 2018. Posttranslational Modifications of Pyruvate Kinase M2: Tweaks that Benefit Cancer. Front Oncol 8, 22.
Presek, P., Glossmann, H., Eigenbrodt, E., Schoner, W., Rubsamen, H., Friis, R.R., Bauer, H., 1980. Similarities between a phosphoprotein (pp60src)-associated protein kinase of Rous sarcoma virus and a cyclic adenosine 3':5'-monophosphate-independent protein kinase that phosphorylates pyruvate kinase type M2. Cancer Res 40, 1733-1741.
Pucino, V., Certo, M., Bulusu, V., Cucchi, D., Goldmann, K., Pontarini, E., Haas, R., Smith, J., Headland, S.E., Blighe, K., Ruscica, M., Humby, F., Lewis, M.J., Kamphorst, J.J., Bombardieri, M., Pitzalis, C., Mauro, C., 2019. Lactate Buildup at the Site of Chronic Inflammation Promotes Disease by Inducing CD4(+) T Cell Metabolic Rewiring. Cell Metab 30, 1055-1074 e1058.
Qian, J., Huang, C., Wang, M., Liu, Y., Zhao, Y., Li, M., Zhang, X., Gao, X., Zhang, Y., Wang, Y., Huang, J., Li, J., Zhou, Q., Liu, R., Wang, X., Cui, J., Yang, Y., 2024. Nuclear translocation of

metabolic enzyme PKM2 participates in high glucose-promoted HCC metastasis by strengthening immunosuppressive environment. Redox Biol 71, 103103.
Qian, Y., Yang, Y., Qing, W., Li, C., Kong, M., Kang, Z., Zuo, Y., Wu, J., Yu, M., Yang, Z., 2022. Coxsackievirus B3 infection induces glycolysis to facilitate viral replication. Front Microbiol 13, 962766.
Rana, N.K., Singh, P., Koch, B., 2019. CoCl(2) simulated hypoxia induce cell proliferation and alter the expression pattern of hypoxia associated genes involved in angiogenesis and apoptosis. Biol Res 52, 12.
Rankin, E.B., Giaccia, A.J., 2008. The role of hypoxia-inducible factors in tumorigenesis. Cell Death Differ 15, 678-685.
Rastogi, M., Sharma, N., Singh, S.K., 2016. Flavivirus NS1: a multifaceted enigmatic viral protein. Virol J 13, 131.
Ray, D., Shah, A., Tilgner, M., Guo, Y., Zhao, Y., Dong, H., Deas, T.S., Zhou, Y., Li, H., Shi, P.Y., 2006. West Nile virus 5'-cap structure is formed by sequential guanine N-7 and ribose 2'-O methylations by nonstructural protein 5. J Virol 80, 8362-8370.
Ren, L., Zhang, W., Zhang, J., Zhang, J., Zhang, H., Zhu, Y., Meng, X., Yi, Z., Wang, R., 2021a. Influenza A Virus (H1N1) Infection Induces Glycolysis to Facilitate Viral Replication. Virol Sin 36, 1532-1542.
Ren, L.H., Zhang, W.J., Zhang, J., Zhang, J.X., Zhang, H.Y., Zhu, Y., Meng, X.X., Yi, Z.G., Wang, R.L., 2021b. Influenza A Virus (H1N1) Infection Induces Glycolysis to Facilitate Viral Replication. Virologica Sinica 36, 1532-1542.
Ren, X., Song, H., Wang, Y., Wang, Y., Zhang, Q., Yue, X., Wu, Z., Li, C., Gao, L., Ma, C., Liang, X., 2024. TIPE1 limits virus replication by disrupting PKM2/ HIF-1alpha/ glycolysis feedback loop. Free Radic Biol Med 221, 52-63.
Rice, C.M., Lenches, E.M., Eddy, S.R., Shin, S.J., Sheets, R.L., Strauss, J.H., 1985. Nucleotide sequence of yellow fever virus: implications for flavivirus gene expression and evolution. Science 229, 726-733.
Ripoli, M., D'Aprile, A., Quarato, G., Sarasin-Filipowicz, M., Gouttenoire, J., Scrima, R., Cela, O., Boffoli, D., Heim, M.H., Moradpour, D., Capitanio, N., Piccoli, C., 2010. Hepatitis C virus-linked mitochondrial dysfunction promotes hypoxia-inducible factor 1 alpha-mediated glycolytic adaptation. J Virol 84, 647-660.
Ritter, J.B., Wahl, A.S., Freund, S., Genzel, Y., Reichl, U., 2010. Metabolic effects of influenza virus infection in cultured animal cells: Intra- and extracellular metabolite profiling. BMC Syst Biol 4, 61.
Rivas, C.I., Vera, J.C., Guaiquil, V.H., Velasquez, F.V., Borquez-Ojeda, O.A., Carcamo, J.G., Concha, II, Golde, D.W., 1997. Increased uptake and accumulation of vitamin C in human immunodeficiency virus 1-infected hematopoietic cell lines. J Biol Chem 272, 5814-5820.
Roberts, D.J., Miyamoto, S., 2015. Hexokinase II integrates energy metabolism and cellular protection: Akting on mitochondria and TORCing to autophagy. Cell Death Differ 22, 248-257.
Roberts, D.J., Tan-Sah, V.P., Smith, J.M., Miyamoto, S., 2013. Akt phosphorylates HK-II at Thr-473 and increases mitochondrial HK-II association to protect cardiomyocytes. J Biol Chem 288, 23798-23806.
Rochowski, M.T., Jayathilake, K., Balcerak, J.M., Selvan, M.T., Gunasekara, S., Miller, C., Rudd, J.M., Lacombe, V.A., 2024. Impact of Delta SARS-CoV-2 Infection on Glucose Metabolism: Insights on Host Metabolism and Virus Crosstalk in a Feline Model. Viruses 16.
Rosales Ramirez, R., Ludert, J.E., 2019. The Dengue Virus Nonstructural Protein 1 (NS1) Is Secreted from Mosquito Cells in Association with the Intracellular Cholesterol Transporter Chaperone Caveolin Complex. J Virol 93.
Rothan, H.A., Fang, S.Y., Mahesh, M., Byrareddy, S.N., 2019. Zika Virus and the Metabolism of Neuronal Cells. Mol Neurobiol 56, 2551-2557.

Roy, A., Kucukural, A., Zhang, Y., 2010. I-TASSER: a unified platform for automated protein structure and function prediction. Nat Protoc 5, 725-738.
Sahoo, B.R., Pattnaik, A., Annamalai, A.S., Franco, R., Pattnaik, A.K., 2020. Mechanistic Target of Rapamycin Signaling Activation Antagonizes Autophagy To Facilitate Zika Virus Replication. J Virol 94.
Salceda, S., Caro, J., 1997. Hypoxia-inducible factor 1alpha (HIF-1alpha) protein is rapidly degraded by the ubiquitin-proteasome system under normoxic conditions. Its stabilization by hypoxia depends on redox-induced changes. J Biol Chem 272, 22642-22647.
Salter, D.W., Baldwin, S.A., Lienhard, G.E., Weber, M.J., 1982. Proteins antigenically related to the human erythrocyte glucose transporter in normal and Rous sarcoma virus-transformed chicken embryo fibroblasts. Proc Natl Acad Sci U S A 79, 1540-1544.
Sarkar, R., Chhabra, S., Tanwar, M., Agarwal, N., Kalia, M., 2024. Japanese encephalitis virus hijacks ER-associated degradation regulators for its replication. J Gen Virol 105.
Shahid, M., Lee, M.Y., Piplani, H., Andres, A.M., Zhou, B., Yeon, A., Kim, M., Kim, H.L., Kim, J., 2018. Centromere protein F (CENPF), a microtubule binding protein, modulates cancer metabolism by regulating pyruvate kinase M2 phosphorylation signaling. Cell Cycle 17, 2802-2818.
Shang, D., Wu, J., Guo, L., Xu, Y., Liu, L., Lu, J., 2017. Metformin increases sensitivity of osteosarcoma stem cells to cisplatin by inhibiting expression of PKM2. Int J Oncol 50, 1848-1856.
Sharma, N., Kumawat, K.L., Rastogi, M., Basu, A., Singh, S.K., 2016. Japanese Encephalitis Virus exploits the microRNA-432 to regulate the expression of Suppressor of Cytokine Signaling (SOCS) 5. Sci Rep 6, 27685.
Shimojima, M., Takenouchi, A., Shimoda, H., Kimura, N., Maeda, K., 2014. Distinct usage of three C-type lectins by Japanese encephalitis virus: DC-SIGN, DC-SIGNR, and LSECtin. Arch Virol 159, 2023-2031.
Shirai, T., Nazarewicz, R.R., Wallis, B.B., Yanes, R.E., Watanabe, R., Hilhorst, M., Tian, L., Harrison, D.G., Giacomini, J.C., Assimes, T.L., Goronzy, J.J., Weyand, C.M., 2016. The glycolytic enzyme PKM2 bridges metabolic and inflammatory dysfunction in coronary artery disease. J Exp Med 213, 337-354.
Shiratori, R., Furuichi, K., Yamaguchi, M., Miyazaki, N., Aoki, H., Chibana, H., Ito, K., Aoki, S., 2019. Glycolytic suppression dramatically changes the intracellular metabolic profile of multiple cancer cell lines in a mitochondrial metabolism-dependent manner. Sci Rep-Uk 9.
Shu, C., Cui, H., Peng, Y., Wei, Z., Ni, X., Zheng, L., Shang, J., Liu, F., Liu, J., 2024. Understanding the molecular pathway of triclosan-induced ADHD-like behaviour: Involvement of the hnRNPA1-PKM2-STAT3 feedback loop. Environ Int 191, 108966.
Shytaj, I.L., Procopio, F.A., Tarek, M., Carlon-Andres, I., Tang, H.Y., Goldman, A.R., Munshi, M., Kumar Pal, V., Forcato, M., Sreeram, S., Leskov, K., Ye, F., Lucic, B., Cruz, N., Ndhlovu, L.C., Bicciato, S., Padilla-Parra, S., Diaz, R.S., Singh, A., Lusic, M., Karn, J., Alvarez-Carbonell, D., Savarino, A., 2021. Glycolysis downregulation is a hallmark of HIV-1 latency and sensitizes infected cells to oxidative stress. EMBO Mol Med 13, e13901.
Silva, E.M., Conde, J.N., Allonso, D., Nogueira, M.L., Mohana-Borges, R., 2013. Mapping the interactions of dengue virus NS1 protein with human liver proteins using a yeast two-hybrid system: identification of C1q as an interacting partner. PLoS One 8, e57514.
Singh, M., Singh, V.N., August, J.T., Horecker, B.L., 1974a. Alterations in glucose metabolism in chick embryo cells transformed by Rous sarcoma virus. Transformation-specific changes in the activities of key enzymes of the glycolytic and hexose monophosphate shunt pathways. Arch Biochem Biophys 165, 240-246.
Singh, S., Singh, P.K., Suhail, H., Arumugaswami, V., Pellett, P.E., Giri, S., Kumar, A., 2020. AMP-Activated Protein Kinase Restricts Zika Virus Replication in Endothelial Cells by Potentiating Innate Antiviral Responses and Inhibiting Glycolysis. J Immunol 204, 1810-1824.

Singh, V.N., Singh, M., August, J.T., Horecker, B.L., 1974b. Alterations in glucose metabolism in chick-embryo cells transformed by Rous sarcoma virus: intracellular levels of glycolytic intermediates. Proc Natl Acad Sci U S A 71, 4129-4132.
Smallwood, H.S., Duan, S., Morfouace, M., Rezinciuc, S., Shulkin, B.L., Shelat, A., Zink, E.E., Milasta, S., Bajracharya, R., Oluwaseum, A.J., Roussel, M.F., Green, D.R., Pasa-Tolic, L., Thomas, P.G., 2017. Targeting Metabolic Reprogramming by Influenza Infection for Therapeutic Intervention. Cell Rep 19, 1640-1653.
Song, M., Liu, S., Luo, Y., Ji, T., Zhang, Y., Deng, W., 2025. PKM2 Facilitates Classical Swine Fever Virus Replication by Enhancing NS5B Polymerase Function. Viruses 17.
Sorbara, L.R., Maldarelli, F., Chamoun, G., Schilling, B., Chokekijcahi, S., Staudt, L., Mitsuya, H., Simpson, I.A., Zeichner, S.L., 1996. Human immunodeficiency virus type 1 infection of H9 cells induces increased glucose transporter expression. J Virol 70, 7275-7279.
Srivastava, K.S., Jeswani, V., Pal, N., Bohra, B., Vishwakarma, V., Bapat, A.A., Patnaik, Y.P., Khanna, N., Shukla, R., 2023. Japanese Encephalitis Virus: An Update on the Potential Antivirals and Vaccines. Vaccines (Basel) 11.
Srivastava, R., Kalita, J., Khan, M.Y., Misra, U.K., 2009. Free radical generation by neurons in rat model of Japanese encephalitis. Neurochem Res 34, 2141-2146.
Stadler, K., Allison, S.L., Schalich, J., Heinz, F.X., 1997. Proteolytic activation of tick-borne encephalitis virus by furin. J Virol 71, 8475-8481.
Stetak, A., Veress, R., Ovadi, J., Csermely, P., Keri, G., Ullrich, A., 2007. Nuclear translocation of the tumor marker pyruvate kinase M2 induces programmed cell death. Cancer Res 67, 1602-1608.
Strowitzki, M.J., Cummins, E.P., Taylor, C.T., 2019. Protein Hydroxylation by Hypoxia-Inducible Factor (HIF) Hydroxylases: Unique or Ubiquitous? Cells-Basel 8.
Su, Q., Tao, T., Tang, L., Deng, J., Darko, K.O., Zhou, S., Peng, M., He, S., Zeng, Q., Chen, A.F., Yang, X., 2018. Down-regulation of PKM2 enhances anticancer efficiency of THP on bladder cancer. J Cell Mol Med 22, 2774-2790.
Sun, Q., Chen, X., Ma, J., Peng, H., Wang, F., Zha, X., Wang, Y., Jing, Y., Yang, H., Chen, R., Chang, L., Zhang, Y., Goto, J., Onda, H., Chen, T., Wang, M.R., Lu, Y., You, H., Kwiatkowski, D., Zhang, H., 2011. Mammalian target of rapamycin up-regulation of pyruvate kinase isoenzyme type M2 is critical for aerobic glycolysis and tumor growth. Proc Natl Acad Sci U S A 108, 4129-4134.
Sun, Y., Cui, A., Dong, H., Nie, L., Yue, Z., Chen, J., Leung, W.K., Wang, J., Wang, Q., 2024. Intermittent hyperglycaemia induces macrophage dysfunction by extracellular regulated protein kinase-dependent PKM2 translocation in periodontitis. Cell Prolif 57, e13651.
Takenaka, M., Noguchi, T., Sadahiro, S., Hirai, H., Yamada, K., Matsuda, T., Imai, E., Tanaka, T., 1991. Isolation and characterization of the human pyruvate kinase M gene. Eur J Biochem 198, 101-106.
Tang, Q., Ji, Q., Xia, W., Li, L., Bai, J., Ni, R., Qin, Y., 2015. Pyruvate kinase M2 regulates apoptosis of intestinal epithelial cells in Crohn's disease. Dig Dis Sci 60, 393-404.
Tang, Y., Su, R., Gu, Q., Hu, Y., Yang, H., 2023. PI3K/AKT-mediated autophagy inhibition facilitates mast cell activation to enhance severe inflammatory lung injury in influenza A virus- and secondary Staphylococcus aureus-infected mice. Antiviral Res 209, 105502.
Tay, M.Y., Smith, K., Ng, I.H., Chan, K.W., Zhao, Y., Ooi, E.E., Lescar, J., Luo, D., Jans, D.A., Forwood, J.K., Vasudevan, S.G., 2016. The C-terminal 18 Amino Acid Region of Dengue Virus NS5 Regulates its Subcellular Localization and Contains a Conserved Arginine Residue Essential for Infectious Virus Production. PLoS Pathog 12, e1005886.
Teo, C.S., Chu, J.J., 2014. Cellular vimentin regulates construction of dengue virus replication complexes through interaction with NS4A protein. J Virol 88, 1897-1913.
Thaker, S.K., Ch'ng, J., Christofk, H.R., 2019a. Viral hijacking of cellular metabolism. BMC Biol 17, 59.

Thaker, S.K., Chapa, T., Garcia, G., Jr., Gong, D., Schmid, E.W., Arumugaswami, V., Sun, R., Christofk, H.R., 2019b. Differential Metabolic Reprogramming by Zika Virus Promotes Cell Death in Human versus Mosquito Cells. Cell Metab 29, 1206-1216 e1204.
Thompson, J.E., Scypinski, L.A., Gordon, T., Sheppard, D., 1987. Tachykinins mediate the acute increase in airway responsiveness caused by toluene diisocyanate in guinea pigs. Am Rev Respir Dis 136, 43-49.
Tian, M., Liu, W., Li, X., Zhao, P., Shereen, M.A., Zhu, C., Huang, S., Liu, S., Yu, X., Yue, M., Pan, P., Wang, W., Li, Y., Chen, X., Wu, K., Luo, Z., Zhang, Q., Wu, J., 2021. HIF-1alpha promotes SARS-CoV-2 infection and aggravates inflammatory responses to COVID-19. Signal Transduct Target Ther 6, 308.
Tien, C.F., Cheng, S.C., Ho, Y.P., Chen, Y.S., Hsu, J.H., Chang, R.Y., 2014. Inhibition of aldolase A blocks biogenesis of ATP and attenuates Japanese encephalitis virus production. Biochem Biophys Res Commun 443, 464-469.
Turtle, L., Solomon, T., 2018. Japanese encephalitis - the prospects for new treatments. Nat Rev Neurol 14, 298-313.
Uemura, E., Greenlee, H.W., 2006. Insulin regulates neuronal glucose uptake by promoting translocation of glucose transporter GLUT3. Exp Neurol 198, 48-53.
Umareddy, I., Chao, A., Sampath, A., Gu, F., Vasudevan, S.G., 2006. Dengue virus NS4B interacts with NS3 and dissociates it from single-stranded RNA. J Gen Virol 87, 2605-2614.
Unni, S.K., Ruzek, D., Chhatbar, C., Mishra, R., Johri, M.K., Singh, S.K., 2011. Japanese encephalitis virus: from genome to infectome. Microbes Infect 13, 312-321.
van de Wetering, C., Aboushousha, R., Manuel, A.M., Chia, S.B., Erickson, C., MacPherson, M.B., van der Velden, J.L., Anathy, V., Dixon, A.E., Irvin, C.G., Poynter, M.E., van der Vliet, A., Wouters, E.F.M., Reynaert, N.L., Janssen-Heininger, Y.M.W., 2020. Pyruvate Kinase M2 Promotes Expression of Proinflammatory Mediators in House Dust Mite-Induced Allergic Airways Disease. J Immunol 204, 763-774.
Van Der Spoel, D., Lindahl, E., Hess, B., Groenhof, G., Mark, A.E., Berendsen, H.J., 2005. GROMACS: fast, flexible, and free. J Comput Chem 26, 1701-1718.
Vander Heiden, M.G., Cantley, L.C., Thompson, C.B., 2009. Understanding the Warburg effect: the metabolic requirements of cell proliferation. Science 324, 1029-1033.
Vashi, Y., Nehru, G., Kumar, S., 2023. Niclosamide inhibits Newcastle disease virus replication in chickens by perturbing the cellular glycolysis. Virology 585, 196-204.
Vastag, L., Koyuncu, E., Grady, S.L., Shenk, T.E., Rabinowitz, J.D., 2011. Divergent effects of human cytomegalovirus and herpes simplex virus-1 on cellular metabolism. PLoS Pathog 7, e1002124.
Wang, C., Jiang, J., Ji, J., Cai, Q., Chen, X., Yu, Y., Zhu, Z., Zhang, J., 2017a. PKM2 promotes cell migration and inhibits autophagy by mediating PI3K/AKT activation and contributes to the malignant development of gastric cancer. Sci Rep 7, 2886.
Wang, G.L., Jiang, B.H., Rue, E.A., Semenza, G.L., 1995. Hypoxia-inducible factor 1 is a basic-helix-loop-helix-PAS heterodimer regulated by cellular O2 tension. Proc Natl Acad Sci U S A 92, 5510-5514.
Wang, H.J., Hsieh, Y.J., Cheng, W.C., Lin, C.P., Lin, Y.S., Yang, S.F., Chen, C.C., Izumiya, Y., Yu, J.S., Kung, H.J., Wang, W.C., 2014. JMJD5 regulates PKM2 nuclear translocation and reprograms HIF-1alpha-mediated glucose metabolism. Proc Natl Acad Sci U S A 111, 279-284.
Wang, K., Zou, C., Wang, X., Huang, C., Feng, T., Pan, W., Wu, Q., Wang, P., Dai, J., 2018. Interferon-stimulated TRIM69 interrupts dengue virus replication by ubiquitinating viral nonstructural protein 3. PLoS Pathog 14, e1007287.
Wang, P., Liu, X., Li, Q., Wang, J., Ruan, W., 2021. Proteomic analyses identify intracellular targets for Japanese encephalitis virus nonstructural protein 1 (NS1). Virus Res 302, 198495.
Wang, P., Sun, C., Zhu, T., Xu, Y., 2015. Structural insight into mechanisms for dynamic regulation of PKM2. Protein Cell 6, 275-287.

Wang, X., Li, S.H., Zhu, L., Nian, Q.G., Yuan, S., Gao, Q., Hu, Z., Ye, Q., Li, X.F., Xie, D.Y., Shaw, N., Wang, J., Walter, T.S., Huiskonen, J.T., Fry, E.E., Qin, C.F., Stuart, D.I., Rao, Z., 2017b. Near-atomic structure of Japanese encephalitis virus reveals critical determinants of virulence and stability. Nat Commun 8, 14.
Wang, X., Perez, E., Liu, R., Yan, L.J., Mallet, R.T., Yang, S.H., 2007. Pyruvate protects mitochondria from oxidative stress in human neuroblastoma SK-N-SH cells. Brain Res 1132, 1-9.
Wang, Y., Liu, J., Jin, X., Zhang, D., Li, D., Hao, F., Feng, Y., Gu, S., Meng, F., Tian, M., Zheng, Y., Xin, L., Zhang, X., Han, X., Aravind, L., Wei, M., 2017c. O-GlcNAcylation destabilizes the active tetrameric PKM2 to promote the Warburg effect. Proc Natl Acad Sci U S A 114, 13732-13737.
Wessel, A.W., Dowd, K.A., Biering, S.B., Zhang, P., Edeling, M.A., Nelson, C.A., Funk, K.E., DeMaso, C.R., Klein, R.S., Smith, J.L., Cao, T.M., Kuhn, R.J., Fremont, D.H., Harris, E., Pierson, T.C., Diamond, M.S., 2021. Levels of Circulating NS1 Impact West Nile Virus Spread to the Brain. J Virol 95, e0084421.
Weyand, C.M., Zeisbrich, M., Goronzy, J.J., 2017. Metabolic signatures of T-cells and macrophages in rheumatoid arthritis. Curr Opin Immunol 46, 112-120.
Wheaton, W.W., Chandel, N.S., 2011. Hypoxia. 2. Hypoxia regulates cellular metabolism. Am J Physiol Cell Physiol 300, C385-393.
Wongtrakul, J., Thongtan, T., Pannengpetch, S., Wikan, N., Kantamala, D., Kumrapich, B., Suwan, W., Smith, D.R., 2020. Phosphoproteomic analysis of dengue virus infected U937 cells and identification of pyruvate kinase M2 as a differentially phosphorylated phosphoprotein. Sci Rep 10, 14493.
Wu, N., Zheng, B., Shaywitz, A., Dagon, Y., Tower, C., Bellinger, G., Shen, C.H., Wen, J., Asara, J., McGraw, T.E., Kahn, B.B., Cantley, L.C., 2013. AMPK-dependent degradation of TXNIP upon energy stress leads to enhanced glucose uptake via GLUT1. Mol Cell 49, 1167-1175.
Wu, R.H., Tsai, M.H., Chao, D.Y., Yueh, A., 2015. Scanning mutagenesis studies reveal a potential intramolecular interaction within the C-terminal half of dengue virus NS2A involved in viral RNA replication and virus assembly and secretion. J Virol 89, 4281-4295.
Wu, S., Le, H., 2013. Dual roles of PKM2 in cancer metabolism. Acta Biochim Biophys Sin (Shanghai) 45, 27-35.
Wu, X., Zhou, Y., Zhang, K., Liu, Q., Guo, D., 2008. Isoform-specific interaction of pyruvate kinase with hepatitis C virus NS5B. FEBS Lett 582, 2155-2160.
Wu, Y.H., Yang, Y., Chen, C.H., Hsiao, C.J., Li, T.N., Liao, K.J., Watashi, K., Chen, B.S., Wang, L.H., 2021. Aerobic glycolysis supports hepatitis B virus protein synthesis through interaction between viral surface antigen and pyruvate kinase isoform M2. PLoS Pathog 17, e1008866.
Xia, L., Qin, K., Wang, X.R., Wang, X.L., Zhou, A.W., Chen, G.Q., Lu, Y., 2017. Pyruvate kinase M2 phosphorylates H2AX and promotes genomic instability in human tumor cells. Oncotarget 8, 109120-109134.
Xiangyun, Y., Xiaomin, N., Linping, G., Yunhua, X., Ziming, L., Yongfeng, Y., Zhiwei, C., Shun, L., 2017. Desuccinylation of pyruvate kinase M2 by SIRT5 contributes to antioxidant response and tumor growth. Oncotarget 8, 6984-6993.
Xie, S., Lin, X., Yang, Q., Shi, M., Yang, X., Cao, Z., Cao, R., 2025. The Japanese encephalitis virus NS1 protein concentrates ER membranes in a cytoskeleton-independent manner to facilitate viral replication. J Virol 99, e0211324.
Xie, S., Yang, X., Yang, X., Cao, Z., Wei, N., Lin, X., Shi, M., Cao, R., 2024. Japanese encephalitis virus NS1 and NS1' proteins induce vimentin rearrangement via the CDK1-PLK1 axis to promote viral replication. J Virol 98, e0019524.
Xie, X., Zou, J., Zhang, X., Zhou, Y., Routh, A.L., Kang, C., Popov, V.L., Chen, X., Wang, Q.Y., Dong, H., Shi, P.Y., 2019. Dengue NS2A Protein Orchestrates Virus Assembly. Cell Host Microbe 26, 606-622 e608.

Xu, Q., Liu, L.Z., Yin, Y., He, J., Li, Q., Qian, X., You, Y., Lu, Z., Peiper, S.C., Shu, Y., Jiang, B.H., 2015. Regulatory circuit of PKM2/NF-kappaB/miR-148a/152-modulated tumor angiogenesis and cancer progression. Oncogene 34, 5482-5493.
Xu, Q., Tu, J., Dou, C., Zhang, J., Yang, L., Liu, X., Lei, K., Liu, Z., Wang, Y., Li, L., Bao, H., Wang, J., Tu, K., 2017. HSP90 promotes cell glycolysis, proliferation and inhibits apoptosis by regulating PKM2 abundance via Thr-328 phosphorylation in hepatocellular carcinoma. Mol Cancer 16, 178.
Yang, C.M., Lin, C.C., Lee, I.T., Lin, Y.H., Yang, C.M., Chen, W.J., Jou, M.J., Hsiao, L.D., 2012a. Japanese encephalitis virus induces matrix metalloproteinase-9 expression via a ROS/c-Src/PDGFR/PI3K/Akt/MAPKs-dependent AP-1 pathway in rat brain astrocytes. J Neuroinflammation 9, 12.
Yang, J., Zhang, Y., 2015. I-TASSER server: new development for protein structure and function predictions. Nucleic Acids Res 43, W174-181.
Yang, K., Li, X., Yang, S., Zheng, Y., Cao, S., Yan, Q., Huang, X., Wen, Y., Zhao, Q., Du, S., Lang, Y., Zhao, S., Wu, R., 2024. Japanese encephalitis virus infection induces mitochondrial-mediated apoptosis through the proapoptotic protein BAX. Front Microbiol 15, 1485667.
Yang, L., Xie, M., Yang, M., Yu, Y., Zhu, S., Hou, W., Kang, R., Lotze, M.T., Billiar, T.R., Wang, H., Cao, L., Tang, D., 2014a. PKM2 regulates the Warburg effect and promotes HMGB1 release in sepsis. Nature Communications 5, 4436.
Yang, L., Xie, M., Yang, M., Yu, Y., Zhu, S., Hou, W., Kang, R., Lotze, M.T., Billiar, T.R., Wang, H., Cao, L., Tang, D., 2014b. PKM2 regulates the Warburg effect and promotes HMGB1 release in sepsis. Nat Commun 5, 4436.
Yang, P., Li, Z., Li, H., Lu, Y., Wu, H., Li, Z., 2015. Pyruvate kinase M2 accelerates pro-inflammatory cytokine secretion and cell proliferation induced by lipopolysaccharide in colorectal cancer. Cell Signal 27, 1525-1532.
Yang, W., Xia, Y., Cao, Y., Zheng, Y., Bu, W., Zhang, L., You, M.J., Koh, M.Y., Cote, G., Aldape, K., Li, Y., Verma, I.M., Chiao, P.J., Lu, Z., 2012b. EGFR-induced and PKCepsilon monoubiquitylation-dependent NF-kappaB activation upregulates PKM2 expression and promotes tumorigenesis. Mol Cell 48, 771-784.
Yang, W., Xia, Y., Hawke, D., Li, X., Liang, J., Xing, D., Aldape, K., Hunter, T., Alfred Yung, W.K., Lu, Z., 2012c. PKM2 phosphorylates histone H3 and promotes gene transcription and tumorigenesis. Cell 150, 685-696.
Yang, W., Xia, Y., Ji, H., Zheng, Y., Liang, J., Huang, W., Gao, X., Aldape, K., Lu, Z., 2011. Nuclear PKM2 regulates beta-catenin transactivation upon EGFR activation. Nature 480, 118-122.
Yang, W., Zheng, Y., Xia, Y., Ji, H., Chen, X., Guo, F., Lyssiotis, C.A., Aldape, K., Cantley, L.C., Lu, Z., 2012d. ERK1/2-dependent phosphorylation and nuclear translocation of PKM2 promotes the Warburg effect. Nat Cell Biol 14, 1295-1304.
Yang, X., Qian, K., 2017. Protein O-GlcNAcylation: emerging mechanisms and functions. Nat Rev Mol Cell Biol 18, 452-465.
Yano, H., Baranov, S.V., Baranova, O.V., Kim, J., Pan, Y., Yablonska, S., Carlisle, D.L., Ferrante, R.J., Kim, A.H., Friedlander, R.M., 2014. Inhibition of mitochondrial protein import by mutant huntingtin. Nat Neurosci 17, 822-831.
Yap, T.L., Xu, T., Chen, Y.L., Malet, H., Egloff, M.P., Canard, B., Vasudevan, S.G., Lescar, J., 2007. Crystal structure of the dengue virus RNA-dependent RNA polymerase catalytic domain at 1.85-angstrom resolution. J Virol 81, 4753-4765.
Yin, Y.Q., Liu, L.L., Jiang, Y.T., Xing, J.C., Qi, W.B., Huang, L.H., 2024. SLC25A12 inhibits Japanese encephalitis virus replication by interacting with the NS1 and enhancing the type I interferon response. Vet Microbiol 297, 110199.
Youn, S., Li, T., McCune, B.T., Edeling, M.A., Fremont, D.H., Cristea, I.M., Diamond, M.S., 2012. Evidence for a genetic and physical interaction between nonstructural proteins NS1 and NS4B that modulates replication of West Nile virus. J Virol 86, 7360-7371.

Yu, I.M., Zhang, W., Holdaway, H.A., Li, L., Kostyuchenko, V.A., Chipman, P.R., Kuhn, R.J., Rossmann, M.G., Chen, J., 2008. Structure of the immature dengue virus at low pH primes proteolytic maturation. Science 319, 1834-1837.
Yuan, L., Wang, Y., Chen, Y., Chen, X., Li, S., Liu, X., 2023. Shikonin inhibits immune checkpoint PD-L1 expression on macrophage in sepsis by modulating PKM2. Int Immunopharmacol 121, 110401.
Yun, S.I., Lee, Y.M., 2018. Early Events in Japanese Encephalitis Virus Infection: Viral Entry. Pathogens 7.
Yusof, R., Clum, S., Wetzel, M., Murthy, H.M., Padmanabhan, R., 2000. Purified NS2B/NS3 serine protease of dengue virus type 2 exhibits cofactor NS2B dependence for cleavage of substrates with dibasic amino acids in vitro. J Biol Chem 275, 9963-9969.
Zahra, K., Dey, T., Ashish, Mishra, S.P., Pandey, U., 2020. Pyruvate Kinase M2 and Cancer: The Role of PKM2 in Promoting Tumorigenesis. Front Oncol 10, 159.
Zhang, J., Li, M., Cheng, J., Wang, Y., Ma, C., Yin, L., Wang, J., Gao, X., Liang, W., Wei, L., 2025a. CypA inhibits respiratory syncytial virus (RSV) replication by suppressing glycolysis through the downregulation of PKM2 expression. J Virol 99, e0007425.
Zhang, J.Y., Yao, M.X., Xia, S.T., Zeng, F.C., Liu, Q.Y., 2025b. Systematic and comprehensive insights into HIF-1 stabilization under normoxic conditions: implications for cellular adaptation and therapeutic strategies in cancer. Cell Mol Biol Lett 30.
Zhang, L., Liu, X., Mao, J., Sun, Y., Gao, Y., Bai, J., Jiang, P., 2023. Porcine reproductive and respiratory syndrome virus-mediated lactate facilitates virus replication by targeting MAVS. Vet Microbiol 284, 109846.
Zhang, L., Nan, X., Zhou, D., Wang, X., Zhu, S., Li, Q., Jia, F., Zhu, B., Si, Y., Cao, S., Ye, J., 2024a. Japanese encephalitis virus NS1 and NS1' protein disrupts the blood-brain barrier through macrophage migration inhibitory factor-mediated autophagy. J Virol 98, e0011624.
Zhang, L.F., Lou, J.T., Lu, M.H., Gao, C., Zhao, S., Li, B., Liang, S., Li, Y., Li, D., Liu, M.F., 2015. Suppression of miR-199a maturation by HuR is crucial for hypoxia-induced glycolytic switch in hepatocellular carcinoma. EMBO J 34, 2671-2685.
Zhang, X., Jiang, L., Weng, G., Shen, C., Zhang, O., Liu, M., Zhang, C., Gu, S., Wang, J., Wang, X., Du, H., Zhang, H., Zhang, K., Wang, E., Hou, T., 2025c. HawkDock version 2: an updated web server to predict and analyze the structures of protein-protein complexes. Nucleic Acids Res.
Zhang, Y., 2008. I-TASSER server for protein 3D structure prediction. BMC Bioinformatics 9, 40.
Zhang, Y., Chang, L., Xin, X., Qiao, Y., Qiao, W., Ping, J., Xia, J., Su, J., 2024b. Influenza A virus-induced glycolysis facilitates virus replication by activating ROS/HIF-1alpha pathway. Free Radic Biol Med 225, 910-924.
Zhang, Y.J., Chang, L.F., Xin, X., Qiao, Y.X., Qiao, W.N., Ping, J.H., Xia, J., Su, J., 2024c. Influenza A virus-induced glycolysis facilitates virus replication by activating ROS/HIF-1α pathway. Free Radical Bio Med 225, 910-924.
Zhang, Z., Deng, X., Liu, Y., Liu, Y., Sun, L., Chen, F., 2019. PKM2, function and expression and regulation. Cell Biosci 9, 52.
Zhang, Z., Li, Y., Loh, Y.R., Phoo, W.W., Hung, A.W., Kang, C., Luo, D., 2016. Crystal structure of unlinked NS2B-NS3 protease from Zika virus. Science 354, 1597-1600.
Zhang, Z., Liu, Q., Che, Y., Yuan, X., Dai, L., Zeng, B., Jiao, G., Zhang, Y., Wu, X., Yu, Y., Zhang, Y., Yang, R., 2010. Antigen presentation by dendritic cells in tumors is disrupted by altered metabolism that involves pyruvate kinase M2 and its interaction with SOCS3. Cancer Res 70, 89-98.
Zhao, Y., Soh, T.S., Lim, S.P., Chung, K.Y., Swaminathan, K., Vasudevan, S.G., Shi, P.Y., Lescar, J., Luo, D., 2015. Molecular basis for specific viral RNA recognition and 2'-O-ribose methylation by the dengue virus nonstructural protein 5 (NS5). Proc Natl Acad Sci U S A 112, 14834-14839.
Zheng, D., Jiang, Y., Qu, C., Yuan, H., Hu, K., He, L., Chen, P., Li, J., Tu, M., Lin, L.J.T.A.j.o.p., 2020. Pyruvate kinase M2 tetramerization protects against hepatic stellate cell activation and liver fibrosis. 190, 2267-2281.

Zhou, X., Chen, Y., Kang, X., Zhao, A., Yang, S., 2024. Transcriptome and Proteome Analyses Revealed Differences in JEV-Infected PK-15 Cells in Response to Ferroptosis Agonists and Antagonists. Animals (Basel) 14.
Zhu, Y., He, Z., Qi, Z., 2023. Virus-host Interactions in Early Japanese Encephalitis Virus Infection. Virus Res 331, 199120.
Zou, J., Xie, X., Lee le, T., Chandrasekaran, R., Reynaud, A., Yap, L., Wang, Q.Y., Dong, H., Kang, C., Yuan, Z., Lescar, J., Shi, P.Y., 2014. Dimerization of flavivirus NS4B protein. J Virol 88, 3379-3391.
Zou, J., Xie, X., Wang, Q.Y., Dong, H., Lee, M.Y., Kang, C., Yuan, Z., Shi, P.Y., 2015. Characterization of dengue virus NS4A and NS4B protein interaction. J Virol 89, 3455-3470.
Zwerschke, W., Mazurek, S., Massimi, P., Banks, L., Eigenbrodt, E., Jansen-Dürr, P., 1999. Modulation of type M2 pyruvate kinase activity by the human papillomavirus type 16 E7 oncoprotein. Proc Natl Acad Sci U S A 96, 1291-1296.

Publications

From thesis

1. **Bohara VS**, Kumar S. Japanese encephalitis virus promotes its replication in neuronal cells by enhancing glycolysis via hypoxia-inducible factor-1α. **Virology**. 2025 Nov 6;614:110736. Doi: 10.1016/j.virol.2025.110736.

2. **Bohara VS**, Deshmukh A, Kumar S. Pyruvate kinase M2 modulates Japanese encephalitis virus replication in neuronal cells. **J Gen Virol**. 2025 Sep;106(9):002140. Doi: 10.1099/jgv.0.002140.

3. **Bohara VS**, Kumar S. Decoding the Metabolic Crosstalk Between Glycolysis and RNA Viral Pathogenesis. **Virology**. Doi.org/10.1016/j.virol.2025.110766.

In collaboration

1. Gupta A, **Bohara VS**, Chauhan AS, Mohapatra A, Kaur H, Sharma A, Chaudhary N, Kumar S. Alpha-synuclein expression in neurons modulates Japanese encephalitis virus infection**. J Virol.** 2024 Dec 17;98(12):e0041824. Doi: 10.1128/jvi.00418-24.

2. Gupta A, **Bohara VS**, Siddegowda YB, Chaudhary N, Kumar S. Alpha-synuclein and RNA viruses: Exploring the neuronal nexus. **Virology**. 2024 Sep;597:110141. Doi: 10.1016/j.virol.2024.110141.

3. Mohapatra A, **Bohara VS**, Kumar S, Chaudhary N. Polymyxin B accelerates the α-synuclein aggregation. **Biophys Chem**. 2021 Oct;277:106628. Doi: 10.1016/j.bpc.2021.106628.

Book chapters

1. **Bohara VS**, Kumar S. Viral Vaccines. Textbook of General Virology, 1ST Edition. 2025. CRC Press, Taylor & Francis Group.

2. **Bohara VS**, Kumar S. Viruses and Their Significance. Textbook of General Virology, 1ST Edition. 2025. CRC Press, Taylor & Francis Group.

3. **Bohara VS**, Bora NR, Sevda S, Kumar S. Development of a new vaccine at the laboratory scale. Bioreactor Design Concepts for Viral Vaccine Production. 2024 Jan 1 (pp. 83-113). Academic Press.

4. Bhattacharya S, **Bohara VS**, Sevda S, Kumar S. Vaccine, and vaccine types. Bioreactor Design Concepts for Viral Vaccine Production.2024 Jan 1 (pp. 73-82). Academic Press.

5. **Bohara VS**, Kumar S.Transgenic animal models. Textbook for Gene Therapy. Springer Nature. (To be published).

6. **Bohara VS**, Kumar S. Genome editing tools. Textbook for Gene Therapy. Springer Nature. (To be published).

Conferences/workshops

1. Presented a poster in the Research and Industrial Conclave (RIC) 2025, Indian Institute of Technology Guwahati, India, on the topic "**Japanese encephalitis virus facilitates its replication in neuronal cells by inducing glucose metabolism via Hypoxia-inducible factor-1α**.

2. Presented a poster in the international symposium "Zoonotic and Transboundary Diseases: Breaking the chain through Multidisciplinary Approach" and XVIIIth Annual conference of Indian Association of Veterinary Public Health Specialists (IAVPHS), organised by Indian Council of Agricultural Research (ICAR) Research Complex for NEH region, Umium, Meghalaya, India.

3. Participated in hands-on training on **Next Generation sequencing technologies and data analysis** jointly organized by Gujarat Biotechnology Research Centre and Anand Agriculture University.

4. Attended mini-symposium on Emerging Viral Diseases of Animals in India on 26th June 2021, organized by the Department of Biosciences and Bioengineering, Indian Institute of Technology Guwahati, Assam, Government of India.